

University of Strathclyde  
Naval Architecture and  
Marine Engineering Department

**COST ANALYSIS OF  
OFFSHORE WIND TURBINE  
SUPPORT STRUCTURES  
- MONOPILE AND JACKET -**

by

**Joel Gancedo Sustatxa**

A thesis presented in fulfilment of the requirements for the  
degree of Master of Philosophy

2011

## **COPYRIGHT STATEMENT**

This thesis is the result of the author's original research. It has been composed by the author and has not been previously submitted for examination which has led to the award of a degree.

The copyright of this thesis belongs to the author under the terms of the United Kingdom Copyright Acts as qualified by University of Strathclyde Regulation 3.50. Due acknowledgement must always be made of the use of any material contained in, or derived from, this thesis.'

Signed:

Date:

## **ABSTRACT**

Wind turbine support structures account for around a quarter of the total capital expenditure of an offshore wind farm. If a reduction of the total investment is sought in order to promote offshore wind in the future, it is vital to understand how the different driving factors affect the design and final costs of support structures.

Based on the last 10 year experience in the market, the influence of several parameters is analysed and conclusions are made for the next stage of the research.

In this second stage, monopile and jacket support structures are studied in detail. For this purpose, a calculation tool was programmed in Mathcad and Matlab respectively, which enables to design the optimum structure in different conditions. These conditions are based on the turbine power, water depth, soil type and significant wave height. Furthermore, manufacturing and installation costs for each design are also calculated, from which total specific cost curves can be obtained for a simple comparison of all the parameters and a better understanding of their impact in the final cost.

Therefore, principal characteristics and limitations of both the monopile and the jacket can be concluded and the most suitable technology for any location easily selected.

## **ACKNOWLEDGEMENTS**

First and foremost I offer my sincerest gratitude to my supervisor, Professor Nigel Barltrop, whose guidance and support from the initial to the final level enabled me to develop an understanding of the subject. I will never forget his patience and specially his eagerness to contribute with his knowledge and experience to the development of the project.

I am grateful to my second supervisor Professor Atilla Incecik and Dr. Li Xu, for the kind help and valuable assistance and to Gurpreet Grewal for his unconditional computer sharing.

This project could not have been accomplished without the support from Gamesa. I would like to acknowledge my fellows in the company, and among all, Juan Albizua for his proficient management.

In my daily work I have been blessed with a friendly and cheerful group of colleagues from all different countries, in addition to the obliging and cooperative staff of the NAME department. It has been a pleasure being part of that motley family.

Last but not least, I thank my parents for their care and especially my wife, for her encouragement and unending love. You were my sunshine during my stay in Glasgow.

## TABLE OF CONTENTS

1	INTRODUCTION .....	12
1.1	Background .....	12
1.2	Objectives and Scope .....	14
1.3	Organization of the thesis.....	14
1.4	Offshore Wind Energy .....	15
1.4.1	Introduction.....	15
1.4.2	Historical review .....	15
1.4.3	Advantages and disadvantages.....	17
1.4.4	Foundation and substructure types for offshore wind turbines.....	18
1.4.4.1	Fixed substructures .....	19
1.4.4.2	Floating sub-structures.....	26
1.4.4.3	Comparison of the different substructures.....	29
2	OFFSHORE SUPPORT STRUCTURES COSTS. EXPERIENCED BASED ANALYSIS .....	30
2.1	Introduction .....	30
2.2	Analysis of all support structures.....	30
2.2.1	Water depth vs specific cost.....	33
2.2.2	Distance to shore vs specific cost.....	34
2.2.3	OWTG number vs specific cost .....	34
2.2.4	OWTG power vs specific cost .....	35
2.2.5	Conclusions .....	39
2.3	Monopile substructure.....	40
2.3.1	Multiple regression analysis.....	40
2.3.2	Conclusions .....	44
3	OFFSHORE SUPPORT STRUCTURES COSTS. NUMERICAL ANALYSIS	45
3.1	Introduction .....	45
3.2	Cost Method for OWTG's support structures .....	47
3.2.1	O&M costs .....	50

3.2.2	Decommissioning costs.....	54
3.2.3	Other costs.....	55
3.3	Input Parameters.....	55
3.3.1	WTG Power .....	55
3.3.2	Water Depth .....	56
3.3.3	Wave height .....	57
3.3.4	Soil Type .....	57
3.4	Monopile cost analysis .....	58
3.4.1	Introduction.....	58
3.4.2	Mathcad calculation methodology.....	58
3.4.2.1	Static analysis .....	59
3.4.2.2	Dynamic analysis.....	71
3.4.3	Monopile Design.....	73
3.4.4	Validation.....	76
3.4.5	Monopile Manufacturing .....	78
3.4.6	Monopile Installation .....	84
3.5	Jacket cost analysis.....	98
3.5.1	Introduction.....	98
3.5.2	Matlab calculation methodology.....	98
3.5.3	Jacket Design .....	108
3.5.4	Validation.....	109
3.5.5	Jacket Manufacturing.....	110
3.5.6	Jacket Installation.....	115
4	ANALYSIS RESULTS.....	121
4.1	Monopile Results.....	121
4.1.1	OWTG power: 3.6 MW .....	121
4.1.2	OWTG power: 5 MW .....	129
4.1.3	OWTG power: 7 MW .....	139
4.1.4	Conclusions .....	139
4.2	Jacket Results .....	144
4.2.1	OWTG power: 3.6 MW .....	144
4.2.2	OWTG power: 5 MW .....	149

4.2.3	OWTG power: 7 MW .....	154
4.2.4	Conclusions .....	158
4.3	Monopile – Jacket costs comparison .....	162
5	conclusions and recommendations .....	164
5.1	Conclusions .....	164
5.2	Recommendations .....	166
6	REFERENCES .....	168
APPENDIX A	Offshore Wind Farms Table .....	A-1





## **LIST OF SYMBOLS AND ABBREVIATIONS**

The following symbols are used and may not have a specific definition in the text where they appear.

AP	Apparent Fixity
API	American Petroleum Institute
CAPEX	Capital Expenditure
dof	Degrees of freedom
DNV	Det Norske Veritas
DS	Distributed Springs
FLS	Fatigue Limit State
GL	Germanischer Lloyd
GBS	Gravity Based Structure
HLV	Heavy Lift Vessel
LPC	Levelised Production Cost
MPI	Magnetic Particle Inspection
MWL	Mean Water Level
m.s.l.	Mean sea level
NDT	Non Destructive Testing
OPEX	Operating Expenses
OWF	Offshore Wind Farm
OWTG	Offshore Wind Turbine Generator
PWHT	Post Weld Heat Treatment

ROV	Remotely Operated Vehicle
THM	Top Head Mass
TP	Transition Piece
ULS	Ultimate Limit State
UT	Ultrasonic Test
WTG	Wind Turbine Generator
$C_d$	Drag coefficient
$C_m$	Inertia coefficient
$D$	Pile diameter
$\delta_{tip}$	Displacement at pile tip node
$\varepsilon_c$	strain occurring at 50% of the ultimate resistance
$F_s$	Force vector of the substructure as seen by the connection node
$f_0$	First natural frequency of the structure
$K_s$	Stiffness matrix of the substructure as seen by the connection node
$H_s$	Significant wave height
$H_{max}$	Extreme wave height
$p$	Actual lateral resistance per area
$p_u$	Ultimate lateral resistance per area
$q$	end bearing per area
$q_{max}$	maximum end bearing per area

$s_u$	Undrained shear strength
$\sigma_{\max}$	Design maximum axial stress
$t$	skin friction per area
$t_{\max}$	maximum skin friction per area
$T_z$	Mean zero crossing period
$\tau_{\max}$	Design maximum shear stress
$th$	Pile thickness
$y$	Actual lateral deflection
$y_c$	displacement occurring at 50% of the ultimate resistance
$\gamma_m$	Material factor
$z$	axial displacement
$z_c$	axial displacement at which maximum skin friction is mobilised

## LIST OF TABLES

Table 1.1. Comparison of different substructure types for offshore wind turbines ...	29
Table 2.1. Data summary for the multiple regression analysis .....	41
Table 3.1. Reference OWTG data.....	56
Table 3.2 Water range included in the study for each substructure.....	57
Table 3.3. Compared sea states .....	57
Table 3.4. Compared clay types.....	58
Table 3.5. Minimum expected $\sigma_{\max}$ and $\tau_{\max}$ from Grade 355 steel depending on the plate thickness .....	70
Table 3.6. Secondary steel weight for each of the considered OWTG powers .....	71
Table 3.7. Monopile substructure weight and diameters for already accomplished projects .....	77
Table 3.8. Monopile transportation costs.....	96
Table 3.9. Estimated times for monopile installation operations.....	97
Table 3.10. Jacket footprint values according to the water depth.....	100
Table 3.11. Jacket top width values according to the WTG power .....	100
Table 3.12. Jacket and pile weights for already accomplished projects .....	109
Table 3.13. Estimated times for jacket installation operations .....	120

## LIST OF FIGURES

Figure 1.1. Division of a wind turbine’s support structure according to [8].....	14
Figure 1.2. Monopile foundation and substructure [9] .....	19
Figure 1.3. Drilled Concrete Monopile Concept [10].....	20
Figure 1.4. Center Column Tripod Substructure [9].....	21
Figure 1.5. Bard Tripile substructure [14] .....	21
Figure 1.6. Jacket substructure [9].....	22
Figure 1.7. Twisted Jacket Concept from Keystone Engineering [16].....	23
Figure 1.8. The monopod and tripod suction can based foundations [23].....	24
Figure 1.9. Shallow water (to the left) and deep water (to the right) gravity based foundations [14] .....	24
Figure 1.10. Guyed Tower Structure [30].....	25
Figure 1.11. Floating platform types according to the used stability method [32] ....	26
Figure 1.12. Spar type floating wind turbine [35].....	27
Figure 1.13. WindFloat floating wind turbine concept [37] .....	28
Figure 1.14. Blue H floating wind turbine concept [35].....	28
Figure 3.1. Typical damages in offshore jacket [53] .....	53
Figure 3.2: Monopile division depending on the linearity of the elements. ....	61
Figure 3.3. Comparison of different methods for the soil-pile interaction calculation [66] .....	63
Figure 3.4. Slope of p-y curves differ at different depths and loadings [70].....	65
Figure 3.5. Different soil resistances to consider in the whole soil-pile interaction [74] .....	66
Figure 3.6.Offshore wind turbine modelled as a mass on pole [78] .....	72
Figure 3.7.Pile Mode 1 example. Scale 1:100 .....	73
Figure 3.8 Frequency intervals for a variable speed turbine system.....	75
Figure 3.9. Period range intervals for the design of the OWTG.....	76
Figure 3.10. Monopile manufacturing. Storage of steel plates [82] .....	78
Figure 3.11. Monopile manufacturing. Milling and cutting [82].....	78
Figure 3.12. Monopile manufacturing. Rolling [82].....	79

Figure 3.13. Monopile manufacturing. Inside longitudinal welding [82].....	79
Figure 3.14. Monopile manufacturing. Milling of the longitudinal union [82] .....	79
Figure 3.15. Monopile manufacturing. Outside longitudinal welding [82] .....	80
Figure 3.16. Monopile manufacturing. Calibration [82].....	80
Figure 3.17. Monopile manufacturing. Assembly [82].....	81
Figure 3.18. Monopile manufacturing. Inside circular welding [82].....	81
Figure 3.19. Monopile manufacturing. Milling of the circular union [82] .....	81
Figure 3.20. Monopile manufacturing. Outside circular welding [82] .....	82
Figure 3.21. Monopile manufacturing. NDT inspection [82] .....	82
Figure 3.22. Monopile manufacturing. Secondary steel assembly [82].....	83
Figure 3.23. Monopile manufacturing. Coating [82] .....	83
Figure 3.24. Offshore pile driving [14].....	84
Figure 3.25. Whole monopile structure (pile+TP) transportation in one piece [85]..	85
Figure 3.26. Offshore pile drilling and drill bit [85] .....	86
Figure 3.27. Transition Piece being placed above driven pile [87] .....	88
Figure 3.28. Monopile grouting areas depending on the installation case [88] .....	89
Figure 3.29. Side stone dumping vessel (on the left) and flexible fall pipe vessel (on the right) [89] .....	90
Figure 3.30. Typical installed monopole [65].....	91
Figure 3.31. Jack-up type vessel transporting piles and transition pieces to site [95]92	
Figure 3.32. TP transportation by barge [96] and flotation [85].....	92
Figure 3.33: Jacket substructure and piles union detail [65].....	102
Figure 3.34: Different technologies for the jacket Transition Piece: steel bracing [100] (on the left), concrete [65] (in the middle) and steel cone [46] (on the right).102	
Figure 3.35: Welded joints [104] (to the left) and cast node [46] (to the right) comparison .....	112
Figure 3.36: Assembled part of jacket substructure [46] .....	113
Figure 3.37: Erection of a jacket substructure [46].....	114
Figure 3.38: Representation of global and local scour in a jacket structure [106]..	115
Figure 3.39: Prepiling with seabed template [107] .....	116
Figure 3.40: Positioning of the jacket substructure (including TP) [107].....	117
Figure 3.41: Jacket frame (on the left) and TP (on the right) positioning [65].....	118

Figure 3.42: Typical jacket and pile connections by in line piles (to the left) and by sleeves (to the right) .....	118
Figure 4.1. Traditional pile design [110] .....	121
Figure 4.2. Natural frequency of a mass pole structure in which the end mass is much greater than the beam mass .....	126
Figure 4.3. Tapered pile design [110] .....	130

## LIST OF DIAGRAMS

Diagram 1.1 OWF CAPEX cost breakdown [4].....	13
Diagram 2.1 Specific cost, water depth and number of installed OWTG in different OWFs for several substructure types .....	32
Diagram 2.2 Water depth vs specific cost for different OWF .....	33
Diagram 2.3 Distance to shore vs specific cost for different OWF .....	34
Diagram 2.4. OWTG number vs specific cost for different OWF.....	35
Diagram 2.5 OWTG power vs specific cost for different OWF .....	36
Diagram 2.6 OWTG power (in columns) and specific cost (in line) for different monopile supported OWF .....	38
Diagram 2.7 CAPEX level in the last decade in absolute value (blue) and taking into account the different constraints (green) [43]. .....	39
Diagram 2.8 Multiple regression predicted and actual costs of a monopile supported OWTG for the year 2010 at different cable lengths.....	42
Diagram 2.9 Multiple regression predicted and actual costs of a monopile supported OWTG for the year 2010 at different water depths. ....	43
Diagram 2.10 Specific cost of monopile supported OWTG vs water depth and cable length for the year 2010 .....	44
Diagram 3.1 Cost Method Overview for offshore substructures.....	49
Diagram 3.2 O&M costs split based on 2 vessels availability [6] .....	52
Diagram 3.3 Monopile static calculation summary with Mathcad .....	59
Diagram 3.4 Horizontal velocity under crest at MWL: Airy theory as % of regular theory [60].....	62
Diagram 3.5. Typical lateral resistance p-y curve [70].....	67
Diagram 3.6 Summary of the monopile dynamic calculation with Mathcad .....	71
Diagram 3.7 Volume of clay spoil for different drilled depths and diameters .....	87
Diagram 3.8 Scour protection thickness variation depending on the water depth (m) .....	94
Diagram 3.9. $\lambda$ variation at different water depths.....	95
Diagram 3.10 Scour protection cost for a 5 m diameter pile .....	95



Diagram 3.11 HLV hiring cost as a function of the lifting capacity [98] .....	96
Diagram 3.12 Annual average weather windows of minimum 6 hours duration based on 4 North Sea sites. [84] .....	97
Diagram 3.13 Summary of the jacket calculation with Matlab .....	99
Diagram 3.14 Whole structure division in parts with different element properties. ....	101
Diagram 3.15 Horizontal velocity under crest at MWL: Airy theory as % of regular theory [60].....	103
Diagram 3.16 Illustration of the two loading cases for the jacket support structure	104
Diagram 3.17 Jacket support structure partition in two, with 4 connection nodes between them .....	105
Diagram 3.18 Example of the maximum stress per node (MPa) for the whole structure.....	106
Diagram 3.19 Jacket mode 1 example. Scale 10:1.....	107
Diagram 4.1 3.6 MW pile and TP mass (only static criterion considered).....	122
Diagram 4.2. 3.6 MW pile and TP mass (static and dynamic criterion considered)	123
Diagram 4.3. Comparison between wave and wind overturning moment at seabed for different depths and wave heights.....	124
Diagram 4.4 Parameters affecting the circle to break between the wave loading and the pile diameter.....	125
Diagram 4.5 Pile penetration and diameter variation with water depth for the 3.6 MW monopile.....	127
Diagram 4.6 Cost per MW trendline for 3.6 MW OWTG monopile (pile and TP). ....	128
Diagram 4.7. 3 areas in the cost per MW trendline for 3.6 MW OWTG monopile (pile and TP).....	129
Diagram 4.8. 5 MW pile and TP mass (only static criterion considered).....	131
Diagram 4.9. 5 MW pile and TP mass (static and dynamic criterion considered) ..	132
Diagram 4.10. Comparison between wave and wind moment at seabed for different pile diameters and wave heights .....	134
Diagram 4.11. Pile penetration and diameter variation with water depth for 5 MW monopile.....	135
Diagram 4.12. Cost per MW trendline for 5 MW OWTG monopile (pile and TP) ....	136
Diagram 4.13 Cost per MW trendline for 5 MW WTG monopile (pile and TP) ....	137

Diagram 4.14 Cost per MW trendline for 5 MW WTG monopile (pile and TP) ....	138
Diagram 4.15. Monopile costs division in varying water depth .....	140
Diagram 4.16 3.6 MW and 5 MW OWTG monopile (pile and TP) costs comparison in several soil and wave heights conditions .....	141
Diagram 4.17 3.6 MW jacket support structure total weight and 1 <sup>st</sup> natural frequency .....	146
Diagram 4.18 Wind and wave generated moment comparison at mudline for the 3.6 MW jacket case.....	147
Diagram 4.19 Wind and wave generated shear force comparison at mudline for the 3.6 MW jacket case.....	147
Diagram 4.20 Piles total weight for the 3.6 MW jacket case.....	148
Diagram 4.21 Cost per MW trendline for 3.6 MW OWTG jacket support structure .....	149
Diagram 4.22 5 MW jacket support structure total weight and 1 <sup>st</sup> natural frequency .....	151
Diagram 4.23 Wind and wave generated moment comparison at mudline for the 5 MW jacket case.....	152
Diagram 4.24 Wind and wave generated shear force comparison at mudline for the 5 MW jacket.....	152
Diagram 4.25 Piles total weight for the 5 MW jacket case.....	153
Diagram 4.26 Cost per MW trendline for 5 MW OWTG jacket support structure .	154
Diagram 4.27 7 MW jacket support structure total weight and 1 <sup>st</sup> natural frequency .....	155
Diagram 4.28 Wind and wave generated moment comparison at mudline for the 7 MW jacket case.....	156
Diagram 4.29 Wind and wave generated shear force comparison at mudline for the 7 MW jacket.....	156
Diagram 4.30 Piles total weight for the 7 MW jacket case.....	157
Diagram 4.31 Cost per MW trendline for 7 MW OWTG jacket support structure .	158
Diagram 4.32 Cost division for jacket support structure at different conditions.....	159
Diagram 4.33 Cost per MW trendline of the jacket support structure for different turbine powers in average soil conditions.....	160

Diagram 4.34. Monopile and jacket support structures total costs comparison for  
average soil ..... 162

# 1 INTRODUCTION

## 1.1 Background

Renewable energy has become the main new generating capacity in Europe, with wind accounting for almost 40% of the new installations in the European Union during 2009 [1].

In the next decade, offshore wind is expected to become one of the main electricity generators in Europe. In the UK, in order to meet the ambitious target of 15% renewable energy consumption by 2020 [2], offshore wind energy is expected to play the main role (up to half of the new generation capacity planned until 2020). Other countries such as Germany, the Netherlands, France or Denmark will be developing large offshore wind projects, which will help to lower carbon emissions and fulfil the European overall 20% energy consumption share from renewable energy by the same year [3].

If these figures are to become real, the offshore industry needs a technological revolution similar to the one lived by the onshore wind industry since the nineties. This would allow a cost reduction in the CAPEX and OPEX of such installations, and therefore their development in a large scale by making this technology more attractive to developers

Furthermore, the needs of the industry are rapidly becoming more challenging as the offshore wind farms locations are moving further from shore into deeper and harsher environments, where the current technology cannot fulfil the minimum requirements.

For all these reasons, research and development in several fields is crucial. One of these main areas is related to the support structures of the offshore wind turbines. It is widely agreed that they account for around 22 to 25% of the total investment [4], [5], [6], [7], and consequently the correct design choice becomes an important decision to be made at an early stage for the project profitability (see Diagram 1.1.).

# OWF CAPEX cost breakdown

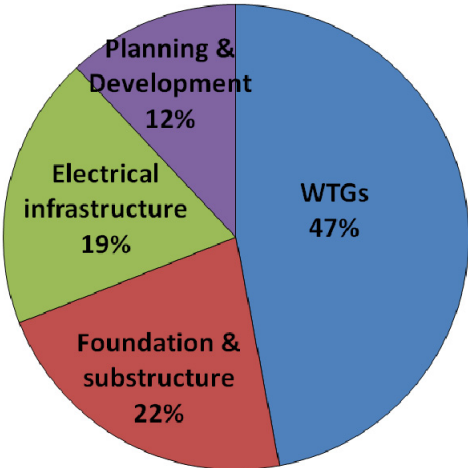
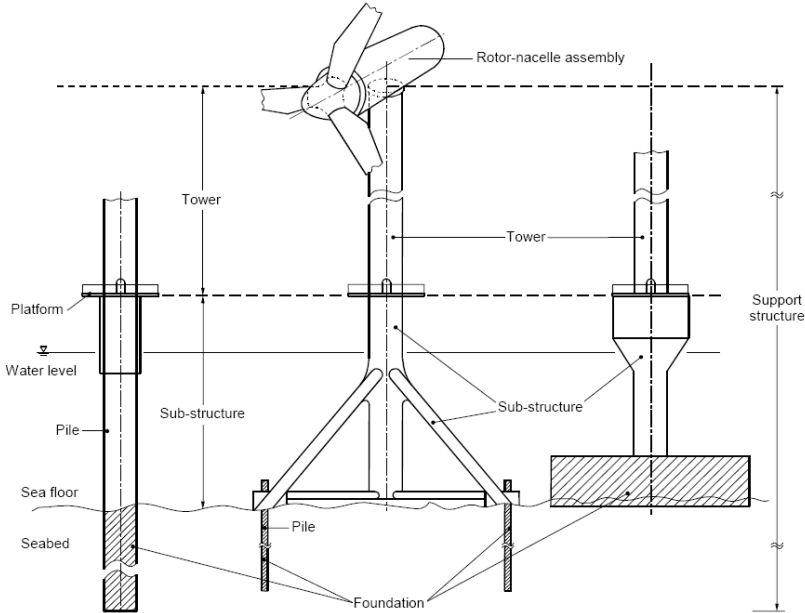


Diagram 1.1 OWF CAPEX cost breakdown [4]

This thesis will be studying both the foundation and substructure costs according to the division made at [8], and depicted in

Figure 1.1. Therefore, for simplification, whenever support structure is used in this thesis, it will be designating the whole structure composed of foundation and substructure (without including the tower of the WTG).



## **1.2 Objectives and Scope**

The first step to achieve the previously stated cost reduction of the offshore wind turbine support structures is to understand what their main design and cost driving factors are and how they affect the final cost.

Besides, a detailed analysis of the monopile and jacket type supports is sought, for representing the present and future of the industry. Their potential and limitations will be established which will help to shape the most suitable offshore wind farm locations and characteristics for each of them.

## **1.3 Organization of the thesis**

The thesis is divided in 5 chapters. The covered parts are briefly summarised hereafter.

Chapter one gives a general introduction to the offshore wind energy and its main characteristics. It also describes different foundation and substructure types at several development stages in order to give a clearer idea of the current state of the art.

In chapter two, establishing general specific costs for different support structures and understanding their effect in the final cost is intended. This is achieved based on the current experience of the industry, which is rather limited as it will be demonstrated. For this reason, only for the monopile general costs and driving equations can be established.

Chapter three is a detailed description of the analysis methodology carried out for the monopile in Mathcad and for the jacket in Matlab, which includes both statics and dynamics. Besides, a general overview of their manufacturing and installation process is also included along with their cost estimations.

In chapter four all the results from the analysis are included in order to understand how the main input parameters affect the structure design and final cost. The results are presented for each studied wind turbine power.

Finally, a summary of the study and its conclusions are listed in chapter five along with some recommendations for the future work.

## **1.4 Offshore Wind Energy**

### **1.4.1 Introduction**

Offshore wind is considered as one of the most promising renewable energies to be developed in the next decades. Despite still being in its infancy, offshore wind potential is enormous when compared to its onshore counterpart and it is expected that its capacity will grow exponentially just like onshore wind did in the past 20 years.

A brief introduction to offshore wind history and its main pros and cons are described hereafter. Then, currently available or possible future offshore support structures along with their advantages and disadvantages are presented.

### **1.4.2 Historical review**

The first offshore projects date from the early 90s. These pioneering projects were characterised by sheltered and shallow locations, in which the onshore turbines technology was directly applied.

Vindeby (1991) in Denmark was the first OWF consisting of 11 gravity based turbines rated at 450 kW. This was followed by Lely (1994) in the Netherlands and Tuno Knob (1995) in Denmark where 500 kW turbines were installed on monopile and gravity based foundations respectively. Bockstigen (1998) in Sweden was the first to use drilled monopiles for 5 offshore 550 kW machines.

Acting as prototypes, they became models for future sites, demonstrating differences of opinion on gravity and monopile foundation design. However, it was not until 2000 when, the first true OWF, exposed to the full North Sea environment was completed at Blyth (Britain) for two 2 MW turbines supported on monopiles.

OWF capacity was less than 5 MW in all these previous projects, until also in 2000, the Middelgrunden (Denmark) wind farm was opened. It consisted of twenty 2 MW turbines on gravity based structures.

Sweden followed with Utgrunden (2000) and Yttre Stengrund (2001) OWFs, which consisted of drilled monopiles totalling less than 10 MW capacity.

However, it was Denmark that continued with its pre-eminent position thanks to the Horns Rev (2002) and Nysted (2003) projects, which relied on monopile and gravity foundations respectively, and had a total capacity of 160 MW and 166 MW. Furthermore, previous installations were completed in very shallow waters (most of them below 5 m depth) and it was Horns Rev the first OWF to be exceeding the 10 m water depth.

Since these first steps, the industry has been rapidly developing and the projects have been located in more challenging sites with increasing turbine size and water depths.

By the end of 2010, almost 3000 MW had been offshore grid connected in 45 wind farms in 9 European countries. Besides, 10 wind farms were under construction totalling another 3000 MW and 19000 MW more had already been fully consented.

During 2010 the average OWF capacity was 155 MW with 3.2 MW turbines in 17.4 m deep waters [1]. These numbers are likely to increase substantially in the following years though.

Europe will continue leading the offshore wind development, specially the UK and Germany where the largest projects have been consented. China has only one OWF constructed so far, the Shanghai Donghai Bridge (2010), which consists of 34 turbines totalling a 100 MW capacity. However, it has shown a great interest in the offshore technology and its capacity is expected to boost rapidly by the end of the decade.

The other big player in onshore wind energy, the USA, is having more problems to spur the development of the offshore industry and no OWF has been constructed yet.



In spite of this, there are currently 10 projects being driven by four different companies.

### **1.4.3 Advantages and disadvantages**

Offshore wind energy is expanding rapidly, especially in the European northern countries. Its main advantages that are detailed hereafter:

Usually geographical conditions or environmental issues prevent the construction of onshore wind farms near dense populated areas, where energy is to be consumed. On the contrary, offshore locations allow the energy to be produced near the consumption areas without these concerns and saving land.

The amount of energy production can be significantly larger than onshore installations. The reasons being:

Wind turbines are usually larger (currently 3.6 to 5 MW) and are fast increasing, latest under development designs doubling these values up to 6 to 10 MW.

Wind speed on the seas is higher than on the land, and wind energy is proportional to the cube of the velocity. This means that a typical 20% wind velocity increase for areas located 10 km or more from land can imply a 70% energy growth.

Wind performance on the seas is steady, incrementing wind farms availability and efficiency.

Sea surface roughness is lower than onshore. Hence, wind shear decreases and offshore tower heights can be smaller. The result is that the structural tower can have a height around or lower than  $\frac{3}{4}$  of the rotor diameter compared with towers on land where a height around or higher than the rotor diameter is common.

Due to the sun radiation running through the sea surface, temperature changes in the atmosphere above sea level are smaller. This, along with the low sea surface roughness, makes offshore wind speed flow less turbulent than onshore, which

means that fatigue loads in the wind turbine will be much smaller and the life cycle greater.

Being far from the coast, visual impact, noise disturbance and shadow problems are avoided, and the turbines can run at higher speeds.

On the contrary, the main disadvantages that this technology needs to overcome are explained below.

Cost is the major drawback. Construction cost of an offshore wind farm is considerably greater than an onshore one. Installation and transmission expenses increase substantially when working in an offshore environment.

Operation and maintenance becomes a problem due to the limited access of the OWFs. Accessibility is very conditioned by weather and available resources that are very costly as well. Furthermore, O&M needs to take into account new important issues like the saltwater corrosion and the substructure inspections.

Higher technical expertise is required in the offshore environment due to the hydrodynamic action on the structure and the submerged foundation. Overall, a more advanced technology is required, especially in the coupling design of the wind farms.

Navigation effect on shipping or impact on fishing can be an issue when selecting the location of an OWF. In addition, influences on marine ecology during construction or visual impact from shore have to be addressed before the construction of an OWF can be consented.

#### **1.4.4 Foundation and substructure types for offshore wind turbines**

Hereafter, a summary of different foundation and substructure types for offshore wind turbines is presented, some already proven, other in research and development or testing stage, but most of them based on the oil&gas experience. A project's unique characteristics will determine which foundation better fulfils the requirements for each case.

### 1.4.4.1 Fixed substructures

There are various concepts available for bottom founded sub-structures:

#### 1.4.4.1.1 Pile based foundations

A simple steel pile embedded to the seabed acts as a link to transfer the loads from the structure to the soil. The pile can be connected to the structure by grouting or swaging technique.

One pile (monopod) or multiple piles (tripod or tetrapod) can support the structure. Hence, the following foundations can be found:

- Monopod.

It is an extension of the onshore turbine tower below the sea surface and driven or drilled 25-40 m into the seabed. The loads are transferred mainly by lateral force to the soil. The steel monopile, with a diameter ranging from 4 to 6 m and a thickness between 40 to 80 mm is currently the simplest, most economic and by far the most widely installed foundation type. Scour protection could be needed depending on the metocean conditions and the pile diameter.

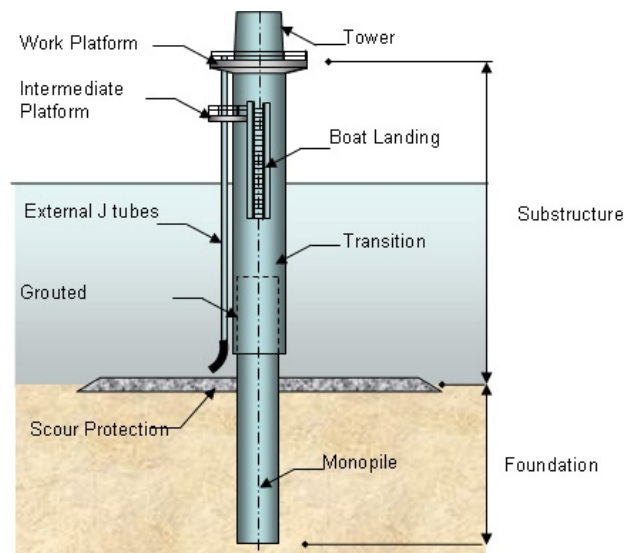


Figure 1.2. Monopile foundation and substructure [9]

Other monopile concepts include:

Concrete monopile: this concept was developed by Ballast Nedam and MT Piling [10]. Because the pile cannot be driven, the foundation is placed by drilling, first inside and then below the prefabricated concrete monopile. The main advantage over the steel monopile is the lower concrete price, which is less dependent on the market changes than the steel.

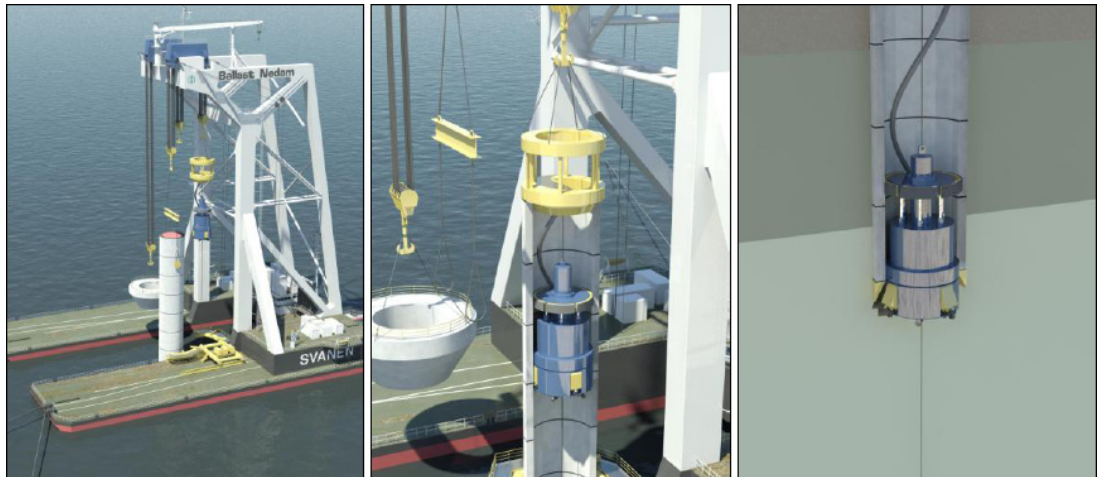


Figure 1.3. Drilled Concrete Monopile Concept [10]

Compliant monopile: basically it is based on the same concept as the monopile, but on the contrary to most of the fixed structures where the first natural frequency is designed to be above wave frequencies to avoid resonance, in this case, the intention is opposite. A very soft structure is created with smaller diameter and thickness. In practice it has only been used in oil & gas industry, as the wind interaction at low frequencies poses many problems and the second natural frequency can coincide with high energy wave frequencies.

- Tripod

It consists of three relatively slender braces that support the main pile from the wind turbine tower and connect it to the seabed by piles. On the contrary to the monopile, the force is transferred to the soil axially by a “push and pull” system.

Braces can be symmetrically placed around the central pile (Center Column Tripod) or the central pile can be lengthened into the seabed and two off-centred

braces added on one side (Flat Faced Tripod). This could simplify the fabrication process, reducing the amount of scaffolding required and the fabrication costs, though increasing the total weight [11]. Comparison of both designs was presented in [12].

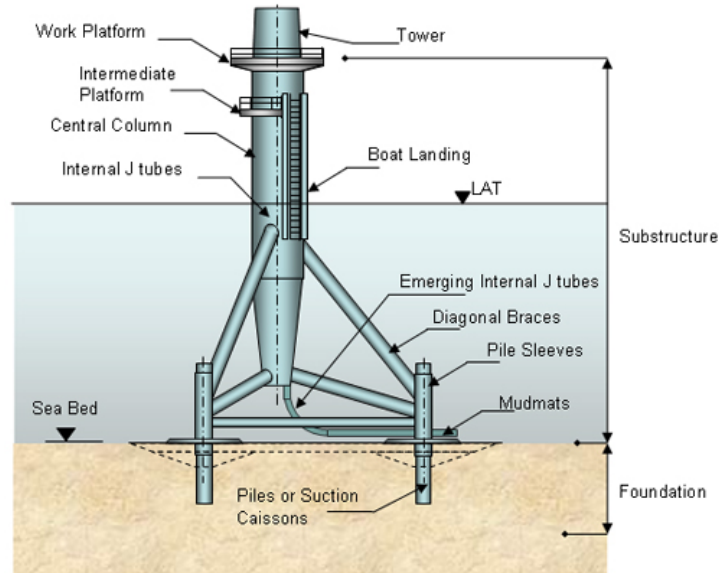


Figure 1.4. Center Column Tripod Substructure [9]

Similarly, the tripile [13] relies on three vertical legs that transfer the loads from the tower to the soil. In this case though, the embedded piles are not connected to the substructure in the seabed but at the mean sea level, just like in the monopod case.



Figure 1.5. Bard Tripile substructure [14]

These substructures are more labour costing than the monopile with higher weights, but can be installed in deeper waters and are less sensitive to wave loading.

- Tetrapod

It is composed of four legs relying on the same “push and pull” method as the tripod so that the soil is mainly loaded in the axial direction. The only installed tetrapod so far, is the jacket type (in Beatrice [15], Alpha Ventus and Ormonde OWFs), which consists of four legs connected by slender braces, creating a highly transparent lattice structure that reduces wave loading significantly.

Fabrication is labour intensive due to the high quantity of connection nodes to be welded. Similarly to the tripod, it needs longer installation time for positioning and the structure is more difficult to handle logistically.

The jacket seems to be a promising foundation type to fulfil the needs of the future offshore locations.

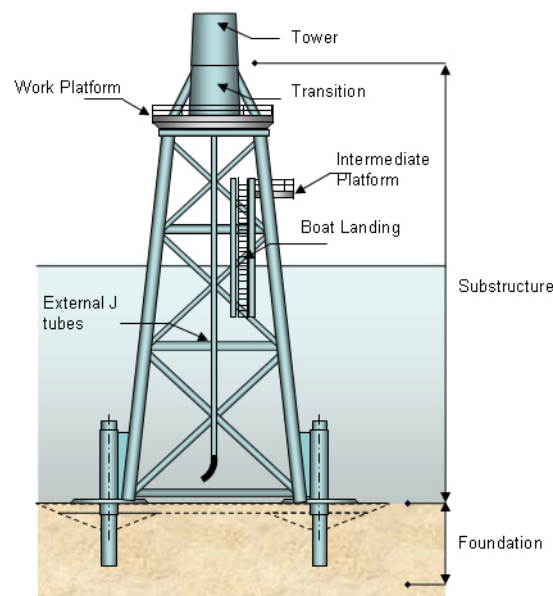


Figure 1.6. Jacket substructure [9]

New designs include the twisted jacket by Keystone Engineering which simplifies installation and decreases total weight by a new concept that consists on a central wider pile and three inclined slenderer legs [16].

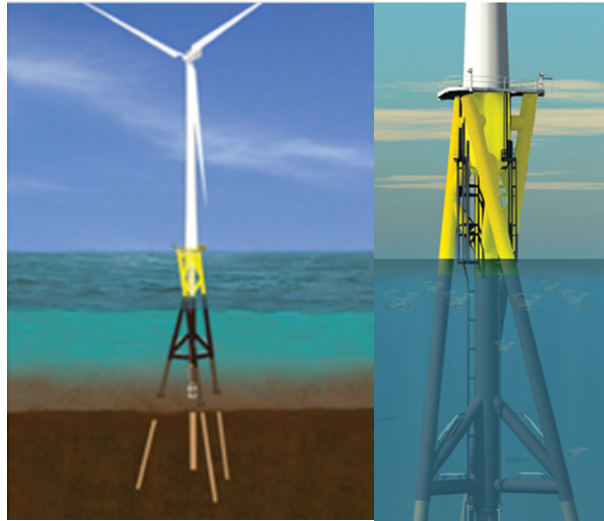


Figure 1.7. Twisted Jacket Concept from Keystone Engineering [16]

#### *1.4.4.1.2 Suction can based foundations*

A large steel cylinder with the open end towards the seabed is sunk and penetrates into the soil by its own weight. Then water is pumped out from the hollow inner volume which creates a negative pressure inside. This, added to the outer water pressure, sucks the can down driving the foundation into the seabed.

Just like the piled based foundations, they can be divided in monopods, tripods or tetrapods substructures depending on the number of anchors that the structure relies on [17]. They are relatively cheap due to lower material usage (compared with their piled founded counterparts) and simpler installation process, but are more dependent on soil conditions (for sand and soft clays) and therefore more prone to be scour protected.

Tests have undergone to prove its viability for offshore wind turbines [18], [19], [20], but it is not still a proven foundation method. However, the recent experience of a monopod met mast installation in Horns Rev 2 [21] and the fact that two of the Carbon Trust foundation competition finalist are a monopod and a tripod [22] type bucket foundation, evidence that this technology could become a reality in the future.



Figure 1.8. The monopod and tripod suction caisson based foundations [23]

#### 1.4.4.1.3 Gravity based foundations

It consists of a huge concrete shell that is filled with cheap ballast in order to obtain a low centre of gravity and a large base that can withstand the overturning moment of the turbine and loads. It can be equipped with skirts, that is, vertical walls that protrude below the base, thus increasing shear resistance and helping to avoid scour below the base. The loading forces are being absorbed by the immense deadweight that the soil has to be able to withstand. For this reason, the soil plays an important role and liquefaction beneath the base is an issue that must be addressed.



Figure 1.9. Shallow water (to the left) and deep water (to the right) gravity based foundations [14]



The use of concrete as the main material means lower fabrication costs when compared to steel structures, especially if the investment costs are spread out on a large number of foundations. On the contrary, it needs the preparation of the seabed before installation and scour protection afterwards, which increases the installation costs.

It is a proven technology in shallow waters [24], [25], but new improved designs aim to install these foundations even in deep waters [26], [27]. This has derived in hybrid substructures, in which the cylinder part is made of steel in order to withstand the higher stresses while reducing the hydrodynamic wave loads with smaller diameters (see [28] as an example). Besides, as the transportation of deep GBS structures in vessels is not viable due to their huge weight, they are designed as self floating.

#### 1.4.4.1.4 *Guyed tower*

Even though the basic concept for fixing the sub-structure to the seabed relies in the previously explained foundation technologies, the guyed tower has some differences when compared to the previous cases. The tower of the turbine is lengthened down to the mudline where a small base gives the necessary footprint for withstanding the vertical loading, while the main lateral forces rely on lead guy lines, anchored to the seabed, and fender lines [29].

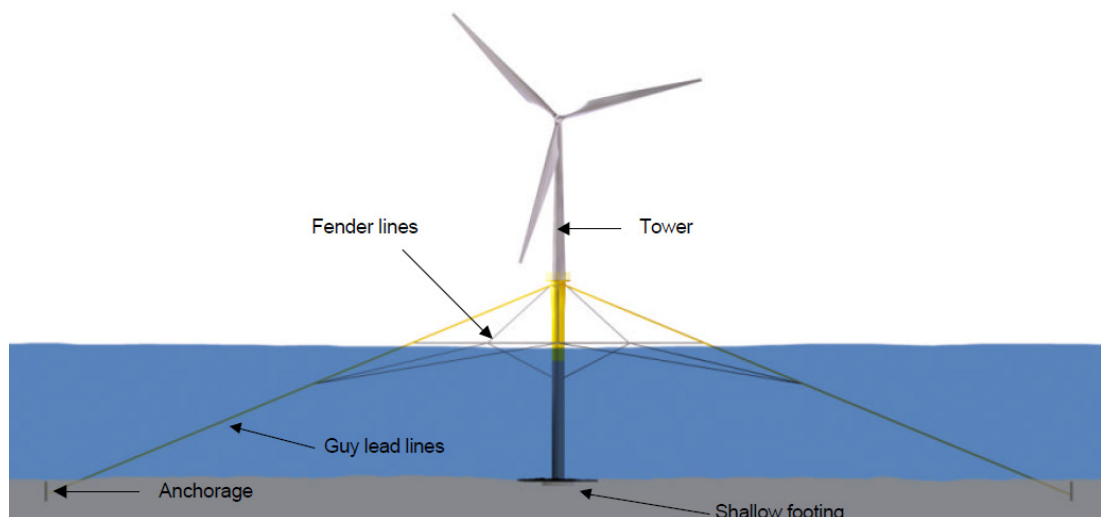


Figure 1.10. Guyed Tower Structure [30]

The fabrication is simplified and the weight of the structure decreased, however, installation of the guyed tower is rather complex and needs accurate positioning. Besides, the guy lines need periodical re-tensioning and inspection to assure the stability over time. Even though there is experience in the oil & gas industry, it has not been proven for the wind industry.

#### 1.4.4.2 Floating sub-structures

The idea is to place a floating substructure near the water surface and attach it to the seabed by several anchor lines that can be either catenary or taut. The loads are transferred through the wires to the anchors which can be driven piles, suction cans or gravity based. They usually require a minimum depth so the technology can be applied.

They are categorised based on the physical principle or strategy that is used to achieve static stability (see

Figure 1.1): ballast, mooring line or buoyancy. Advantages and disadvantages of each method are explained in [31]. In practice all floating concepts are hybrid designs in more or less extent.

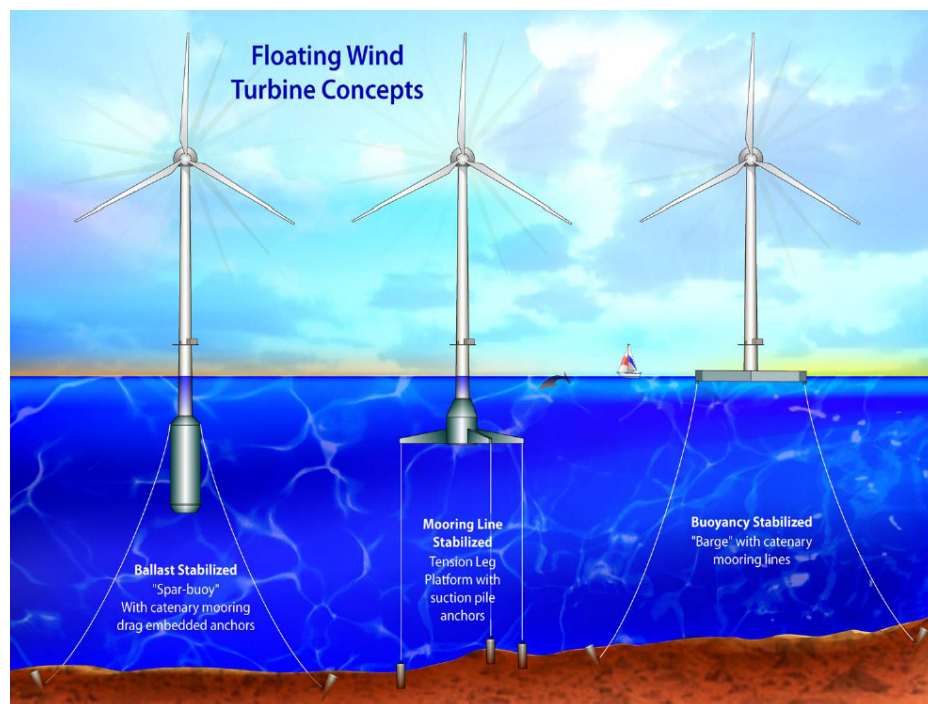


Figure 1.11. Floating platform types according to the used stability method [32]

In general, they provide less stability, but at high depths, it is the only feasible technology that can be cost effective, due to the high steel quantity that their fixed counterparts would need. Even though they are not commercially available at the moment, in the medium term floating substructures might see a breakthrough.

There are three main concepts in development at different stages.

#### *1.4.4.2.1 Spar type*

It consists of a long and slender hollow cylinder with soft and hard tanks. It uses ballast to ensure that centre of gravity is below centre of buoyancy and hence keep wind turbine stable. The soft and hard tanks are filled with sea water and rocks respectively. It has good heave performance but a big pitch and roll motion.

First full-scale prototype was installed in Norway in 2009 by Statoil [33]. Similarly, a downwind wind turbine concept is also being developed by Sway [34].



Figure 1.12. Spar type floating wind turbine [35]

#### *1.4.4.2.2 Semi-submersible type*

It mainly consists of columns, a truss structure, mooring lines and anchor basis. It depends on balance between gravity, buoyancy and mooring lines to ensure the stability. It has a shallow draft and good operational and transit stability.

Feasibility studies have been carried out for a trifoater design [36] and there is also a patented side towered variation by Principle Power (the WindFloat [37]), in which

water entrapment (heave) plates at the base of each column improves the motion performance.



Figure 1.13. WindFloat floating wind turbine concept [37]

#### 1.4.4.2.3 TLP type

The tension leg platform is tethered to the seabed by permanently tensioned cables (tendons) by the uplift created by the hollow platform. It has good heave and rotational motions but complex mooring system.

Blue H installed a demonstrator in 2008, which has lead to the patented “Submerged Deepwater Platform” [38]. In this case, the buoyant body is connected to a counterweight which lies on the sea bottom.

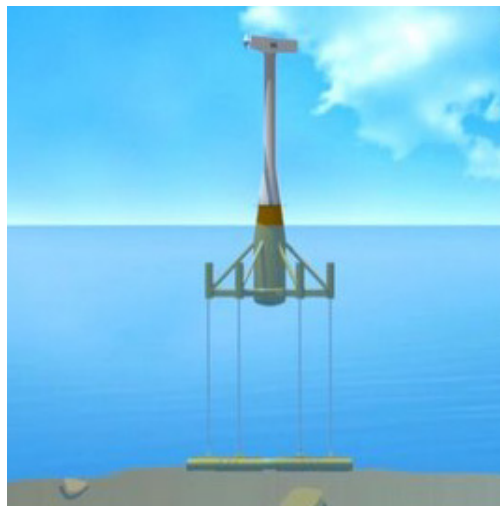


Figure 1.14. Blue H floating wind turbine concept [35]

### 1.4.4.3 Comparison of the different substructures

A summary of the main substructures is presented in Table 1.1 comparing different important issues that have to be addressed when deciding the support concept for a wind turbine in a certain location. The given descriptions and values are just general as in reality each project is unique and should always be studied in particular. Sand and clay soil types have been covered, however if rock or chalk soils are to be considered the results may be different.

	Monopile	Tripod/ Tripile	Jacket	Shallow GBS	Deep GBS crane-free	Monopod bucket	tripod bucket	Floating
State of the art	mature	prototype	pre-serial	mature	not tested	Demonstrator	not tested	Demonstrator
Manufacturing complexity	Low	Moderate	Moderate	On site	On site	Low	Moderate	Low
Transportation complexity	Moderate	Moderate	Moderate	High	Moderate	Moderate	Moderate	Low
Installation complexity	Moderate	Moderate -High	Moderate -High	High	Moderate	Moderate	Moderate	Low
Scour Protection need	Moderate	Low	Low	Very high	Very High	Moderate	Moderate	Low
Decommissioning complexity	Moderate	High	High	Moderate	Low- Moderate	Low	Low	Low
Dependency on soil conditions	High	Low	Low	High	Very High	High	Moderate	Low
Dependency on hydrodynamic conditions	High	Moderate	Low	Moderate	High	High	Moderate	Moderate
Dependency on WTG loads	High	Moderate	Low	Low	Low	High	Moderate	High
Self-weight	Moderate	High	High	High	Very high	Low	High	High
Depth application	< 30 m	25 - 40 m	30 - 60 m	< 20 m	30 - 60 m	< 20 m	25 - 40 m	>80 m

Table 1.1. Comparison of different substructure types for offshore wind turbines

## **2 OFFSHORE SUPPORT STRUCTURES COSTS. EXPERIENCED BASED ANALYSIS**

### **2.1 Introduction**

When looking into the absolute costs of the offshore support structures many difficulties are encountered due to the limited publicly available data. Even when this data is available, different sources have been found to disagree in the values in considerable amount (as an example [39] and [40]). Furthermore, when dividing these costs into different key offshore wind components and their contribution in the overall capital and operating expenditure of a project, the information is scarcer and less reliable. For all these reasons, caution is advised when making conclusions. Unique nature of each project and the fast development and changing economics of the offshore market due to the wide range of factors affecting the project initial budget prevents from concluding absolute values for each component or operation type.

Hence, the aim of this preliminary analysis is to obtain a simple tool for shaping the offshore market costs and get an idea of the cost drivers from the support structure's point of view by analysing real offshore wind farms projects data.

### **2.2 Analysis of all support structures.**

The main source for the data compilation was [40]. 37 European offshore wind farms, 17 of them from the UK, projected from 2002 to 2010, were included in this study. Previous offshore experience was discarded for considering it too outdated, which would just add uncertainty in the final results reliability. A table containing detailed information from already commissioned and under construction offshore wind farms is included in the Appendix A.

The first conclusion that can be extracted from Diagram 2.1 is that the monopile is clearly the main support structure installed so far (23 OWF out of 37), followed by the gravity base structures (8 OWF out of 37). In absolute numbers, the monopile is the undisputed preferred substructure with an extended experience (over 1000 installations) and second the GBS (over 150). The rest of the substructures (jacket, tripod and bucket) are novel or prototype projects that are looking into expanding offshore wind energy into deeper waters. In fact, none of the monopile have been installed in waters deeper than around 20-25 m and none of the GBS foundations above 15 m depth, which gives an idea of the current technology limitations (only in shallow waters) and the constraints that the industry is facing.

The second conclusion is that the stated total costs for the whole project strongly varies from site to site which reflects the difficulties of averaging offshore costs. In order to understand how different factors determine this final cost, a more detailed analysis of individual variables is carried out.

### Foundation vs water depth vs specific cost

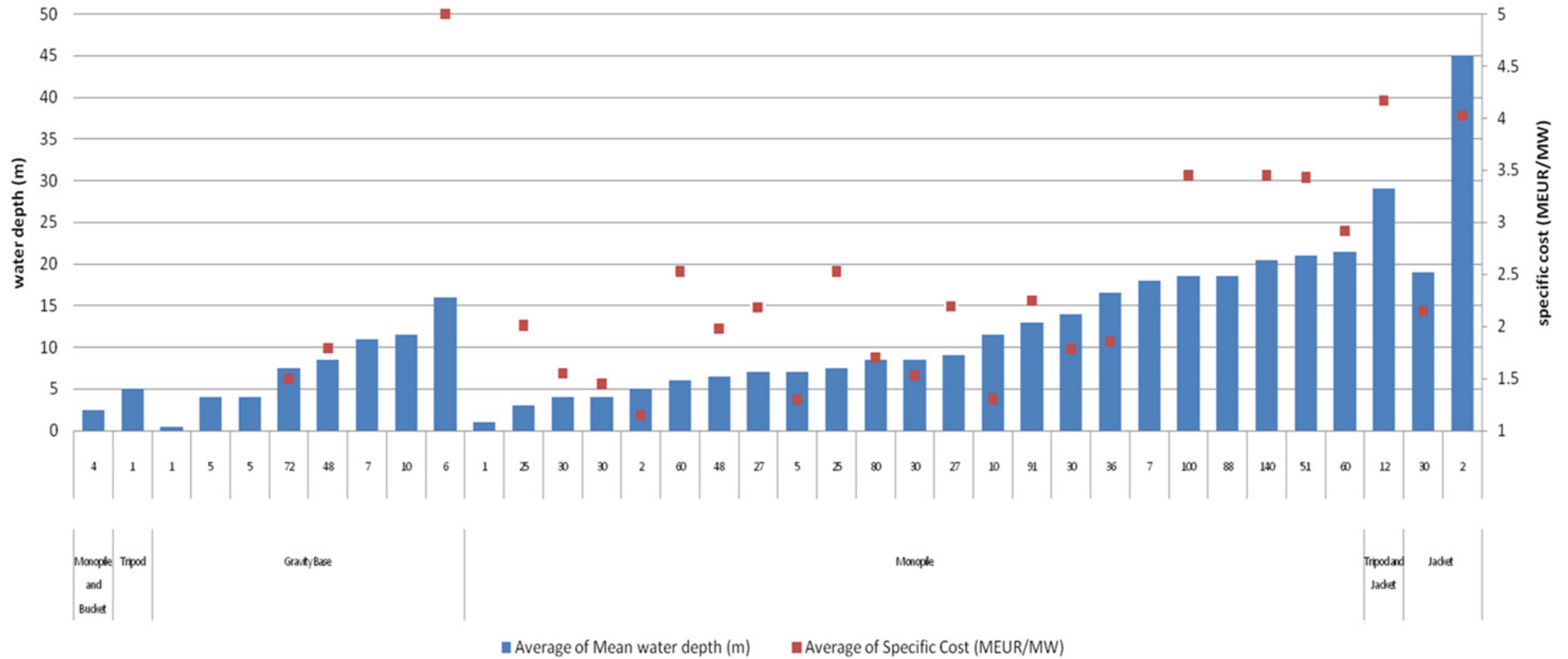


Diagram 2.1 Specific cost, water depth and number of installed OWTG in different OWFs for several substructure types



## 2.2.1 Water depth vs specific cost

As it can be seen in Diagram 2.2, overall, a logical pattern is followed by the analysed values, increasing the total costs of the projects the deeper the water depth of the site.

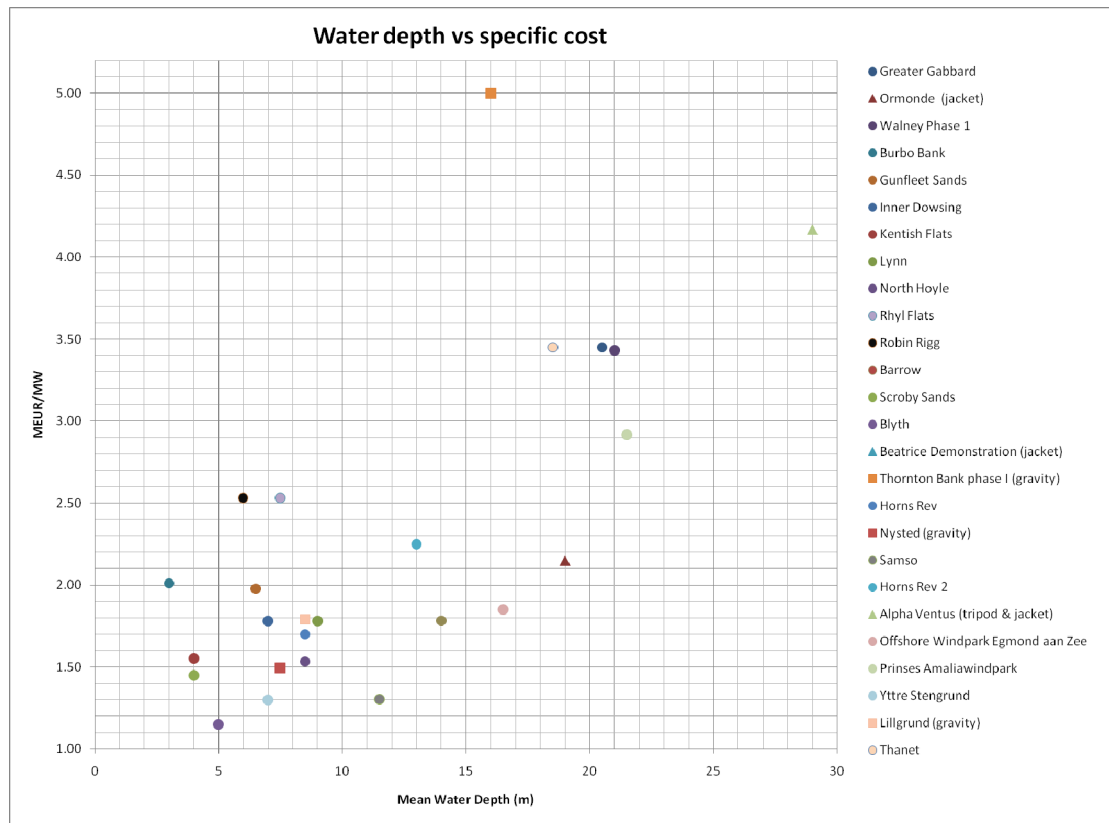


Diagram 2.2 Water depth vs specific cost for different OWF

As previously stated, construction in deeper waters brings higher manufacturing and installation costs, due to higher loading of the OWTG (from the expected harsher environmental conditions and longer structures under these loads), the added costs for vessels capable of handling heavier structures and the increased installation time that this means. Implicitly, deeper waters usually also mean longer distance to shore which affects the costs as it will be explained later.

Most of the projects so far, have been undertaken in less than 15 m water depths, but this is just the beginning of an industry that is moving fast to deeper locations.

## 2.2.2 Distance to shore vs specific cost

The distance to shore mainly affects the installation costs, increasing them due to the higher transportation times needed from the logistic port to the construction site (see Diagram 2.3). On the other hand, the implicit variable would be that further from shore the depth usually increases which also affects the total budget as previously stated.

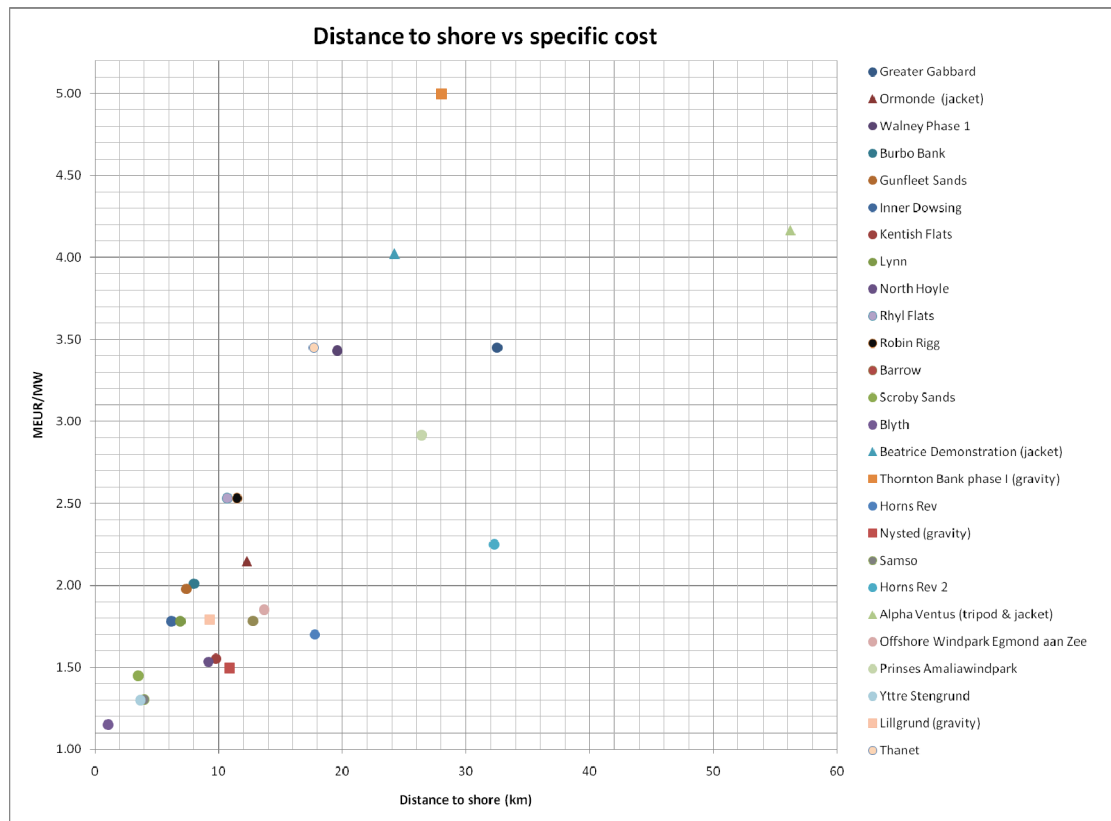


Diagram 2.3 Distance to shore vs specific cost for different OWF

## 2.2.3 OWTG number vs specific cost

No clear pattern is obtained from Diagram 2.4. It seems logical that increasing the OWTG would lead to a decrease in the total cost per MW, due to the lower specific cost of fixed costs and the lower installation time related to the increasing learning curve during the installation process. However, the particular characteristics of each

OWF project could somehow disguise this tendency. Furthermore, bigger projects have often to deal with bigger setbacks during its execution.

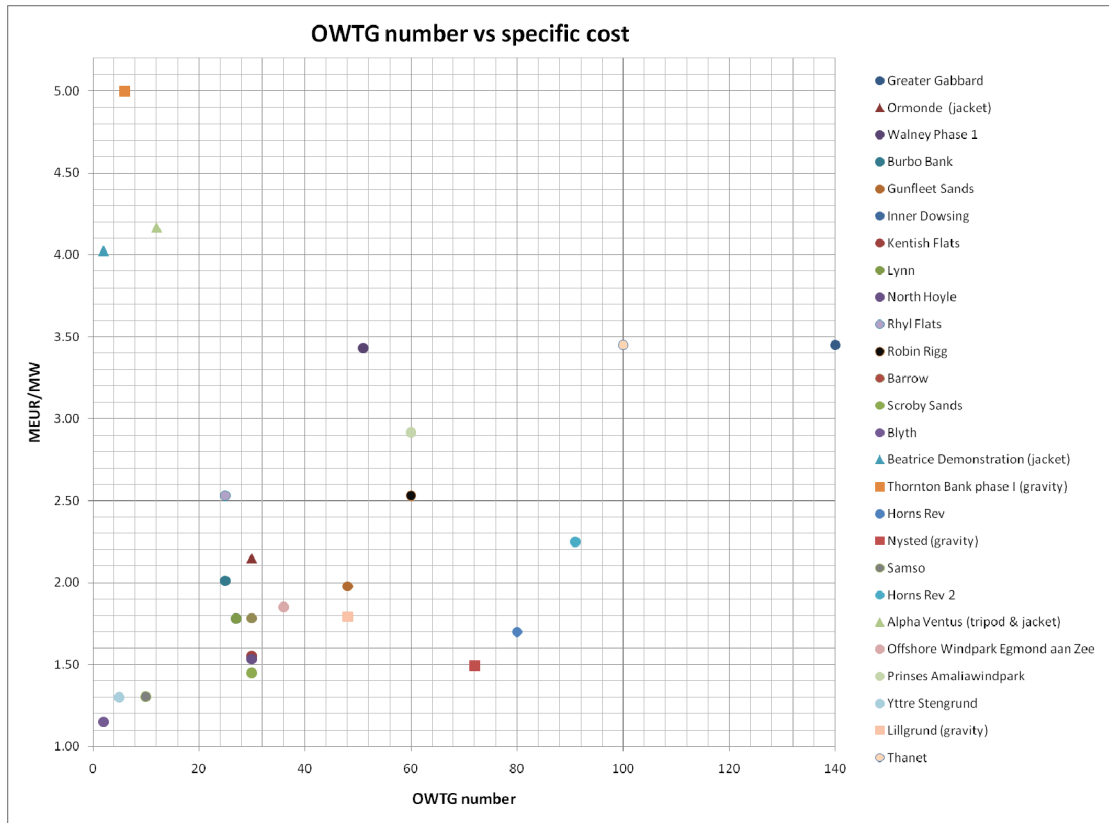


Diagram 2.4. OWTG number vs specific cost for different OWF

## 2.2.4 OWTG power vs specific cost

The tendency showed in Diagram 2.5 seems to be that the higher the OWTG power, the cost is increased. Different reasons can be the cause of this, which are explained by Diagram 2.6, in which power and specific cost of the project is represented for several monopile supported OWFs commissioned at different years.

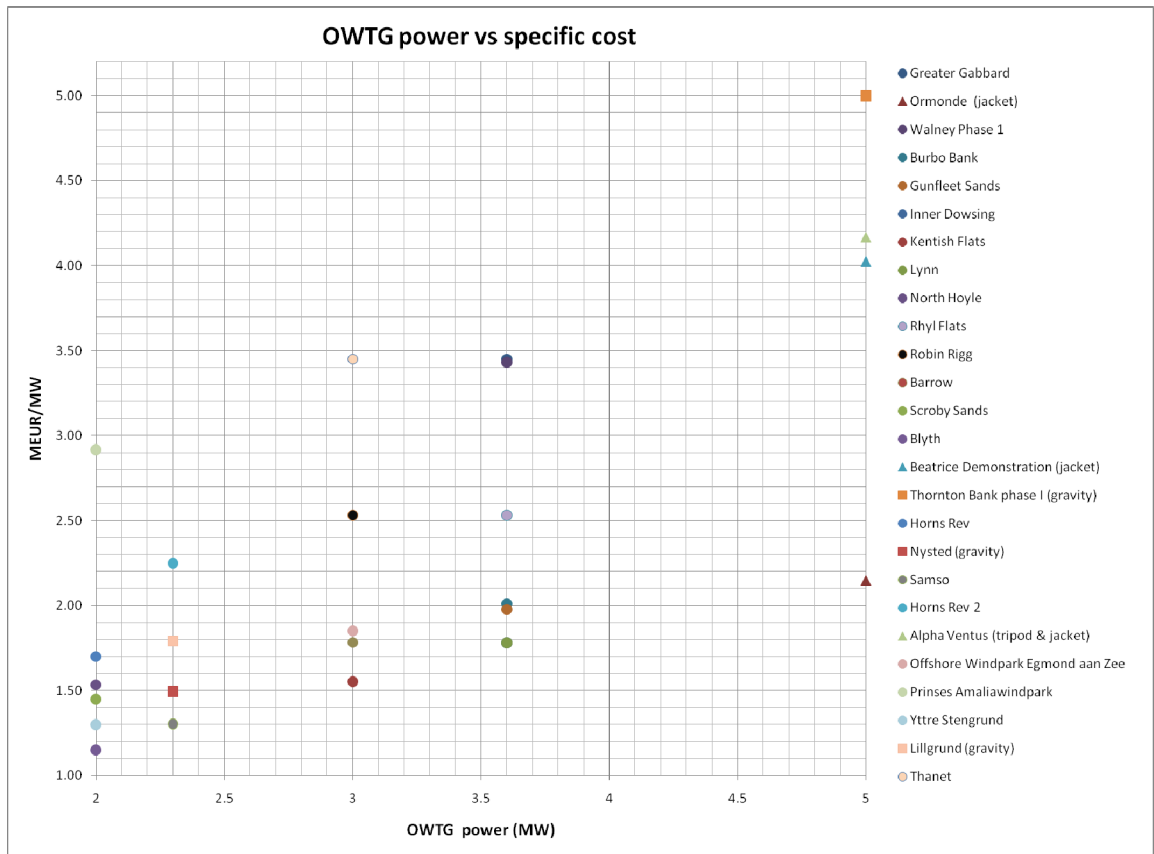


Diagram 2.5 OWTG power vs specific cost for different OWF

After careful analysis of Diagram 2.6, it can be concluded that the highest power projects which are the most recent ones, are in fact more expensive (averaging 2.5 to 3.5 M€/MW) than the small-medium older projects (averaging 1.5 to 2 M€/MW). This is logical as stated in the previous section and agrees with values given in [41]. Moreover, these more recent bigger size and power projects had to deal with many constraints that increased the specific cost, especially since 2006 [4], [6]. Main ones are listed hereafter:

- Supply chain constraints. Given the offshore projects increase in the last years and the relatively small number of OWTG manufacturers (mainly Vestas and Siemens have dominated the whole market), it could be that competitiveness is not yet strong. In addition, the offshore market is in competition with the onshore one, which was also in short supply of some

components during this period. Similarly, installation costs have also risen due to the constraints on the availability of installation vessel and services.

- Level of investment for Research & Development and production capacity expansion. These investments necessary for the supply chain in the last years could be reflected in the WTG prices.
- Rapid rise of steel prices between 2006 and 2008, which strongly affects foundation and substructure costs.
- Copper prices rise, which mainly affect cable costs that account up to the 10% of the total project cost [42].

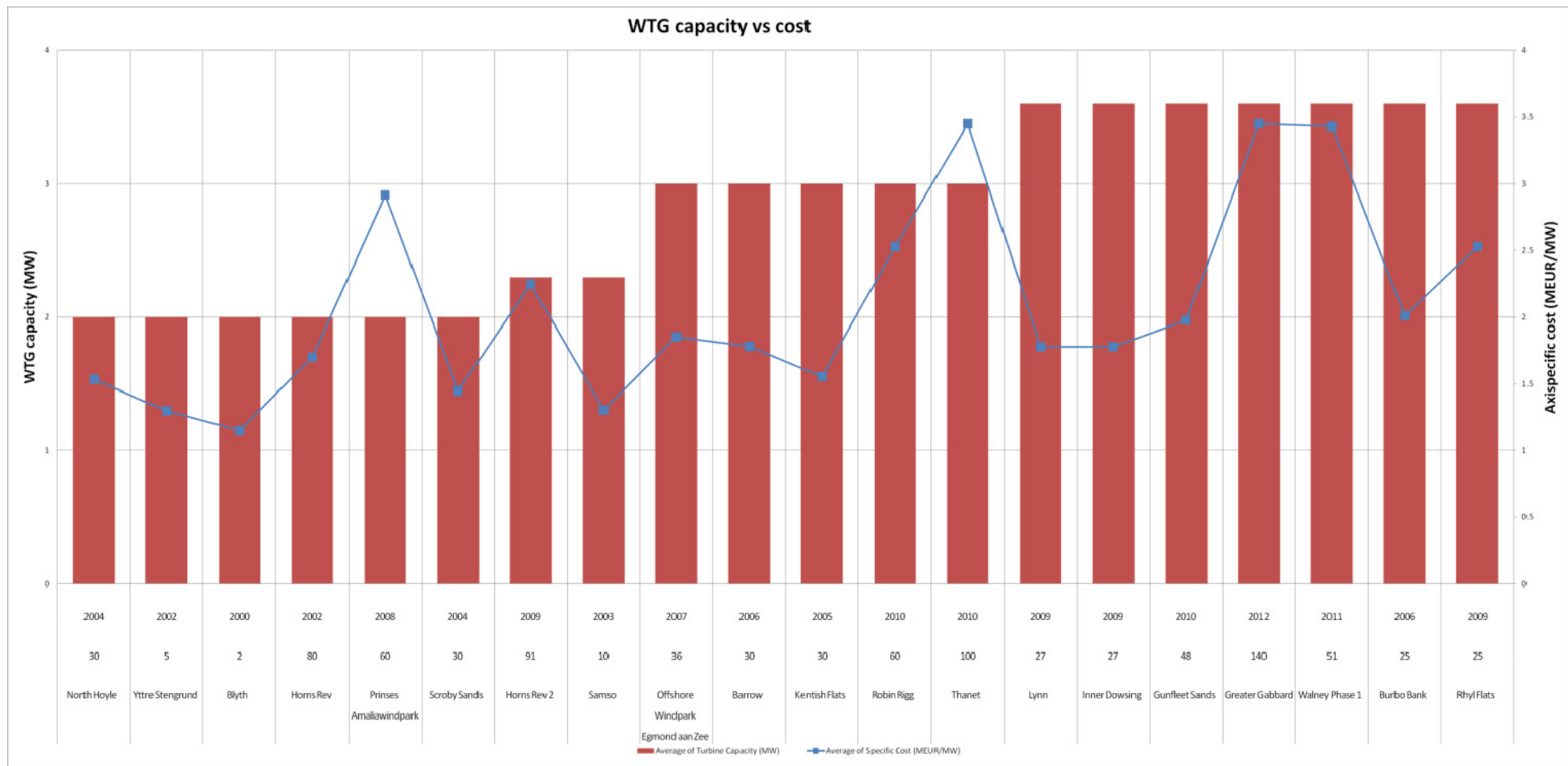


Diagram 2.6 OWTG power (in columns) and specific cost (in line) for different monopile supported OWF

If all the previous reasons are taken into account and we add other reasons like the inflation rate and the fact that the most recent projects have been undertaken in deeper waters, further from shore, it could be considered that overall, the costs have maintained, as shown in Diagram 2.7 from [43].

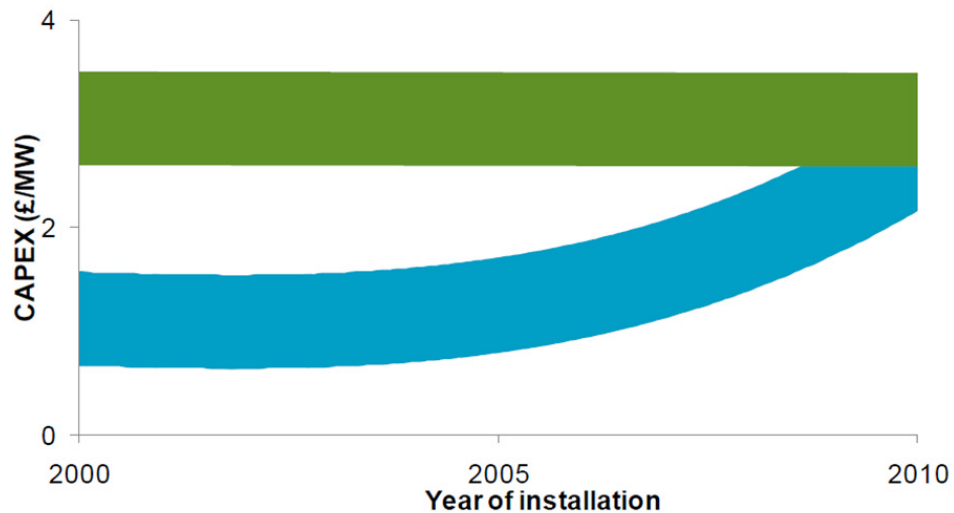


Diagram 2.7 CAPEX level in the last decade in absolute value (blue) and taking into account the different constraints (green) [43].

## 2.2.5 Conclusions

Based in the last decade offshore experience, how different variables affect the total OWF project cost and consequently the support structure costs have been assessed. The complexity and interrelation of different factors such as, water depth, distance to shore, OWTG number and OWTG power has been demonstrated.

There are just a couple of projects with full available costs data of the GBS foundations. On the other hand, tripod, jackets and bucket substructures have barely been installed (one or two OWF, mostly prototypes). In the next years, more OWF are expected to be constructed using this technology, but currently just suppositions can be made.

This lack of experience prevents any conclusion to be made about any support structure type except the monopile, which has been the preferred among all, followed

by the GBS. Overall, the monopile is the chosen substructure in shallow and sheltered waters due to its simplicity in design, manufacturing and installation, which results in more economical structures.

Taking this into account and in order to increase the reliability of the results, a more thorough study is carried out based only on the experience of monopile supported OWFs.

## 2.3 Monopile substructure

### 2.3.1 Multiple regression analysis

The following cost analysis was carried out using the data of 19 OWF that used the monopile for supporting their turbines and commissioned or to be commissioned from 2000 to 2012. Some of the available main factors that drive the total cost of the project budget were included in this study. The data, obtained from [40], and summarised in

Table 2.1, was used in a linear multiple regression analysis. With this analysis, a simple equation that showed the weight of each driving factor was sought.

Wind Farm Name	Number of Turbines	Turbine Capacity (MW)	Shore Distance (km)	Year Online	Total cable length (km)	Mean water depth (m)	Specific Cost (MEUR/MW)
Walney Phase 1	51	3.6	19.6	2011	89	21	3.43
Burbo Bank	25	3.6	8	2006	40	3	2.01
Gunfleet Sands	48	3.6	7.4	2010	43.3	6.5	1.98
Inner Dowsing	27	3.6	6.2	2009	26	7	1.78
Kentish Flats	30	3	9.8	2005	30.8	4	1.55
Lynn	27	3.6	6.9	2009	26	9	1.78
North Hoyle	30	2	9.2	2004	34	8.5	1.53
Rhyl Flats	25	3.6	10.7	2009	29	7.5	2.53
Robin Rigg	60	3	11.5	2010	44.5	6	2.53
Thanet	100	3	17.7	2010	101.3	18.5	3.45
Barrow	30	3	12.8	2006	48	14	1.78
Scroby Sands	30	2	3.5	2004	21.3	4	1.45
Horns Rev 2	91	2.3	32.3	2009	70	13	2.25
Offshore Windpark Egmond aan Zee	36	3	13.7	2007	45	16.5	1.85
Prinses Amaliawindpark	60	2	26.4	2008	73	21.5	2.92
Belwind Phase I	55	3	52	2010	90	41	3.76
Blyth	2	2	1.1	2000	1.5	5	1.15
Greater Gabbard	140	3.6	32.5	2012	245.5	20.5	3.45
Blyth	2	2	1.1	2000	1.5	5	1.15



Table 2.1. Data summary for the multiple regression analysis

The results of the multiple regression analysis were assessed based on 3 conditions that had to be fulfilled.

- $R^2 > 85\%$ . Percentage of the costs variation that the equation explains.
- $|t| > 1$ . If the factor being analysed is driving the output characteristic, then  $|t|$ , the statistical absolute value must be above 1.
- $p < 0.05$ . The p value must smaller than 0.05 in order to obtain a minimum 95% confidence result.

Several multiple analyses were carried out, mixing different inputs and the output, which in this case is the specific CAPEX cost. Among all the input parameters the ones that fulfilled all these requirements are described hereafter:

- Year online. This factor will give the influence for the inflation along with the steel and copper price increase. Besides, it will also include the supply chain constraints that worsened in the last years.
- Water depth. It will include the influence of the monopile design dimensions in the total cost. The deeper the water, the monopile will be heavier and thus more costly.
- Total Cable length: this length, which includes the total infield and export cable length, gives an idea of the number of OWTGs (infield length) and the shore distance (export length) apart from the valuable total cable cost that means up to 10% of the project cost [42].

The only factor that does not seem to be included in the equation in a direct or indirect way is the turbine power. Actually, as it was explained in the previous section, the turbine power has not an easy to assess influence in the final cost. It was

found difficult to reliably extract its sole impact in the cost from such a small studied population under the influence of so many factors.

The obtained equation is thus summarised as follows:

$$\text{CAPEX (M€/MW)} = -231.43 + 0.116 \cdot \text{Year} + 0.01 \cdot \text{Total Cable (km)} + 0.035 \cdot \text{Depth (m)}$$

This equation has an average residual value of 11.5%. In

Diagram 2.8 and

Diagram 2.9, the predicted and the actual total costs are compared for different cable lengths and water depths for the year 2010.

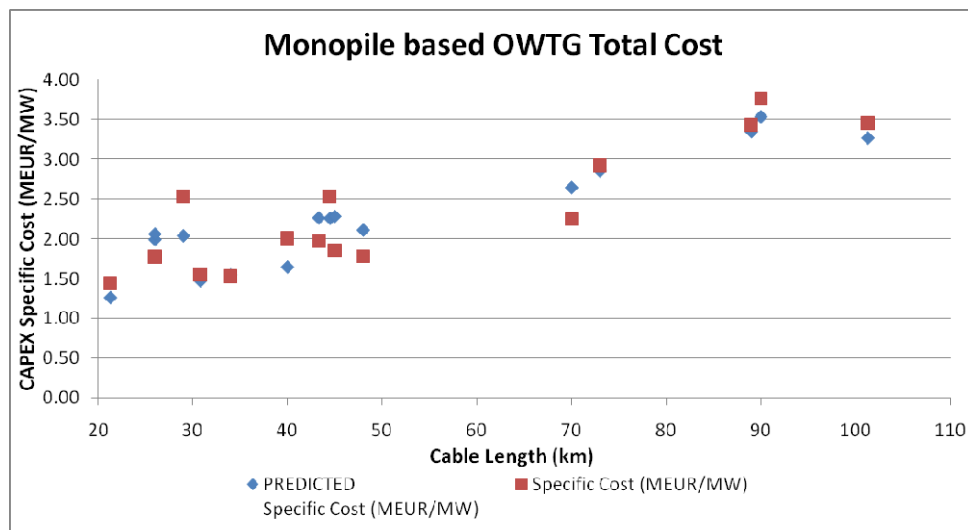


Diagram 2.8 Multiple regression predicted and actual costs of a monopile supported OWTG for the year 2010 at different cable lengths

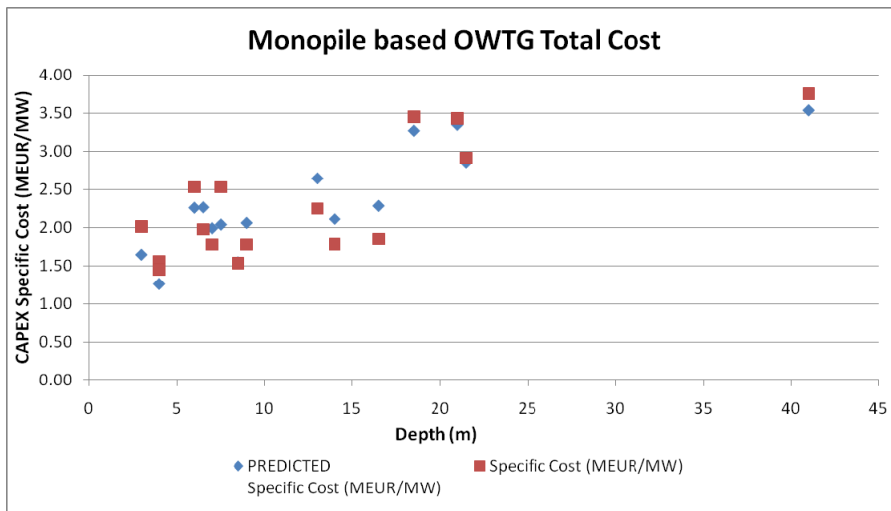


Diagram 2.9 Multiple regression predicted and actual costs of a monopile supported OWTG for the year 2010 at different water depths.

A 3D graph can be plotted from this equation as shown in

Diagram 2.10, in which the current construction sites are marked. This area, which is in the 20-25 m water depth and 50-70 km cable length range, give a total CAPEX of 2.8-3.2 M€/MW. This value is very similar to other recently published values that established the current cost at 3 M€/MW [43], 3.2 M€/MW [4], or 3-4 M€/MW [41].

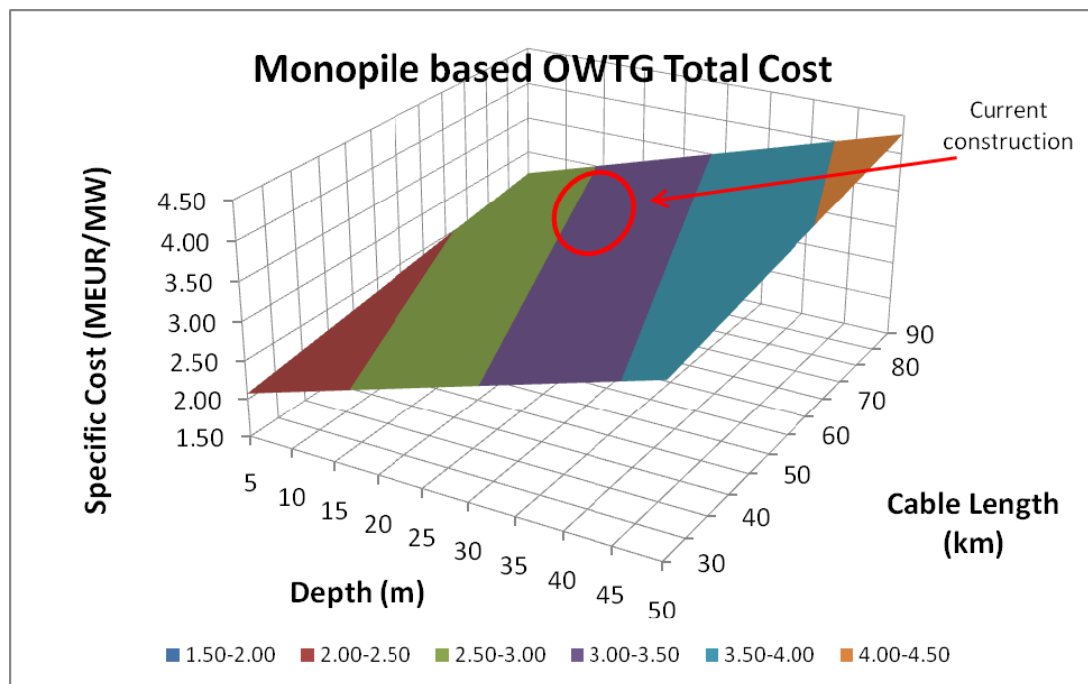


Diagram 2.10 Specific cost of monopile supported OWTG vs water depth and cable length for the year 2010

### **2.3.2 Conclusions**

A multiple regression analysis was undertaken for different design factors of 19 monopile based OWFs with the aim of obtaining a simple cost driving equation for the monopile and a better understanding of their influence.

From the obtained equation and its slopes, it can be concluded that if the year and the factors that it includes (inflation, steel and copper price increase...) are not taken into account, water depth is the input that bigger impact has in the final cost, affecting both manufacturing and installation costs.

This explains why until now the water depth range has increased slowly in the last 10 years. Most recent and deepest OWF are 20-25 m water depth, but most of the current experience is below 15 m (see Diagram 2.2).

This equation can be roughly used for the monopile costs calculation, estimating that it represents 22 to 25 % of the total cost [4], [5], [6], [7]. This assumption would indicate that currently the monopile cost is in the 0.6-0.8 M€/MW range.

## **3 OFFSHORE SUPPORT STRUCTURES COSTS. NUMERICAL ANALYSIS**

### **3.1 Introduction**

As previously stated, offshore support structure accounts for almost a fourth of the total CAPEX cost of an OWF [4], [5], [6], [7], and it is of vital importance to choose the most economical design for each location

If the profitability of the project is to be maximised, a deep interrelation study of the main inputs encountered when designing, manufacturing, installing, operating, maintaining and decommissioning an offshore support structure is needed.

However, the scarce available public data mainly accounts for the whole project budget and just gives rough ideas of the entire project cost drivers as demonstrated in the section before. Furthermore, the current experience does not give much data about other substructure rather than the monopile.

All this prevents reliable conclusions to be made about each support structure and deciding the most economical choice for specific sites becomes rather uncertain. It is necessary to assess and understand the costs from the very initial driver factors if a sensible decision is to be made.

The two substructures with the highest future installation potential in the midterm are selected for study. According to the experienced based study from chapter two, the monopile is the leading and most mature technology among all, and therefore will continue to be the preferred option whenever is possible to be installed.

On the other hand, UK and Germany, the European leading countries in the development of offshore wind, will be facing unprecedented site characteristics both

in the British Round 3 and the recently approved German windparks [44], further from shore and in deeper and harsher waters.

The jacket seems to be the most promising substructure in order to fulfil most of these new requirements and it is expected to take the biggest market share among all other support structures (60% of the UK market according to [45]).

In [12], the tripod and quadrapod were compared and the results showed a better general performance for the jacket type substructure, also obtaining lighter total weights as stated in [46]. After a thorough study of different available technologies (see [11]) the jacket was also the chosen substructure for the Beatrice project, which has a similar water depth (45 m) and environmental conditions to many offshore windfarms to be developed in the next decade.

Regarding the foundation type for the jacket substructure, two alternatives are being used, piles and suction buckets. Steel piles are more common as suction buckets have only been used for some Oil & Gas projects and research regarding its applicability for offshore wind turbines is currently being conducted. So far, the stability under high cyclic tensile loading could not be demonstrated sufficiently. Furthermore, scour protection is an issue for suction buckets which is normally not required in the case of piles.

For all these reasons, both the monopile and the jacket are chosen to be studied in detail with a numerical tool that enables the design and then the cost calculation of these substructures in different conditions.

This new tool can provide a clear objective influence of the main designing drivers of an OWF for a wide range of locations that will be assessed by water depth, soil type and wave height. All these inputs that compose some of the key factors of an OWF design are related to different WTG powers, thus enabling the selection of the most suitable and economical choice for each particular case.

Details of the developed cost model are explained in the following section.

## 3.2 Cost Method for OWTG's support structures

A simplification of all the variables affecting the OWTG support structure design is required for a straightforward analysis and understanding of its costs. The whole process is reduced to 4 main parameters that mostly drive the design and therefore the costs of an OWTG support structure: water depth, wave height, soil type and WTG power.

As it has been described in the previous sections, water depth is the primary factor. Higher depths mean bigger and heavier substructures and foundations, thus more costly manufacturing and installations costs.

Another big challenge for the wind industry when moving from onshore to OWFs, is the fact of having to deal with the hydrodynamic loading. Wave loads became a key designing issue in offshore structures. Low, medium and large wave heights are studied, represented by their significant wave ( $H_s$ ), that is, the average height of the highest one third of the waves, within a 3 hour sea state. Hence,  $H_s=4$  m,  $H_s=7$  m and  $H_s=12$  m are the 3 analysed sea states, representing low, medium and high wave loading respectively.

Offshore foundations transfer the structure loads to the soil. It is important to understand how different soil types can affect the final cost of a support structure. 3 different clay types regarded as soft, average and hard were used in the calculations.

WTG power usually established in the FEED stage of the project will mainly affect the support structure design by changes in the nacelle weight and the tower height. These will be essential during the static but especially the dynamic calculation of the structure. Hence, 3 WTG power will be compared, 3.6 MW, 5 MW and 7 MW, which gather the present, the near future and the medium term future of the offshore wind industry development.

Wind loading is not considered as another key factor for the support structure design. A certain WTG is designed for a range of conditions and no big differences are

expected from site to site in mean wind speeds and turbulences. In this case, average values were used for each WTG power.

Distance to shore and installed number of OWTG are two variables considered fixed in this analysis. They have an influence in the total cost (as showed in previous analysis based on experience data), especially regarding the manufacturing and installation of the infield and export cable.

However, regarding the OWTG support structure, the installed number influences the manufacturing costs in a reduced manner, as it is very difficult to set how much the price of the processed steel is reduced depending on the size of the order to the manufacturing company.

Distance to shore on the other hand, will affect installation costs as the transport time can be increased. In spite of this, its influence is not considered a key factor. First of all, it will only account for a very small portion of the total cost (the whole installation of the support structure means around a fourth of its total cost [6]). Secondly, other factors such as transport vessel speed, its operational maximum wave height, mean sea significant wave, and consequently weather downtime, will have a bigger impact in the total transport time.

For these reason distance to shore is considered fixed at 25 km. This is an average value of the UK Round 2 OWF projects. Number of OWTG is set to 100, as an average size.

Having described all the inputs that will be used in the study, Diagram 3.1 shows a schematic overview of the applied cost method.



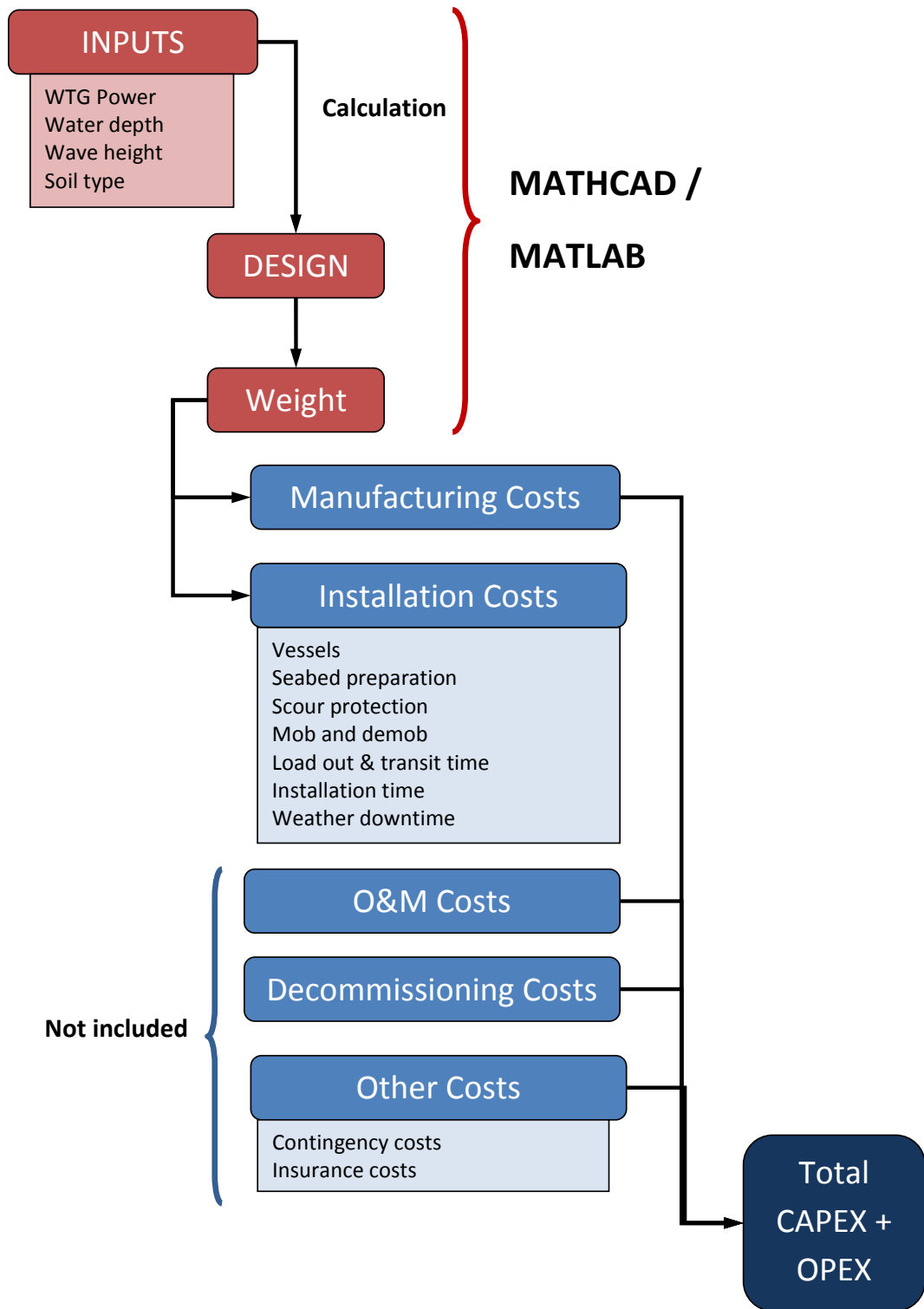


Diagram 3.1 Cost Method Overview for offshore substructures

As it can be seen in the sketch, the method fundamental is an optimum foundation and substructure design according to the input characteristics. The calculation of the

design is carried out by Mathcad software for the monopile and by Matlab software for the jacket, which allows simple modifications of the input values and easy and fast iteration of the design parameters, such as thicknesses, diameters, lengths, etc.

The support structure design gives a total mass, which is the leading parameter for an approximate calculation of manufacturing costs. Besides, the weight and dimensions of the support structure also serves for the installation costs estimation. The installation costs include seabed preparation and scour protection whenever necessary, mob and demob costs, transport vessel hiring costs (which will depend on the load out and transport times) and the Heavy Lift Vessel hiring costs (which will depend on the installation times). Logically, these times will be affected by the weather downtime.

It is important to remark that only the CAPEX costs of the support structure have been included in this study and OPEX costs like the O&M, decommissioning and other associated costs have been excluded. The reasons to do so are explained hereafter.

### **3.2.1 O&M costs**

Currently, the costs of maintaining an offshore wind farm are estimated to be around 25% of the Levelised Production Cost (LPC) [7], [47], [48]. The LPC is the cost of one production (kWh) averaged over the wind power station's entire expected lifetime, expressed in €/ kWh.

With an expected CAPEX reduction in the years to come, this figure could be increased up to a 33% of a lifetime cost. Other sources set the current O&M costs around 70000 €/MW per year [4], which gives a similar overall result.

Nevertheless, these are rough estimations open to discussion and they could strongly vary in the future. The main reasons being:

- Limited operational life of all offshore wind farms to date. This means that there is no experience in the final stage of an OWF life, when the O&M costs are expected to be the highest.

- For the above reason, most of the WTG are still under warranty, which prevents O&M real costs disclosure by the manufacturers.
- This lack of experience also could lead to an underestimation of the initial projects budgeting that is been amended as experience is gained in frequency of parts replacement, accessibility, performance and availability levels, etc. See [49] for further information.
- Evolution of the O&M strategies. Even though historically they were formulated under the assumption of a 20 year project life which enabled limited preventive maintenance usage, this strategy has recently moved towards a more conservative approach seeking to extend project life, as there are lease terms as much as 50 years. Therefore, the current figure of 2-4 days per WTG of yearly planned O&M labour [50] is expected to be altered in the future.

Taking all this into account and the fact that materials and services for O&M are largely related to the WTG market, costs have also been affected by past rises in commodity, labour and steel prices, and thus, it is not surprising the 58% increase in O&M costs between UK Round I and II offshore wind farm projects [4].

On the other hand, as turbine technology develops to provide greater reliability, O&M costs should also be decreasing.

Diagram 3.2 is an indication of the main cost contributors operating an OWF, based on 2 vessels availability [6].

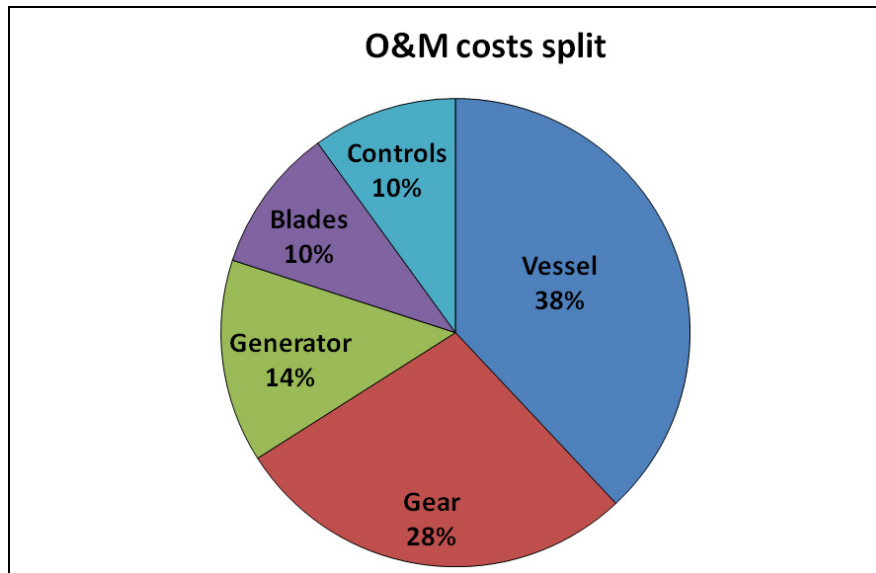


Diagram 3.2 O&M costs split based on 2 vessels availability [6]

From these chart, it can be concluded that vessel hiring costs, which account for the biggest part of the total costs, will potentially increase as wind farms are sited further offshore, with higher transport times and greater risk of weather downtime. Nevertheless, it should be noted that a great effort is being accomplished for the improvement of access methods less sensitive to wind and wave conditions [50].

Further adaptation to the harsh marine environment carried out by WTG manufacturers should help to reduce the O&M costs associated to the main WTG troublesome components, [51], [52]. Several measures are being addressed, such as reducing overall number of parts, simplifying design, increasing reliability, using modular designs, developing effective condition monitoring and remote control systems or improving maintenance strategies for service and repair actions.

General guidelines for the inspection methodologies for offshore wind turbines are given in [53], which is mainly based on the oil & gas facilities. Issues such as corrosion, fatigue, mechanical damage (e.g., from dropped objects and vessel impact), and structural response to extreme events are intended to be located so that remedial action can be taken before the structural strength is compromised (see Figure 3.1).

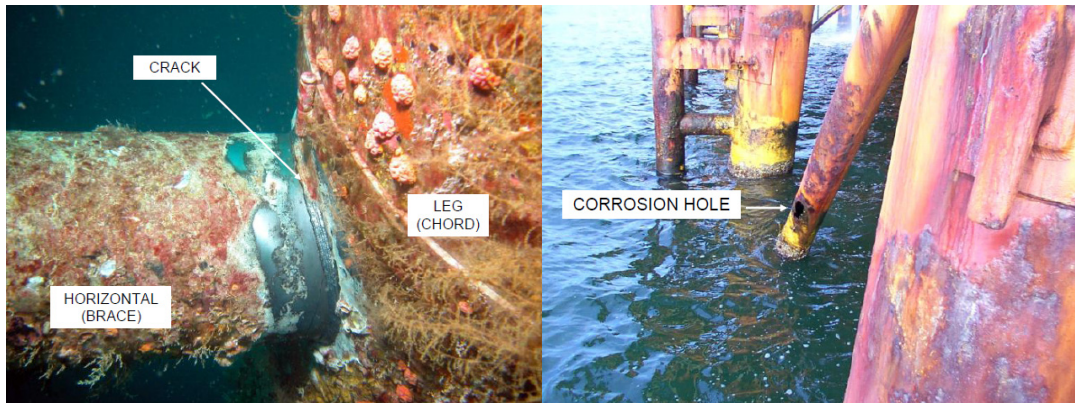


Figure 3.1. Typical damages in offshore jacket [53]

In the case of substructure inspections, their O&M are divided based on their cycling in 3 categories [53],:

- Annual: performed every year. Its targets are primarily above water along with cathodic protection measurements and splash zone visual inspection.
- Intermediate: executed every 3-5 years in addition to the annual one. Higher level of effort is needed. A diver or ROV assesses the condition of the subsea structure and equipment including the general condition, physical damage, and marine growth present.
- Extended: accomplished every 6-10 years. The critical subsea structural connections are cleaned of marine growth and inspected to assess the general condition, identify cracks or damage to welds, identify deterioration of concrete surfaces, and enable definition of potential anomalies.

Notwithstanding, as shown in,

Diagram 3.2 it is clear that WTG substructures are not one of the main O&M costs drivers. Furthermore, lack of experience in the young offshore wind industry, prevents particular costs associated with each support structure type to be considered. This, together with the uncertainty involved in all O&M cost calculations due to the

reasons explained before, have lead to its exclusion from the support structures cost analysis, in order to facilitate comparison between different structures.

### **3.2.2 Decommissioning costs**

Decommissioning provisions are to be made in a yearly basis as stated in [54]. All the same, not much is known about offshore decommissioning and even the more experienced oil & gas industry is now starting to deal with the challenges involved in the process, mainly based in the nuclear power industry. These experiences in the following years will be important for a more accurate future estimation of its costs.

Until recently, it was assumed to require almost the same equipment and time as installation. Decommissioning of components above the water level could be a little faster, because it may be done less precisely. However, foundation decommissioning could take longer and require more specific equipment for the purpose. Its costs are taken equal to installation costs [55], but due to interest and inflation the net present value should be less.

Furthermore, regarding support structures, reuse by repowering with new/superior wind turbines is encouraged [54], [56]. This would mean a life extension that would consequently reduce decommissioning costs even more.

Latest decommissioning provisions have been determined at 21000 €/MW per year [4]. Based on total costs splits, it seems logical to consider a fourth of this cost to be provided for the support structure. However, this assumption does not make any differentiation among foundation or substructure types, but it rather estimates a fixed specific amount, no matter the structure characteristics.

Offshore wind energy industry is still too recent and does not have, nor will have in the medium term, any decommissioning experience. Hence, introducing this variable in the support structure costs analysis would only add uncertainty to the comparison. In any case, it is set as a fixed value, whatever the foundation or substructure, so it is preferable not to include it in the study for a clearer understanding of the driving factors.

### **3.2.3 Other costs**

Other costs include insurance and contingency costs for the support structure during the construction period, which were estimated at 10% and 7% respectively according to [57]. These values should decrease in the future along with offshore wind industry uncertainties as experience is gained in the field.

These costs were not included in the study because of the difficulty entailed in their calculation for different foundation and substructure types. Moreover, as they are considered a fixed percentage value, similar for all support structure, their exclusion from the analysis allows a simpler cost comparison and more comprehensible results.

## **3.3 Input Parameters**

Two different offshore support structure costs (monopile and jacket) are to be analysed in relation to 4 main designing parameters. These parameters are explained in detail hereafter.

### **3.3.1 WTG Power**

One of the main advantages of offshore wind energy is the avoidance of visual impact when the wind farms are far enough from shore, which allows bigger WTG to be installed. In addition, offshore energy is more expensive due to the harsher environment and more challenging installation to be carried out. These two factors together have led the market to its current tendency to increase the WTG power, aimed to reduce total specific costs (€/MW) of the investment.

3 WTG powers are compared (3.6 MW, 5 MW and 7 MW), gathering the present, the near future and the medium term market installation powers. Each turbine power will generate different loadings from wind and weight for the static and dynamic calculations.

In Table 3.1, the specifications of each reference OWTG are given. This information for the 3.6 MW and 5 MW OWTGs is based on [58]. Data for the 7 MW OWTG is based on estimations.

<b>REFERENCE OWTG</b>	<b>3.6 MW</b>	<b>5 MW</b>	<b>7 MW</b>
Rotor diameter	106	126	164
<b>TOWER DESIGN DATA</b>			
Tower length (m)	71	81	87
Nacelle mass including rotor (Tn)	220	410	480
Tower top D/wall thickness (m / mm)	3.5 / 15	4.5 / 20	5.5 / 25
Tower bottom D/wall thickness (m / mm)	4.5 / 30	6 / 35	6.5 / 35
<b>LOADS AT TOWER BASE</b>			
Horizontal load (MN)	1.42	2.03	2.59
Vertical load (MN)	4.4	7.1	8.37
Moment (MN m)	111.2	180.45	253.75

Table 3.1. Reference OWTG data

Loads at the tower base will make the difference between the various WTG powers when the static analysis of the support structure is being accomplished. On the contrary, the tower design data (especially the THM weight) will have a bigger impact when the natural frequency of the structure is being calculated. The tower diameter and thicknesses are distributed linearly along the whole tower length from the initial value at the top to the final value at the bottom.

In reality, turbine power is not the only parameter affecting the wind loads, as the rotor diameter will have a big impact along with the cut out wind speed among other. However, in this analysis the power output was considered a better parameter in order to compare the specific costs as it gives a clearer idea of the project's economics.

### **3.3.2 Water Depth**

As it has already been mentioned, water depth is the main cost driver for the offshore wind industry. Each support structure has an optimum water depth range that in this analysis is attempted to calculate. The compared depths for each foundation are



summarised in Table 3.2. Monopile water range has been extended to overlap the jacket range for a proper comparison of both substructures.

Substructure	Water Range (m)
Monopile	10 - 45
Jacket	25-85

Table 3.2 Water range included in the study for each substructure

### 3.3.3 Wave height

Depending on the offshore wind farm location, the hydrodynamic loading that the structure will have to withstand can strongly vary. Each substructure has different characteristics, making some of them more prone to resist high wave loading and other being more suitable for sheltered waters. In order to include the whole range, 3 main sea states have been compared as shown in Table 3.3. The 3 sea states (low, medium and high) are represented by the significant wave height ( $H_s$ ). However, the extreme wave height ( $H_{max} = 1.86 \cdot H_s$ ), which is the average height of the highest 1% of all waves in a sea state, is used in the extreme loading calculation of the structure. Each  $H_s$  has also an associated mean zero crossing period ( $T_z$ ) that can be estimated by  $3.54 \cdot H_s^{0.5} \leq T_z \leq 4.56 \cdot H_s^{0.5}$  as per [59].

Sea State	$H_s$ (m)	$H_{max}$ (m)	$T_z$ (s)
Low	4	7.44	7
Medium	7	13.02	9
High	12	22.32	12

Table 3.3. Compared sea states

### 3.3.4 Soil Type

The soil type in which the foundation is being installed is of critical importance. The foundation transfers all the structure loading to the soil, which has to be strong enough to resist. Once again 3 types of soils are covered, soft, average and hard. The chosen material is clay, which is very common in the North Sea. Thus, undrained shear strength ( $s_u$ ) is used for its characterization. Undrained shear strength increases

with soil depth, and a linear increase was used in the calculations from the minimum value at seabed to the maximum value at 60 m depth. Table 3.4 shows the  $s_u$  values for each case. These values are not necessarily a standard type, but the ones considered for this analysis.

Soil Type	$s_u$ (Pa) at seabed	$s_u$ (Pa) at 60 m depth
Soft	50000	200000
Average	150000	300000
Hard	350000	500000

Table 3.4. Compared clay types

### 3.4 Monopile cost analysis

#### 3.4.1 Introduction

The monopile is the first substructure analysis carried out for being the most popular and experienced one. Thanks to its simplicity, it has become the undisputable preferred support structure, at least up to now, when most of the experience is based in sheltered waters below 20 m depth and WTG powers are under 3.6 MW. Its economical limits are sought in this analysis by the calculation of a wide range of input parameters that cover the present and potential future of this substructure.

#### 3.4.2 Mathcad calculation methodology.

The Mathcad programme developed for the monopile, makes 2 types of calculations. First of all, a static analysis is carried out from which the monopile design (diameter, thickness and penetration) is obtained. Then, this design is used for the calculation of the first natural frequency of the whole structure (including tower and nacelle). General calculation method, which is carried out according to [59], [60], is explained hereafter.

### 3.4.2.1 Static analysis

The static analysis is done for the ultimate limit state. In Diagram 3.3 this analysis in Mathcad is resumed.



Diagram 3.3 Monopile static calculation summary with Mathcad

Below, a brief explanation of the steps in Mathcad programme for the monopile static calculation is given.

### *1. Definition of monopile*

Due to the simplicity of the monopile, the calculation can be carried as a 2D structure composed of beam elements. The whole monopile and TP is divided in 7 parts. Each part has its own properties (area, moment of inertia, length, etc.) depending on the entered input data (diameter, thickness and lengths). This allows the possibility to modify the monopile design in accordance with the necessities while minimising the weight ratio.

The platform level or the level at which the transition piece (TP) is connected to the tower can be calculated as [59] or [61]. However, as in this case no tidal range or storm surge is considered, the formula is simplified, so that it only depends on the water depth and the significant wave. The final result has been proved to be similar in real cases. Thus, the platform level was set at the minimum value between  $0.78 \cdot \text{water depth}$  and  $2/3 \cdot H_{\text{max}}$ . No tidal ranges or storm surges were included in the calculation of the platform level, neither a minimum airgap, as for the purpose of this study it has no influence. Run up of the waves were not considered neither.

The pile ends 2 m above m.s.l., which facilitates the installation of the TP, as it can be correctly placed while still in sight. The TP diameter is 0.25 m bigger than the inside pile diameter, which is enough for the grouting of both pieces together. The overlap length will be 2 times the pile diameter, which is a typical value used in the industry [6].

The substructure and the main structure are divided taking the connection node as a reference. Hence, the elements below the connection node (the one in the mudline) correspond to foundation which is governed by the non linearities of the soil, whereas the elements above the connection behave linearly and correspond to the substructure. Figure 3.2 shows this division.

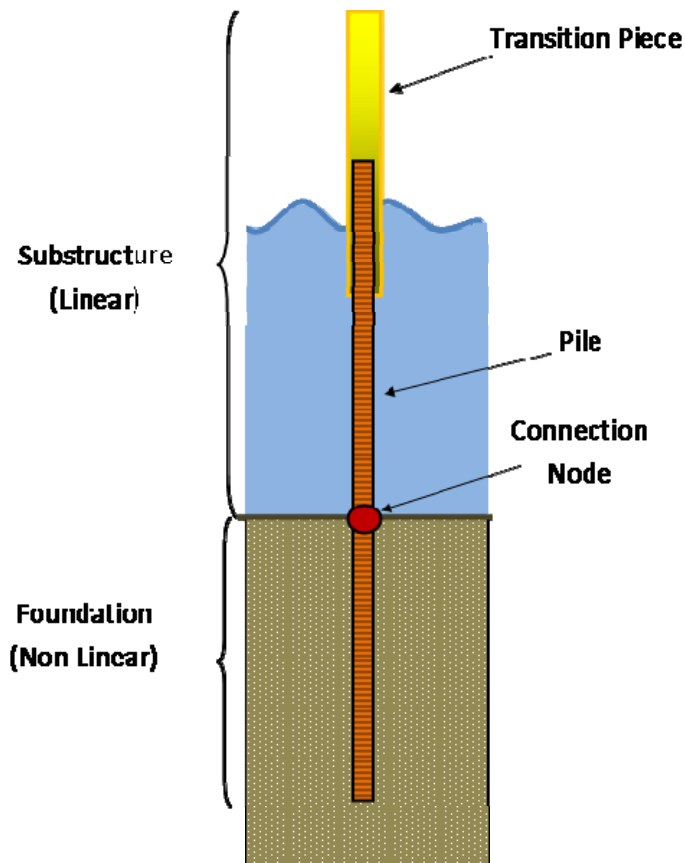


Figure 3.2: Monopile division depending on the linearity of the elements.

## 2. Definition of loads

Turbine weights and wind loads are reduced to a horizontal and vertical load and a moment according to values in Table 3.1.

Water particle velocity due to waves is calculated according to linear wave theory (Airy) [60], [62]. Nevertheless, the use of linear theory in shallow waters, and especially with high wave heights should be limited [63], [64]. In this case, the linear theory was always used for simplification. Even so, as it can be seen in Diagram 3.4, not even a correction coefficient was necessary because the area being studied (according to used wave height and periods) was around 100% of Airy theory [60].

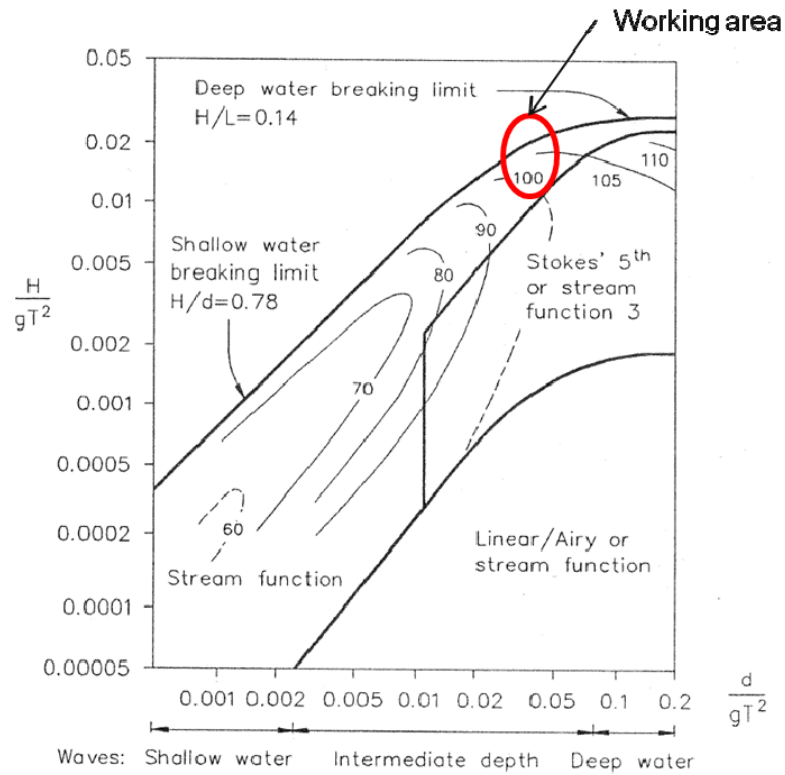


Diagram 3.4 Horizontal velocity under crest at MWL: Airy theory as % of regular theory [60]

In addition to these velocities, a current horizontal velocity of 0.8 m/s is added. Then, the maximum horizontal load corresponding to the water particle velocities are applied according to Morrison's equation, which is of common use for slender structures like the monopile [63]. Drag and inertia coefficients are set to  $C_d=1.05$   $C_m=2$  in order to be conservative [65].

Extreme wind, wave and current loads are applied all together at the same time, which is a conservative approximation. But this approach is satisfactory for the study being carried out.

Finally, the structure weight and the buoyancy of the underwater part are included.

A safety factor of 1.35 is used for the environmental loads and 1 for the permanent loads as per [59].

### 3. Definition of substructure

The stiffness matrix and force vector of the substructure (from the first node above m.s.l. down to the seabed node) are calculated, first in the local coordinates and then transformed to global coordinates.

### 4. Definition of connection node

The force vector and stiffness matrix of the substructure are transformed to  $K_s$  and  $F_s$ , that is, the stiffness and external forces as seen by the connection node. As it has been explained before, this connection node is placed in the seabed. Below this node, non linear behaviour of the structure starts due to the soil non linear properties.

### 5. Calculation of pile under soil structure

The stiffness matrix of the foundation, which is located below the connection node, is calculated according to the properties of its elements. Then, soil stiffness has to be added to the matrix.

There are different methods for a laterally loaded monopile to be modelled as shown in Figure 3.3 [66]:

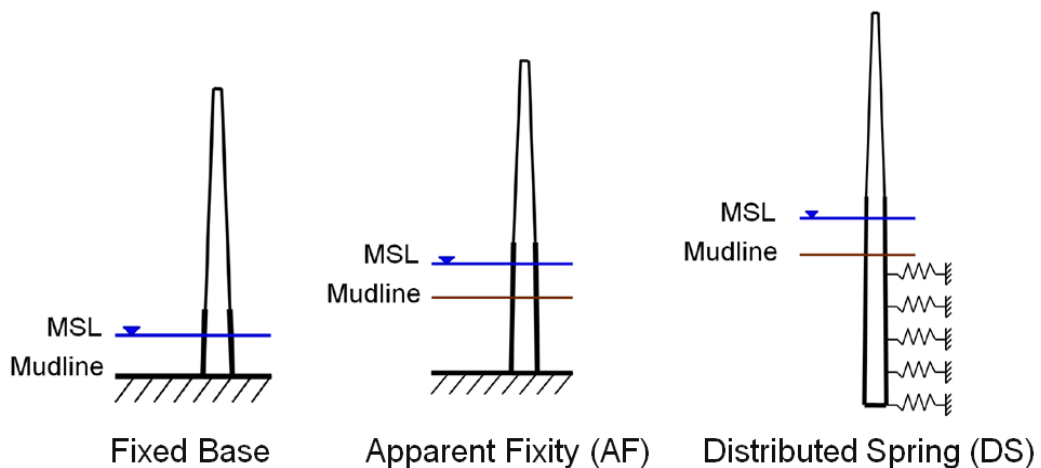


Figure 3.3. Comparison of different methods for the soil-pile interaction calculation [66]

A fixed-base model is the simplest of the three and involves a rigid connection of the turbine's support structure to the sea bed. This model does not take into consideration the soil profile at the turbine site and it also does not allow for lateral or rocking motion at the mudline. Therefore, the results are not reliable.

The apparent fixity (AF) model has a fixed connection that is located a specific depth below the mudline so as to produce an appropriate translation and rotation at the mudline. The length below the mudline will depend on the soil's profile and is usually taken from tables. This method is sometimes used for preliminary dynamic analysis.

The distributed springs (DS) model includes the true length of the foundation and replaces layers of the soil with discrete linear elastic springs along the length of the pile. The stiffness of these springs depends on the loads at the head of the pile. This is because soil under loading does not behave as a linear elastic material; the more soil is loaded, the softer or less stiff it becomes. The stiffness of the soil under a given load and at a specific depth can be determined from available p-y curves (or load-deflection curves).

In addition, each depth has its own associated and independent p-y curve, and the deeper the soil is, the higher the stiffness will be. According to the Winkler-hypothesis the springs act independently of each other. Hence, the subgrade reaction at the pile in a certain depth is not influenced by the pile displacements at other depths.

So, the p-y curves increase their slope the deeper the analysed soil is and decrease it, the more loaded it is (see Figure 3.4). This explains soil's non linear behaviour.

This method is the one commonly used for offshore piles [67], [68] as it is the standard design procedure according to the relevant guidelines in offshore engineering (API, GL, DNV) [69].

In this case, a good representation of the pile bending moment and the stiffness at different depths is needed, therefore DS method is chosen for the study.



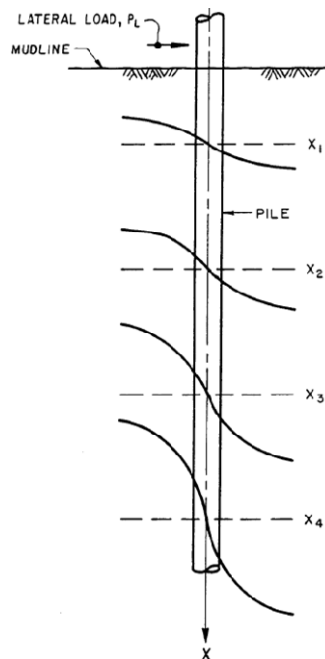


Figure 3.4. Slope of p-y curves differ at different depths and loadings [70]

Notwithstanding, the p-y method has been derived from field test results with pile diameters of up to 0.60 m. By the experiences gained over the last 30 years this method may be acceptable for piles with diameters of up to 1 or 2 m [71]. Even though piles with larger diameters (up to 6.5 m) have been recently designed and installed, no experimental data or long term pile behaviour experience exists.

Many studies have been undertaken [67], [69], [71], [72], [73] to demonstrate the appropriateness of the p-y method for calculating laterally loaded large diameter piles. However, results are not unifying as the design requirement criterion used in the calculations will have a big influence. Overall, it seems that this method leads to an overestimation of the pile-soil stiffness at great depths.

Thus, in the future new calculation methods more appropriate for large diameters will likely be developed. Yet, currently, p-y method is the most widely spread method, and for the cases under study, p-y curves were created for the calculation of the soil lateral, shaft and end bearing stiffness (see Figure 3.5).

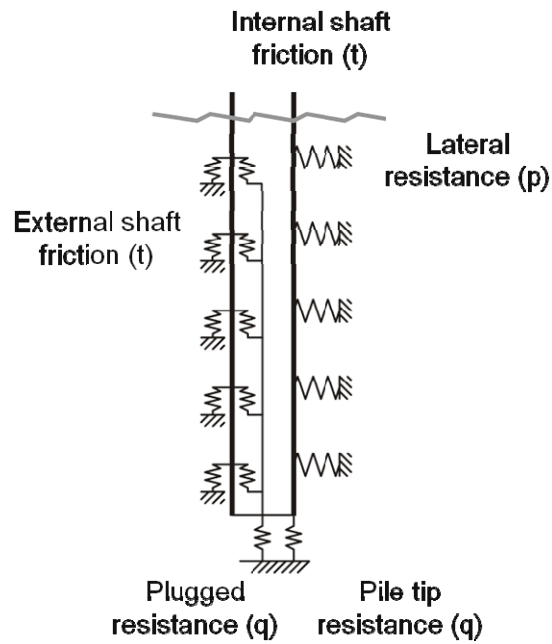


Figure 3.5. Different soil resistances to consider in the whole soil-pile interaction [74]

The equations governing the lateral, shaft and end bearing resistance are calculated according to [59] and [60], which are fundamentally affected by the undrained shear strength ( $s_u$ ) in the case of clay soil.

Hereafter, the used equations are summarized for each resistance type.

Lateral resistance: p-y curve

$$p \left[ \frac{N}{m^2} \right] = 0.5 \cdot p_u \cdot \left( \frac{y}{y_c} \right)^{1/2}, \text{ for } y \leq 8 \cdot y_c, \text{ and}$$

$$p \left[ \frac{N}{m^2} \right] = p_u \text{ for } y > 8 \cdot y_c$$

Where,

$p$  , actual lateral resistance per area

$p_u = 9 \cdot s_{u,c}$  , ultimate lateral resistance per area

$y$  , actual lateral deflection

$y_0 = 2.5 \cdot \varepsilon_c \cdot D$  , displacement occurring at 50% of the ultimate resistance

$\varepsilon_c$  , strain occurring at 50% of the ultimate resistance

$\varepsilon_c = 0.007$  , for soft clays

$\varepsilon_c = 0.005$  , for average clays

$\varepsilon_c = 0.004$  , for hard clays

$D$  , pile diameter

In Diagram 3.5, a typical p-y curve for lateral resistance is shown.

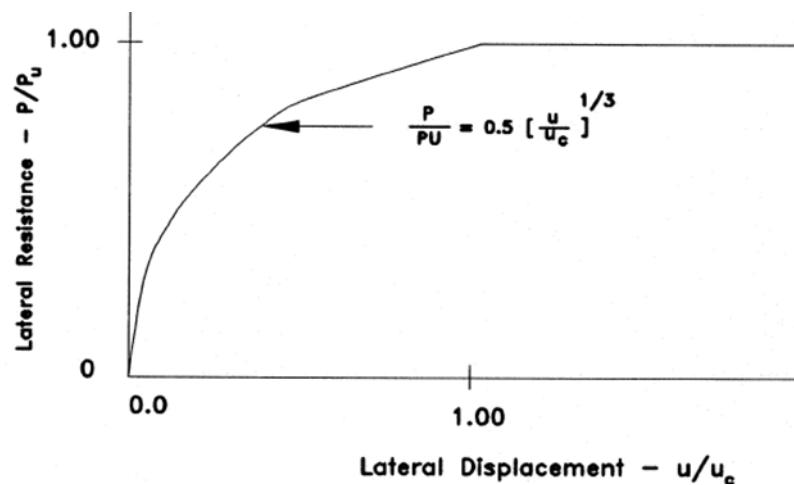


Diagram 3.5. Typical lateral resistance p-y curve [70]

Shaft resistance: t-z curve

$$t \left[ \frac{N}{m^2} \right] = t_{max} \cdot \left[ z \cdot \left( \frac{z}{z_c} \right)^{1/2} - \left( \frac{z}{z_c} \right) \right] , \text{ for } z \leq z_c$$

$$t \left[ \frac{N}{m^2} \right] = 0.8 \cdot t_{max} \cdot z , \text{ for } z > z_c$$

Where,

$t$  , skin friction per area

$t_{max}$  , maximum skin friction per area

$$t_{max} = s_u, \text{ for soft clays}$$

$$t_{max} = 0.5 \cdot s_u, \text{ for average and hard clays}$$

$z$  , axial displacement

$z_c = 9 \text{ mm}$  , axial displacement at which maximum skin friction is mobilised (typical value for offshore piles).

End bearing resistance: q-z curve

$$q \left[ \frac{N}{m^2} \right] = q_{max} \cdot \left( \frac{z}{z_c} \right)^{1/8}, \text{ for } z \leq z_c$$

$$q \left[ \frac{N}{m^2} \right] = q_{max}, \text{ for } z > z_c$$

Where,

$q$  , end bearing per area

$q_{max} = 9 \cdot s_u$ , maximum end bearing per area

$z$  , axial displacement

$z_c = 0.1 \cdot D$  , axial displacement at which maximum skin friction is mobilised

The end bearing capacity of the soil will be equal to the internal shaft friction of the pile plus the end bearing of the pile wall annulus, as long as the pile is not "plugged".

The pile is “plugged” when the internal shaft friction plus the end bearing of the pile wall annulus is smaller than the end bearing of the plug (when the whole end area is resisting). For the calculations, only the smaller of the two resistances will be considered.

From each of the resistance-displacement curve, the soil stiffness (N/m) is calculated by the secant stiffness method (resistance divided by the displacement at that point) and is then added to the main structure stiffness matrix. Then, displacements can be computed again from which the new soil stiffness can be calculated again. Soil’s non linearity makes this iteration necessary for the convergence of the final soil stiffness and displacements in the foundation.

#### *6. Calculation of substructure*

Once the non linear part of the structure has been calculated, deflections of the linear part (above mudline) can be obtained. So, all the results in global coordinates are already known.

#### *7. Calculation of results in local coordinates*

By transforming global deflections to local coordinates, element forces can be calculated using the element’s local stiffness. Finally, element stresses are obtained.

#### *8. Check results*

Design requirements are checked according to several limiting criterion:

- Maximum axial stress  $< \sigma_{\max}$
- Maximum shear stress  $< \tau_{\max}$
- Pile head tilt angle (mudline)  $< 0.7$
- Fixed pile tip ( $\delta_{\text{tip}} < 0.001 \cdot D$ )
- $D/th < 100$

The optimum pile design is manually obtained by changing the diameter, thickness and penetration to get the lightest pile possible while fulfilling all the above limitations.

Steel Grade 355, widely used for offshore monopiles, is considered in the calculations with a material safety factor of 1.1 as per [59]. Maximum axial and shear strength are calculated and limited as per [59], [75].  $\sigma_{\max}$  and  $\tau_{\max}$  vary depending on the steel plate thickness as shown in Table 3.5. [76].

Minimum yield strength (Grade 355) MPa	$\sigma_{\max}$ ( $\gamma_m=1.1$ ) MPa	$\tau_{\max}$ ( $\gamma_m=1.1$ ) MPa
$t < 16$ mm	355	323
$16 < t < 40$ mm	345	314
$40 < t < 63$ mm	340	309
$63 < t < 100$ mm	325	295
$100 < t < 120$ mm	310	282

Table 3.5. Minimum expected  $\sigma_{\max}$  and  $\tau_{\max}$  from Grade 355 steel depending on the plate thickness

Estimating the maximum pile head tilt angle is one the most difficult tasks for engineering design, as also the installation tolerances will have to be taken into account. In this case, the limit was set according to [69] and [71].

Reviewed literature does not agree for the suitability of the zero-toe-kick criterion in large monopile designing. In this study, it is limited and the pile tip is considered fixed pile when its deflection is smaller than  $0.001 \cdot D$  (see [63]), where  $D$  is the diameter of the pile at the tip.

Regarding the tubular members  $D/th$  relation, there are different recommendations to follow from the standards, such as  $th > D/120$  [75] or  $th \geq 6.35 + D/100$  [77]. In this analysis, a in between criterion was adopted,  $t > D/100$ .

#### 9. Recalculate if necessary

If the results do not satisfy the entire designing criterion, the monopile dimensions are modified (diameters, thicknesses and/or penetration) and the whole process is repeated.

### 10. Calculate weight

From the final design of the support structure, the weight of the whole monopile structure (the driven pile, the transition piece and the secondary steel) is calculated with a steel density of 7850 Kg/m<sup>3</sup>. Secondary steel includes J-tube, platform, boat landings and ladders and is summarised in Table 3.6 from values based on [65].

OWTG Power	Secondary Steel Weight (Tn)
3.6 MW	35
5 MW	39
7 MW	45

Table 3.6. Secondary steel weight for each of the considered OWTG powers

#### 3.4.2.2 Dynamic analysis

The dynamic analysis of the monopile includes the calculation of the whole structure first natural frequency (THM, tower, substructure and foundation). Diagram 3.6 is a summary of the steps given in Mathcad to obtain the first natural frequency of the whole OWTG which are explained hereafter.

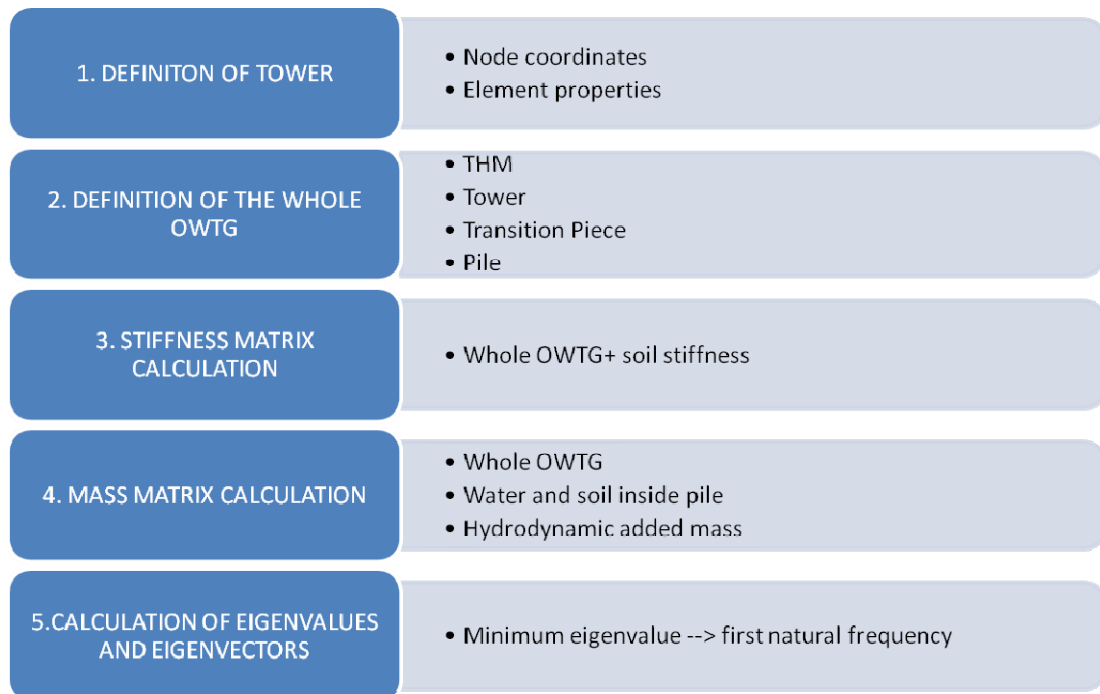


Diagram 3.6 Summary of the monopile dynamic calculation with Mathcad

### 1. Definition of tower

New elements for the tower are created and defined according to the data corresponding to each OWTG.

### 2. Definition of the whole OWTG

The tower elements are added to the existing structure defined for the static calculation. Thus, the whole OWTG element's mass and stiffness can be defined.

### 3. Stiffness matrix calculation

Element stiffness in local coordinates are added together and transformed to global coordinates. Finally, the soil stiffness is also added to the matrix.

### 4. Mass matrix calculation

Element masses in local coordinates are added together and transformed to global coordinates. THM mass is considered as a mass on pole at the top the structure (see Figure 3.6),

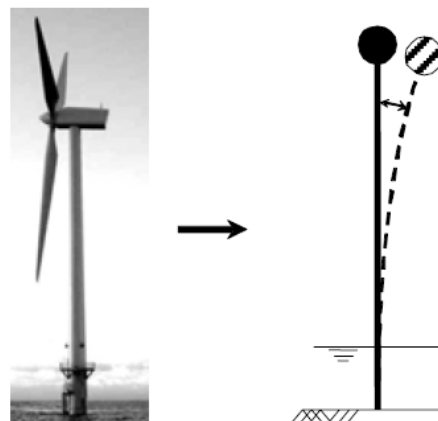


Figure 3.6. Offshore wind turbine modelled as a mass on pole [78]

For the elements under the mudline the soil mass inside the whole driven length is also considered. In the case of the elements above the mudline and up to the m.s.l,



the water mass inside is also added. For these elements too, the hydrodynamic added mass has to be accounted, which in this case, equals to the volume inside the pile multiplied by the sea water density.

### 5. Calculation of eigenvalues and eigenvectors

Once the stiffness and mass matrix are known, both the eigenvalues and eigenvectors (for plotting of the vibration mode as shown in Figure 3.7) can be calculated. Finally, the smallest of the eigenvalues is extracted which corresponds to the 1<sup>st</sup> natural frequency of the OWTG.

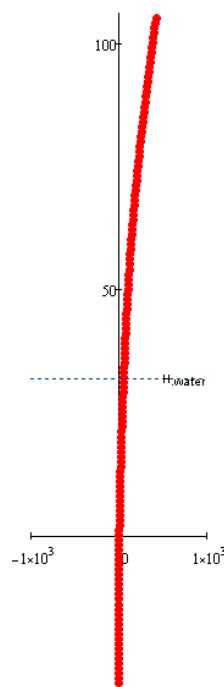


Figure 3.7.Pile Mode 1 example. Scale 1:100

### 3.4.3 Monopile Design

As it has been explained the designing of the monopile was carried out according to the extreme loading calculations and the 1<sup>st</sup> natural frequency. Fatigue limit state was not considered in the design due to lack of time. The effect of structural and foundation damping is also not included.

Fatigue due to combined wind and wave loading is known to be an important aspect for offshore support structures. The turbulent wind and the unsteady sea state lead to high dynamic loads with a number of cycles of about  $10^9$  during the turbine whole life [79]. However, incorporation of a proper model for dynamic, combined (lifetime) loading increases complexity of the design tools with an order of magnitude. Moreover, the focus of this study was on estimating the relative change in weight of the support structure with water depth, wave height, soil conditions and WTG power for a given turbine. It is assumed that fatigue consideration would not affect the relative change.

On the other hand, approximate calculations have already been done by the use of an amplification factor. In [80], the dynamic response is implemented with a simple gust response factor of 1.5 for aerodynamic loading and no dynamic amplification is applied to hydrodynamic loading.

In this study, the extreme loading calculations are carried out for both extreme wind and wave combination at the same time, which can be regarded as a more restrictive static designing than recommended on [59]. In spite of all, fatigue is most likely to affect structural connections and therefore, it could result in a cost increase when compared with this simplified calculations.

Regarding the natural frequency, it cannot coincide with any of the rotational frequencies of the turbine (1P and 3P) and it must also stay away from the frequencies of the waves to prevent resonance and with it, increased fatigue. The 1P frequency refers to the rotor frequency and the 3P frequency refers to blade passing frequency (the set of three blades passing the tower).

Figure 3.8 shows the designing intervals allowable if the aerodynamic resonance is to be avoided.

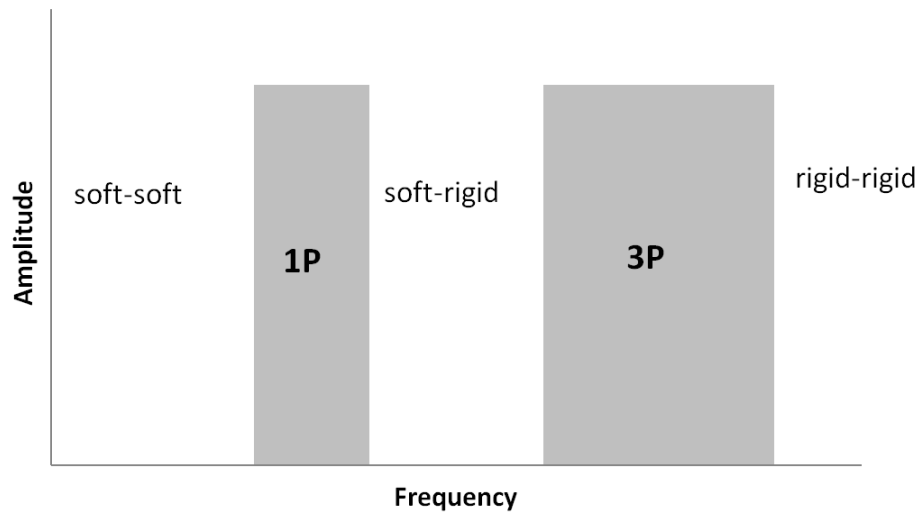


Figure 3.8 Frequency intervals for a variable speed turbine system

A soft-soft (compliant) structure, only requires 30% of the diameter of a stiff-stiff design [78]. The only complication here is that in the soft-soft area wave frequencies are also present, causing potential resonance and fatigue.

This is the reason why bottom mounted support structures are typically designed between the 1P and 3P frequencies of the turbine [81], [74], that is, the soft-rigid area.

A typical operational range between 7 rpm (minimum rotational speed at the cut-in wind speed) and 15 rpm (maximum speed) is considered for the WTGs. The wave period range will be from the minimum of 3.55 s (for the smallest  $H_s=1$  m waves) to a maximum of 12 s (for the largest  $H_s=12$  m waves). Nevertheless, it is sea states with high frequency of occurrence that have the largest effect on fatigue analysis. These are generally short waves with small significant heights (around 1.5 m). A typical wave scatter diagram for the North Sea can be found in [79].

The above implies an allowable period range between 2.86 s and 3.55 s as shown in Figure 3.9. Or, an allowable frequency range between 0.28 and 0.35 Hz. This is very similar to the limitations considered in [61] where a target value of 0.29 Hz is aimed being 0.35 Hz the maximum value.

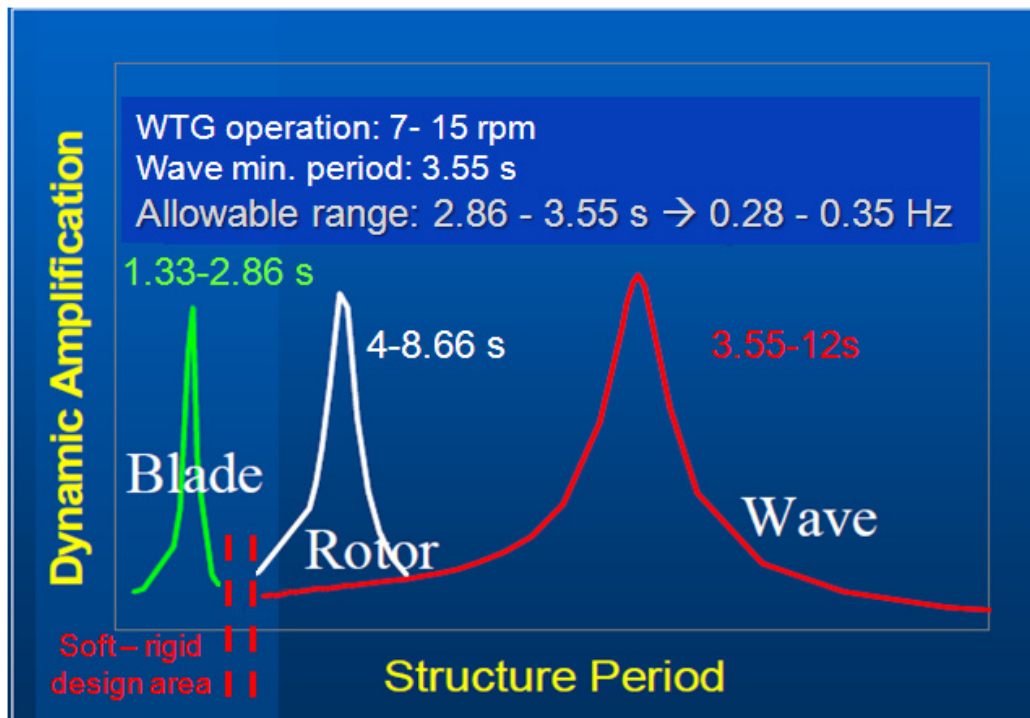


Figure 3.9. Period range intervals for the design of the OWTG

So, during the design process of the monopile, it will be critical to contemplate this limitation as the natural periods of oscillation are likely to fall into the wave excitation zone. If necessary, the monopile diameter and thicknesses are to be increased in order to avoid the restricted area.

### 3.4.4 Validation

The limited available data makes it rather difficult to validate the results with real examples from the industry. Monopile weights and dimensions can be found in the public source; however, detailed information regarding soil profiles, design wave heights or allowable frequency range, is rather confidential.

Monopile weights for several projects at different depths were compared with the obtained values from Mathcad (see Table 3.7). Results showed to be sensible regarding both weights and pile diameters.

Wind Farm	OWTG	Pile diameter (m)	Pile Weight (Tn)	TP Diameter (m)	TP Weight (Tn)	Water depth (m)
Belwind	Vestas 3.0 MW	5	350-500	5	167	20
Lincs	Siemens 3.6 MW	4.74	300-420	5	250	8.5-16
Sheringham Shoal	Siemens 3.6 MW	4.73 - 5.7	375-530	4.7	220	16-22
Gunfleet Sands I and II	Siemens 3.6 MW	4.7	423	5	212	0-10
Robin Rigg	Vestas 3.0 MW	4.3	195-264	4.54	160	0-9
Rhyl Flats	Siemens 3.6 MW	4.7	193-235	5	220	6.5-12.5
Lynn & Inner Dowsing	Siemens 3.6 MW	4.74	200-266	5	181	6-11
Burbo Bank	Siemens 3.6 MW	4.7	195-234	5	225	3.7-7.5
Kentish Flats	Vestas 3.0 MW	4.3	144-184	4.54	90	6.6-7.7
Horn Rev	Vestas 2MW	4	125-155	4.24	80-100	6 - 14

Table 3.7. Monopile substructure weight and diameters for already accomplished projects

A real monopile design for the Kriegers Flak OWF [65] was also compared in similar conditions and the average differences were as follows:

-Monopile and TP weight: -19%

- Monopile diameter: -6%

- Penetration: -13%

- 1<sup>st</sup> natural frequency: -15%

It must be taken into account that the monopile is a very sensitive structure, in which any modification in the input parameters, which were similar but not the same, can have a significant impact in the final results. In any case, the obtained results are considered valid for the purpose of the study. The values with Mathcad were below

the Kriegers Flak values, but this is reasonable taken into account that no fatigue was included in the analysis.

### 3.4.5 Monopile Manufacturing

Manufacturing of a monopile and its transition piece is a relatively simple and automated process. The piles are usually made up of "cans", cylinders of rolled plate with a longitudinal seam. It comprises several fabrication steps that are summarised below with pictures of each of the operations [82]:

1. **Storage of steel plates:** delivered plates from the steel mill are stored in the warehouse. Their wall thicknesses usually range between 50 to 90 mm.



Figure 3.10. Monopile manufacturing. Storage of steel plates [82]

2. **Milling and cutting:** the plate is transformed to the necessary surface area.



Figure 3.11. Monopile manufacturing. Milling and cutting [82]

3. **Rolling:** the plate is rolled into the circular section. Single cans are typically 1,5m long or more.

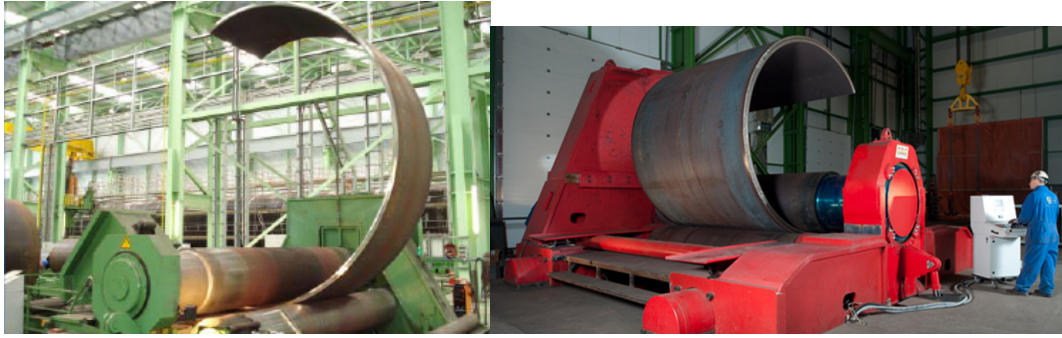


Figure 3.12. Monopile manufacturing. Rolling [82]

4. **Inside longitudinal welding:** first chord of the longitudinal union is welded. Longitudinal seams of two adjacent segments are rotated 90° apart at least.



Figure 3.13. Monopile manufacturing. Inside longitudinal welding [82]

5. **Milling:** the longitudinal union is machined in order to prepare the surface for the second welding chord.



Figure 3.14. Monopile manufacturing. Milling of the longitudinal union [82]

6. **Outside longitudinal welding:** second outer welding chord is necessary due to the high plate thicknesses.



Figure 3.15. Monopile manufacturing. Outside longitudinal welding [82]

7. **Calibration:** the pile can is calibrated in order to correct any misalignment due to rolling and/or welding tensions.



Figure 3.16. Monopile manufacturing. Calibration [82]

8. **Assembly:** pile elements are placed together and prepared for the circular welding.





Figure 3.17. Monopile manufacturing. Assembly [82]

9. **Inside circular welding:** first chord of the circular union between the two cans is welded.



Figure 3.18. Monopile manufacturing. Inside circular welding [82]

10. **Milling:** the circular union is machined in order to prepare the surface for the second welding chord.



Figure 3.19. Monopile manufacturing. Milling of the circular union [82]

11. **Outside circular welding:** second outer welding chord is necessary due to the high plate thicknesses.



Figure 3.20. Monopile manufacturing. Outside circular welding [82]

12. **NDT inspection:** non destructive testing like the ultrasound inspection of the welding chords is necessary in order to assure the quality of the piles.



Figure 3.21. Monopile manufacturing. NDT inspection [82]

In the case of the transition piece, apart from the previous steps, the fabrication continues with some processes more:

13. **Secondary steel assembly:** all the necessary appurtenances are attached to the pile, including ladders, boat landings, platform and J-tube.



Figure 3.22. Monopile manufacturing. Secondary steel assembly [82]

14. **Coating:** surface protection is added.



Figure 3.23. Monopile manufacturing. Coating [82]

Finally, the components are stored and eventually transported to the logistic port where they will be awaiting for the installation process to begin.

Overall, the manufacturing costs of the monopile, have suffered an important increase in recent years mostly due to the steel and commodities price rise which roughly contribute to the 45-50% production costs of the monopile [83].

As it has been explained, the monopile is entirely a steel component with a considerably simple fabrication process. Thus, it is more convenient to account for the manufacturing costs in a cost per weight basis. Most recent estimations by [78], [81] and [84] determined the cost around 2-3 €/kg.

### 3.4.6 Monopile Installation

The construction of a typical monopile consists of the following phases:

1. *Seabed preparation (if needed):*

A "mattress" of rock and stones is placed around the foundation to protect against erosion. Usually, when the pile is to be driven no seabed preparation is needed (except where seabed erosion is a problem). This removes the need of this time consuming underwater operation.

2. *Pile driving or drilling [85]:*

The pile is driven or drilled through the mattress to the planned depth.

When the overburden consist of soils (sands, gravels, clay, etc.) the pile driving is the preferred option by using a variety of means. This can be a hammer system using diesel or hydraulic power; or vibrator or oscillator (see Figure 3.24 ). In general these methods are quicker than drilling but are limited by site conditions. The driving process induces high fatigue stresses in the pile, which prevents incorporation of ladders, platform, flange etc. in the pile fabrication. They have to be provided separately and fitted as additional operations (transition piece installation), thus reducing many of the time benefits of driving.



Figure 3.24. Offshore pile driving [14]

If a site has little or no overburden, a rock socket is drilled in the bedrock to the final elevation and the whole monopile is grouted in position. This produces a very stiff foundation, eliminating many of the uncertainties associated with piling in soils. Figure 3.25 shows a monopile (pile+TP) being transported for a drilling installation.



Figure 3.25. Whole monopile structure (pile+TP) transportation in one piece [85]

Although drilling is flexible in terms of ground conditions, large diameter drilling has slow penetration rates in comparison to driving and also involves multiple operations in deploying the conductor and pile top drill prior to placement of the pile. Subsequently, the placed pile must be surveyed for verticality and then grouted into position; there is then a further delay while the grout is allowed to cure. The conductor or guide casing serves to support the upper part of the hole in the soft unstable material or overburden. In addition, the conductor supports the drill and is employed to align and position the hole. Figure 3.26 shows a typical offshore drilling method and a drill bit.

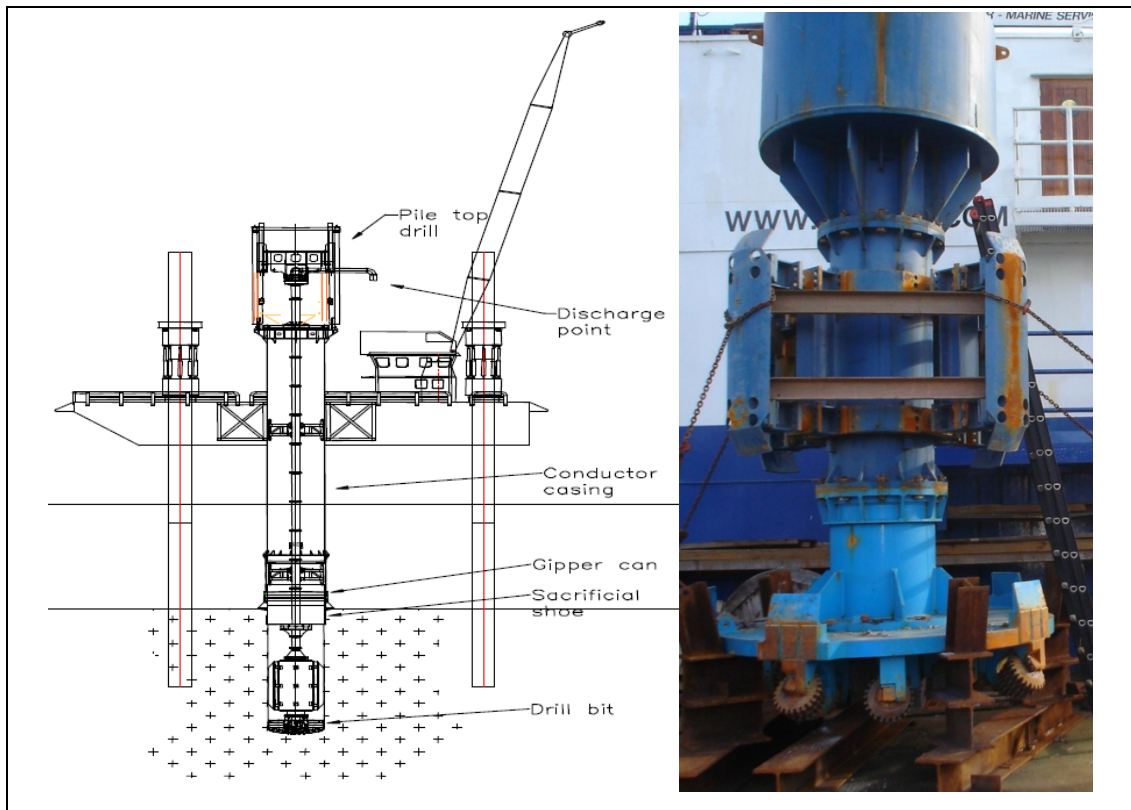


Figure 3.26. Offshore pile drilling and drill bit [85]

Another alternative is the combination of drilling and driving. This is merely a combination of the above. The driving equipment is substituted for a drill when the prevailing ground conditions are no longer favourable. This system tends to fall between the others in terms on speed.

However, when diameters increase above 5-6m, certain problems arise. On the one hand, the hammers necessary to drive the piles could be too heavy to lift with some of the existing cranes. On the other hand, if drilling is the preferred option the volume of spoil is unmanageable and uneconomic to process. Diagram 3.7 shows how the volume of clay excavated from a hole increases with diameter. It can be seen that the volume produced soon becomes very large and uneconomic to treat and transport.

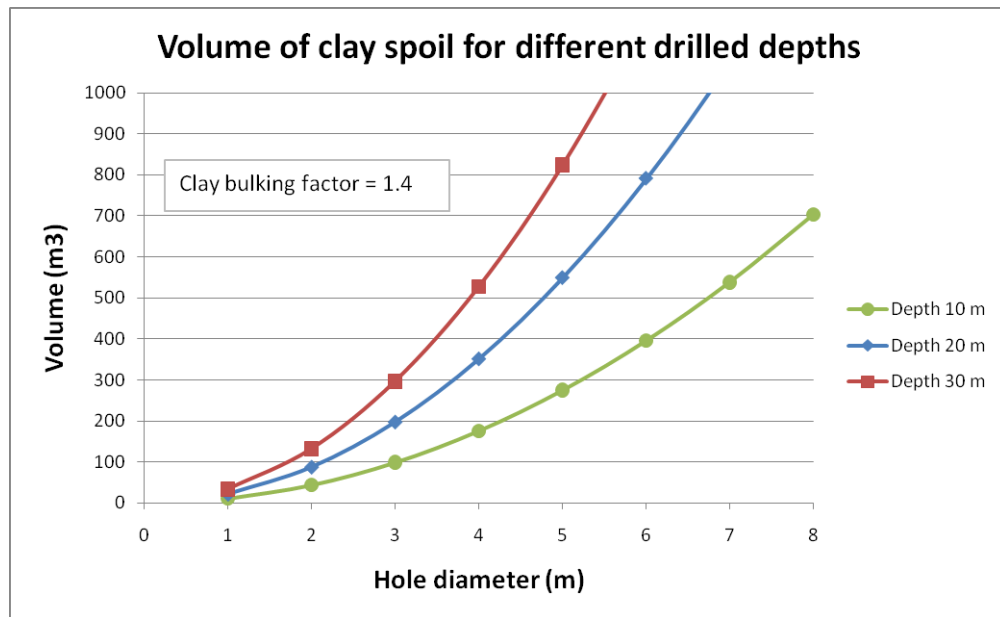


Diagram 3.7 Volume of clay spoil for different drilled depths and diameters

So, currently monopile installation technology is close to its limit: Greater Gabbard, Arklow Bank or Belwind are offshore windfarms with monopile foundations that are around 5 m in diameter installed in water depths about 20 m depth. This entails an important handicap for the monopile foundation and further technological developments will be necessary if this foundation type is to continue being installed in future OWFs. Some of the players are already researching in the simultaneous pile driving [86], in order to be capable of serving future demand.

### 3. Transition Piece positioning (if needed):

The complete TP with pre-installed features such as boat landing arrangement, cathodic protection, cable ducts for submarine cables, turbine tower flange, etc., is placed on position. TP makes it possible to absorb the inaccuracies during the pile installation process. Thus, it allows raising the turbine tower to a completely vertical position even if the foundation is not totally levelled. The top rim of the transition piece is a flange that accommodates bolting of the turbine tower. Brackets are used inside the TP for temporary support before the grouting.

The pile commonly stands out of the water a few meters in order to facilitate the positioning operation (see

Figure 3.27). Moreover, this allows less steel to be consumed as the TP is grouted to the outer pile and therefore has a larger diameter. So the shorter the TP is, the more inexpensive the substructure becomes.



Figure 3.27. Transition Piece being placed above driven pile [87]

#### 4. *Grouting:*

Installation tolerances can easily be accommodated and compensated for within the grouted connections. The grouting process is simple and can be carried out above and below sea level using standard processing equipment.

The most widely used connection is the grouting of the TP to the pile in the mean sea level. This is done by pumping the grout through flexible hoses into the overlapped annuli. Alternatively, if a rock socketed monopile foundation has been installed (when drilling has been necessary); the steel piles are grouted into the socket drilled in the rock. Both cases are depicted in Figure 3.28. Finally, the concrete is left to dry.

Recent problems in the TP – pile grouting have lead the industry to an extensive analysis of the calculations methods and design of this type of unions. Therefore, the



use of shear keys or conical shape unions instead of just cylindrical unions is expected in the future.

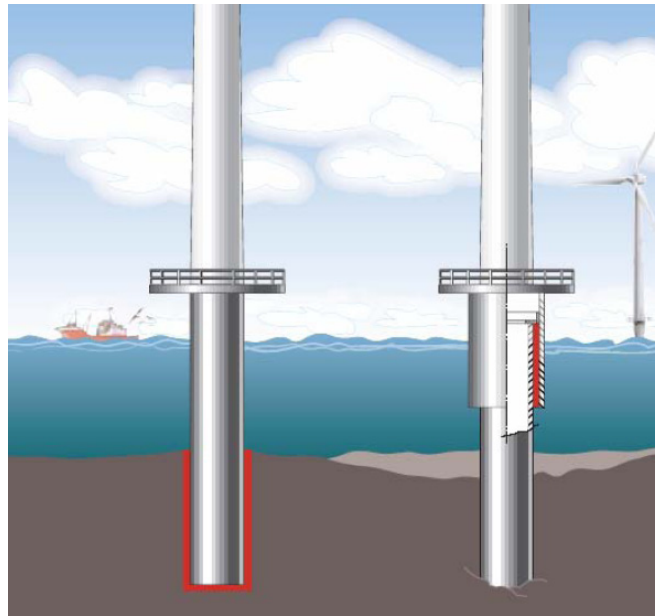


Figure 3.28. Monopile grouting areas depending on the installation case [88]

##### 5. *Scour protection (if needed):*

Several types of scour protection exist, ranging from asphalt to concrete mattresses, but most options require expensive offshore installation. The most cost effective method is therefore the dumping of crushed rock also known as the “rip-rap” solution. The basic idea behind the placing of a layer of rock is that the rock particles are selected in such a way that the increased current around the structure will not be able to wash them away.

This kind of static scours protection (because it is carried out before any scour takes place), can be installed in two different ways:

The side stone dumping consists of loading the rock on a barge equipped with hydraulic shovels. The barge sails along at a constant speed and the rock is pushed overboard onto the target. The barge sail speed and rock dumping rate determines the thickness of the layer of rock left on the seabed.

The flexible fall pipe method utilizes a larger holding tank in the barge and a flexible tube which is lowered into the water and down to the seabed while a remotely operated vehicle (ROV) guides the fall pipe. It allows a higher degree of accuracy and control.

Both the side stone dumping vessel and the flexible fall pipe are shown in Figure 3.29.



Figure 3.29. Side stone dumping vessel (on the left) and flexible fall pipe vessel (on the right) [89]

The need of protection is influenced by the seabed sediment type, tidal currents, waves and pile diameter. Hence, there are cases in which designing a heavier monopile is more economical than application of the scour protection [90]. Some of the OWFs that do not have scour protection for the monopile foundations in the UK are Barrow, Kentish Flats or North Hoyle [91].

Notwithstanding, there are 3 scour effects that have to be taken into account [92]:

- a) Foundation length: When the top part of the soil is removed because of scour, the foundation pile needs to be extended deeper into the ground to ensure sufficient lateral bearing as the pile penetration must be considered to start from the bottom of the hole.
- b) Natural frequency: The increase in the foundation length has an impact in the natural frequency of the structure that will be decreased. In spite of the small variation on the natural frequency that this implies, the fatigue of such a structure will very sensitive to this lowering, and will increase substantially [93]. This relation between small decrease of natural frequency and large increase in fatigue

is typical for the dynamically sensitive monopile supported offshore wind turbines.

- c) J-tube: in case no scour protection will be applied around the monopile, special attention has to be given to the protection of the cable near the monopile to avoid spanning of the cable in the scour hole. Because the power cable is of vital importance for the power production of the offshore wind turbine, damage to the cable should be prevented

Once all the above installation operations have been accomplished, the monopile is ready for the OWTG installation on top of it (see Figure 3.30)



Figure 3.30. Typical installed monopile [65]

Apart from these, during the monopile installation there are other transportation and manipulation operations that depend on the installation method that is employed. This will mainly depend on the distance to the base port [94].

If the offshore wind farm is near the base port (less than 2 hours sailing), only a Heavy Lift Vessel (HLV) will be used in the process, as this vessel can be loaded and then work on site in the monopiles installation (see Figure 3.31).

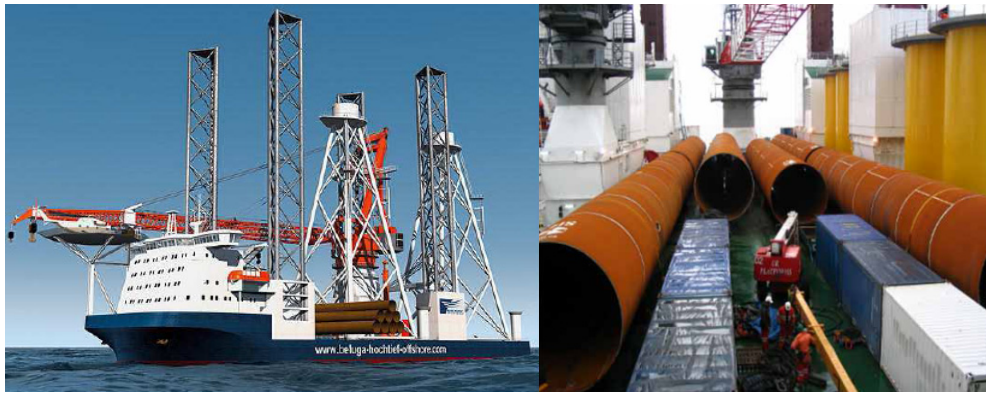


Figure 3.31. Jack-up type vessel transporting piles and transition pieces to site [95]

However, if the OWF is far from the base port (more than 6 hours sailing), hiring a feeder vessel becomes worthwhile. The piles delivery in this case can be done by barge or flotation (see Figure 3.32). In the case of the barge, the pile can be adequately protected and secured for the journey, but it will only allow for a limited space onboard. Alternatively, when dispatched by flotation the ends of the piles are sealed by steel closure plates or rubber diaphragms which should be able to resist wave slamming during the tow. In this case, there is no limit on the size of the vessel or lay down area. It also has inherent advantages for pile handling, which can be carried out easier and by vessels with lower working heights and smaller lifting capacity. This method is attractive where long segments of pile are to be lifted.



Figure 3.32. TP transportation by barge [96] and flotation [85]

It is not the aim of this study to analyse all the different methods, vessels and possibilities that the installation of a support structure would have to consider in order to make the most inexpensive choice. But, typical installation operations will be counted for a simpler comparison between support structures.

Therefore, distance to shore and its impact is not included. Instead, an average future OWF size is considered (composed of 100 WTG) and the need of a feeder vessel (tug boat with a barge) in the installation process in order to reduce transport time. This would help to fulfil the tight deadlines for 100 WTG in one installation season.

Moreover, support structure costs is not largely influenced by the distance to shore as detailed in [84]. A less than 1% increase per 10 km further from shore is obtained in the analysed cases, which include monopiles, gravity based, jacket and tripod.

Analysed soil type is clay, which allows the pile to be driven. Thus, the installation operations (driving, TP placing and grouting) will be accomplished by a HLV vessel.

Therefore, the total installation cost is divided in the following parts:

#### **A. Seabed preparation and scour protection cost**

Protection will be required in order to avoid the scour's 3 main effects, which are even more influenced by the larger pile diameters of bigger turbines.

The cost of the scour protection is calculated by a rock volume cost basis. Hence, the needed protection volume is calculated and then multiplied by 300 €/m<sup>3</sup>, which is the suppliers cost estimation for the procurement and installation, including vessel hiring [89].

For the mattress volume calculation recommendations in [97] are put into practice.

The minimum layer thickness depends on the water depth and has been set as shown in Diagram 3.8. Protection layer is almost 50% thicker from the pile to a distance D

of the pile, to account for the loss of smaller rocks that may be displaced by wave and current action.

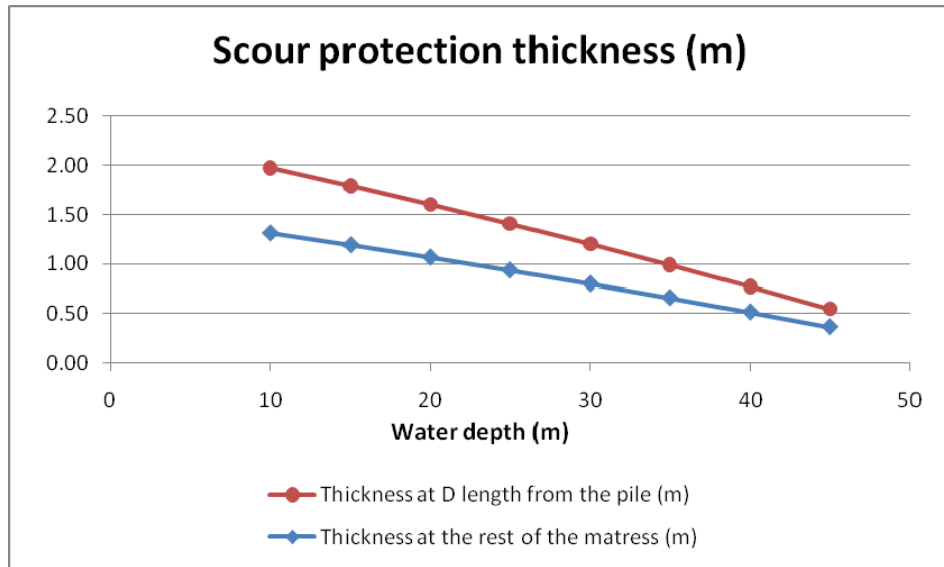


Diagram 3.8 Scour protection thickness variation depending on the water depth (m)

The introduction of the scour protection on the seabed results in increased turbulence at the downstream side of the scour protection which introduces scour of seabed material at its edge. The depth of the scour hole that will form at the edge of the scour protection, as well as the resulting slope influences the soil strength along the pile with increasing depth. By extending the scour protection farther away from the monopile, the effect of the scour hole is reduced.

In this study, the minimum protection length will be calculated as  $L=\lambda \cdot D$ , where  $D$  is the pile diameter at the seabed and  $\lambda$  is a constant with a minimum value of 2 and increases with water depth as shown in Diagram 3.9.

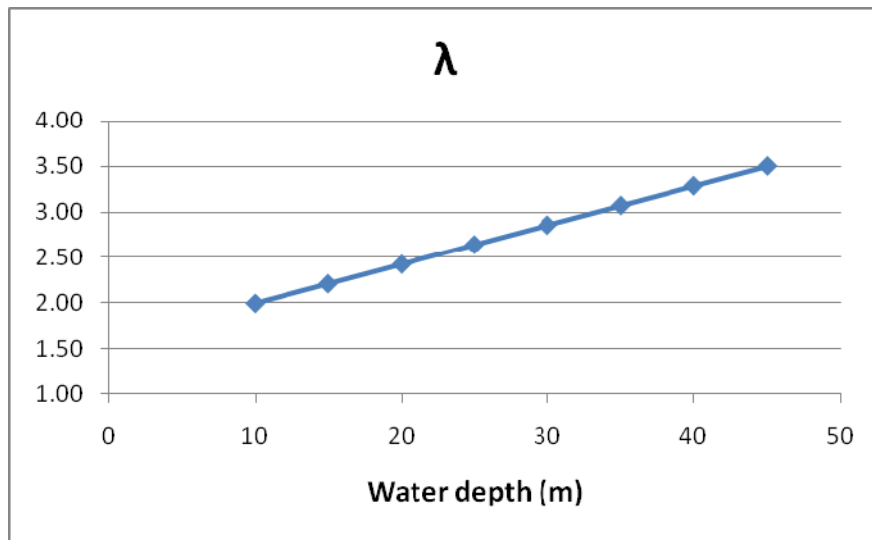


Diagram 3.9.  $\lambda$  variation at different water depths

So, once the thickness (as a function of the depth) and length (as a function of the depth and the monopile diameter at seabed) are known, the necessary rock volume can be calculated and multiplied by the cost. In Diagram 3.10 the scour protection cost for a 5 m diameter monopile at different water depths is presented.

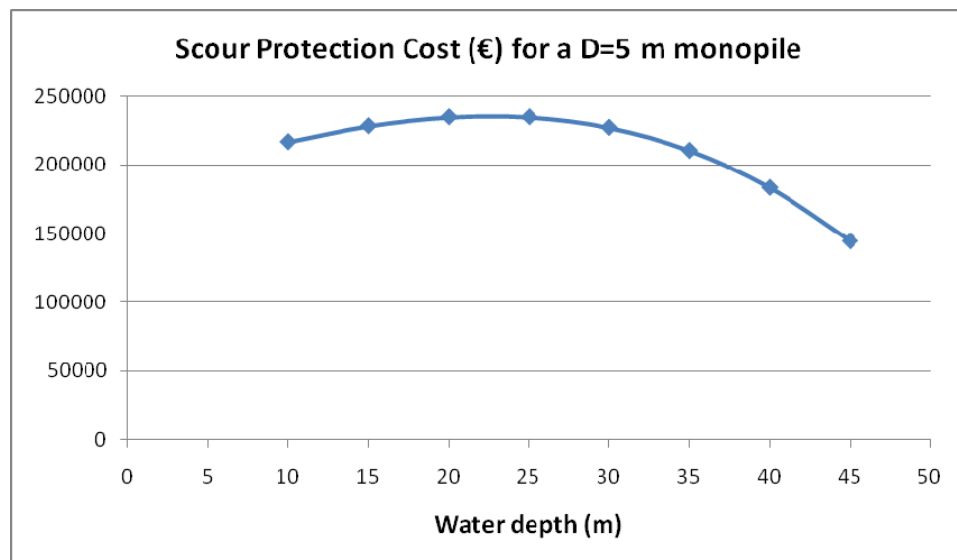


Diagram 3.10 Scour protection cost for a 5 m diameter pile

## B. Pile transportation and installation cost

The piles and transition pieces will be transported from the base port to site by a barge and a tug. Their cost and operation  $H_s$  are summarised in Table 3.8 [84].

Vessel	Operational $H_s$ (m)	Cost (€/day)
Barge (payload 2000 Tn)	1.5	7233
Tug	3	27312

Table 3.8. Monopile transportation costs

So the transportation of the components will have a total cost of 34548 €/day and an operational  $H_s = 1.5$  m.

Pile driving, TP placing and grouting will be accomplished by a HLV. The cost of such vessels has been considered as a function of the lifting capacity, and therefore of the pile weight. This function is charted in Diagram 3.11 [98]. An operational  $H_s = 1.2$  m for its operations is used for the calculations [99].

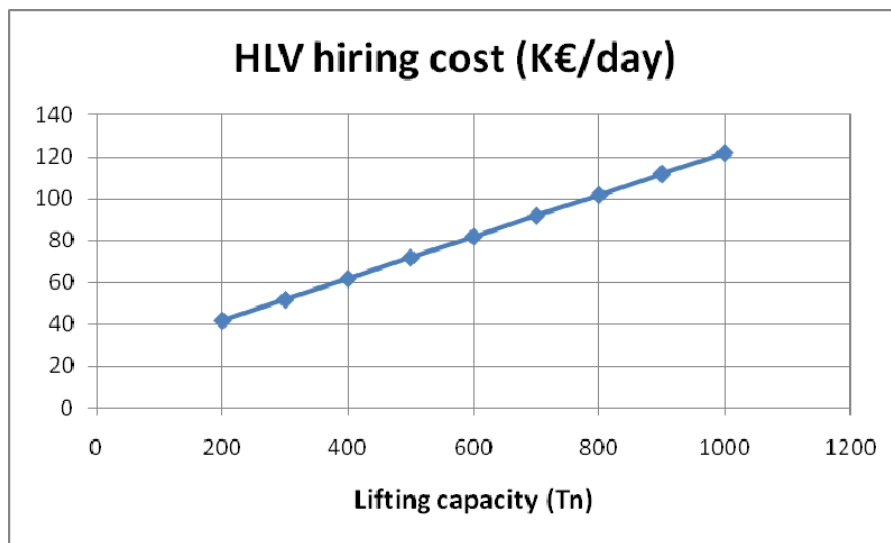


Diagram 3.11 HLV hiring cost as a function of the lifting capacity [98]

The cost of a large piling hammer is estimated at 14011 €/day [84].



Based on recent projects data, the average time for each operation is summarised in Table 3.9. Then, the weather windows for these operations have to be taken into account as a function of the operational  $H_s$  of the vessel. A minimum weather window of 6 hours for the operations to start is considered and its results are shown in Diagram 3.12 from data gathered from 4 North Sea sites [84]. Finally, once the total necessary time and the daily rate of each vessel are known, the total cost can be calculated.

Operation	Time (days)
Pile loading & transportation (go & back)	0.5
TP loading & transportation (go & back)	0.5
Pile installation	1
TP installation	1

Table 3.9. Estimated times for monopile installation operations

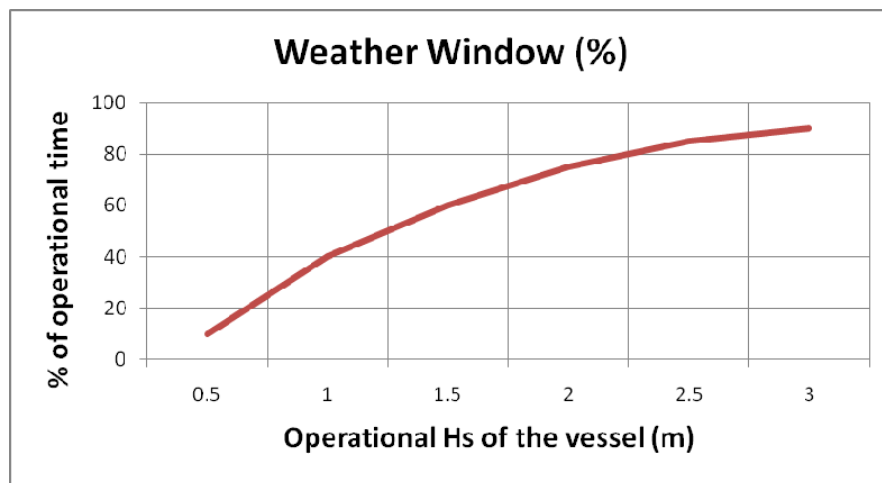


Diagram 3.12 Annual average weather windows of minimum 6 hours duration based on 4 North Sea sites. [84]

### C. Mob and demob cost

Based on [6] and [97] information, a mob and demob fixed cost of 320000 € is considered. When calculating the cost for each monopile, this value is divided by 100 (OWF average number of OWTG), which gives a cost of 3200 € per support structure for the mob and demob expenses.

## **3.5 Jacket cost analysis**

### **3.5.1 Introduction**

In 2006, the two jacket demonstrators in Beatrice wind farm at 45 m water depth had to deal with numerous technical challenges during its design, fabrication and installation [15] becoming the first substructures of its kind. However, since then, new installations in Alpha Ventus (commissioned in 2010) and Ormonde (the first large scale project using jacket substructure) are the first steps of a developing technology that will keep on growing as the already under construction big projects in Thornton Bank phase II (Belgium) and Nordsee Ost (Germany) evidence.

As it has already been affirmed, the jacket is a promising alternative for the evolution of the offshore wind industry, specially taking into account the characteristics of the near future planned OWF.

For this reason the cost analysis of the jacket type substructure is undertaken. This will help to shape and understand its real potential and weaknesses in order to correctly address the necessary improvements for this future jacket revolution to happen.

### **3.5.2 Matlab calculation methodology.**

Firstly, a Mathcad programme was written for the jacket static and dynamic calculation similarly to the monopile foundation, but in this case using 3D elements with 6 degrees of freedom, because of the nature of the structure and the forces involved. However, this programme had to be finally discarded due to the increased complexity of the substructure, the bigger matrices that had to be dealt with and the more complicated optimization procedures needed in order to obtain the lightest structure possible.

Instead, it was decided to reprogramme it in Matlab code, which enabled faster calculations and the possibility to run hundreds of iterations to optimize the design.

Diagram 3.3 summarizes the whole jacket calculation methodology that will be explained in detail hereafter.



Diagram 3.13 Summary of the jacket calculation with Matlab

### 1. Definition of jacket+piles+tower

First of all, the optimum number of storeys is calculated for the jacket lattice. This will depend on the height to cover, the footprint and the top width. Then, the height and widths of each storey are obtained by a least squares curve fitting aiming to achieve the most squared storeys as possible.

The footprint and top width are input values that vary according to the water depth and the OWTG power respectively as shown on Table 3.10 and Table 3.11. The jacket footprint increases with water depth to maintain a constant batter angle between the hub and the considered jacket top widths.

Depth (m)	Footprint (m)
25	16 x 16
35	18 x 18
45	20 x 20
55	22 x 22
65	24 x 24
75	26 x 26
85	28 x 28

Table 3.10. Jacket footprint values according to the water depth

Power (MW)	Top width (m)
3.6	6
5	8
7	9

Table 3.11. Jacket top width values according to the WTG power

Each node of the whole structure is then defined, including the tower, the transition piece, the jacket braces and legs, and the piles according to the entered initial dimensions as shown in Diagram 3.14.

The whole structure is divided in small parts, so that their elements can be defined according to their own properties. Having many parts helps to a better optimization

of the total weight, as the diameter and thickness can be set according to the necessities in each part of the structure. Hence, the following is a summary of the different areas that can be encountered in the jacket substructure and piles:

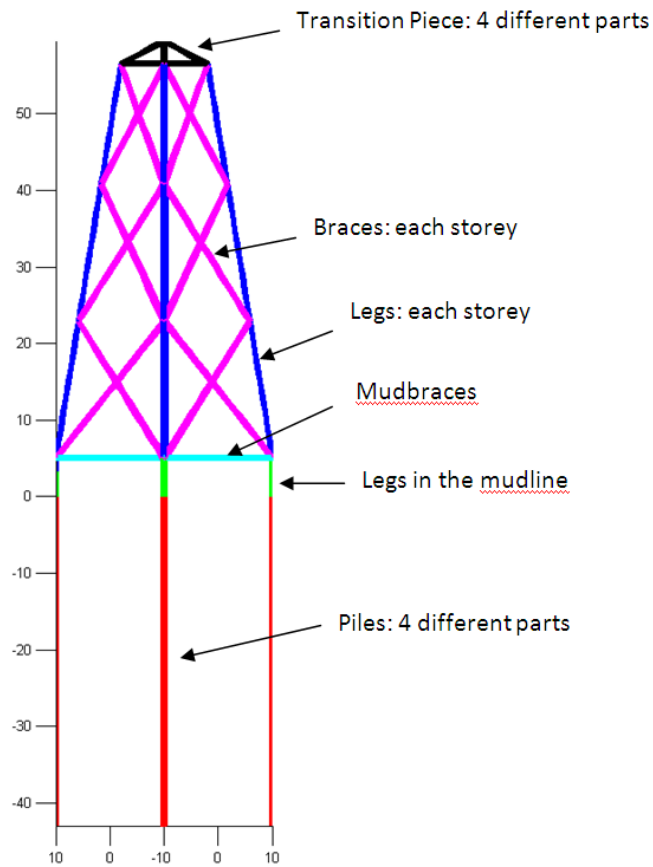


Diagram 3.14 Whole structure division in parts with different element properties

The coordinate system is set in its centre of symmetry at the mudline level, which is at a distance from the mean sea level equal to the water depth plus the considered scouring depth. The total scour is the sum of the global and the local scour, which are equal to 1 m and 2.5 times the pile diameter respectively.

The substructure has in line piles and the union is made by a 0.15 thick grouting (see Figure 3.33).

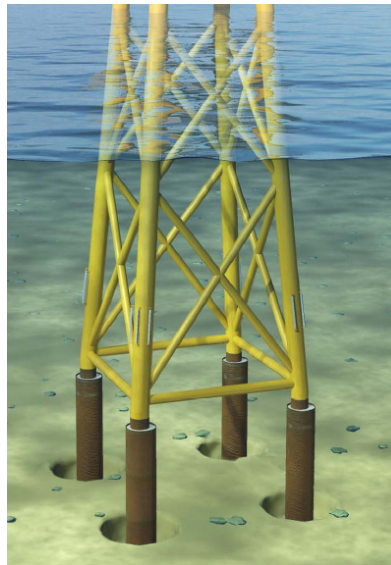


Figure 3.33: Jacket substructure and piles union detail [65]

Transition Piece height above mean sea level was calculated in the same way as it was explained for the monopile so it varies with the considered wave crest. Among the different TP technologies available (see Figure 3.34), the steel bracing was chosen for the calculation. Its height was set at 5 m and it was modelled with 3D beams and 6 dof (just like the rest of the structure) in a pyramid shape with a central vertical beam, following the design of the Beatrice or Alpha Ventus jacket substructures.

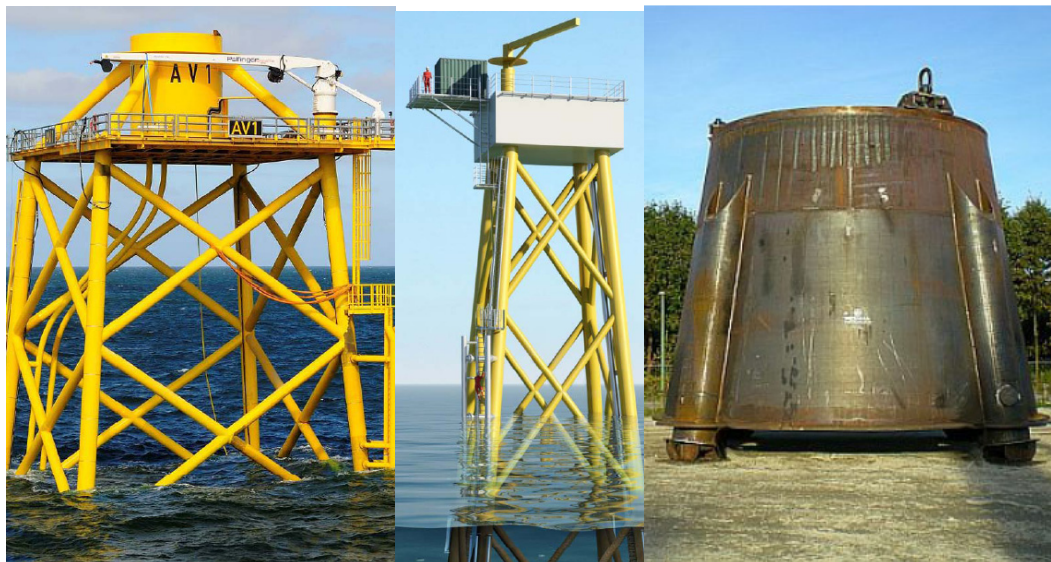


Figure 3.34: Different technologies for the jacket Transition Piece: steel bracing [100] (on the left), concrete [65] (in the middle) and steel cone [46] (on the right).

## 2. Definition of loads

Turbine and wind loads were reduced to a horizontal load and a moment. The same assumptions as with the monopile were taken regarding current velocity and wave loading. Linear wave theory was used without any correction factor for the particle velocities and accelerations, because the working area was around 100% of the Airy theory as shown in Diagram 3.4.

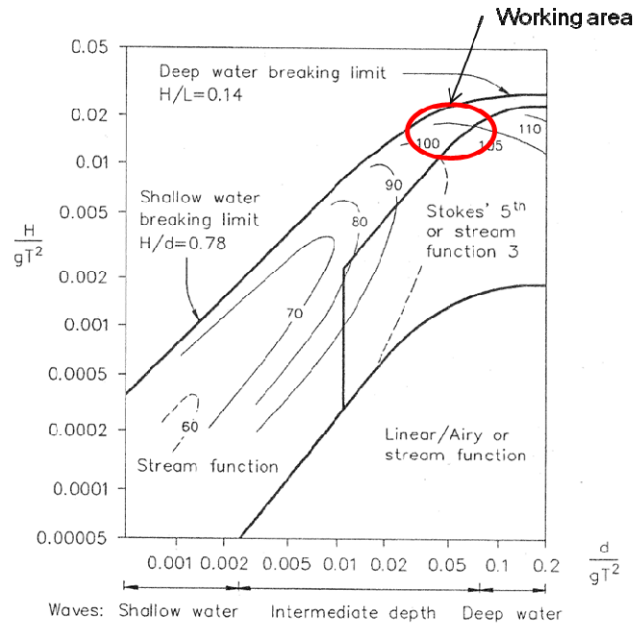


Diagram 3.15 Horizontal velocity under crest at MWL: Airy theory as % of regular theory [60]

The wave was stepped past the substructure with phase increments of  $1^\circ$ . The wave phase angle is chosen for the worst loading case in the mudline.

Wave and wind loads were calculated for two different direction angles, 0 deg and 45 deg (see Diagram 3.16). Therefore, the whole analysis of the structure was carried out twice and the worst case for each node taken into account. The reason is that the piles will have to withstand a higher load when the wave direction is 45 deg, while the worst case scenario for the brace nodes will be when wave and wind direction is in 0 deg.

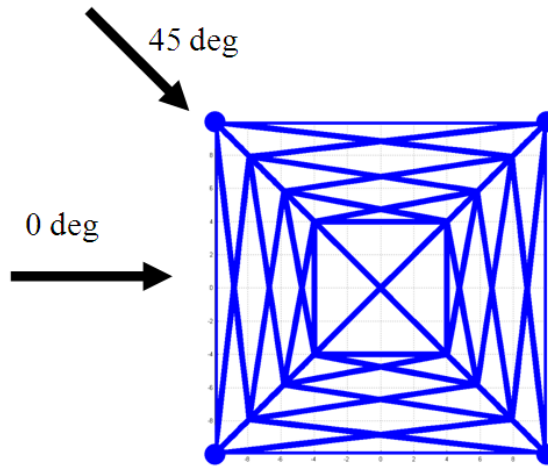


Diagram 3.16 Illustration of the two loading cases for the jacket support structure

Finally, the structure weight and the buoyancy of the underwater part are included.

A safety factor of 1.35 is used for the environmental loads and 1 for the permanent loads as per [59].

### 3. *Definition of substructure*

The stiffness matrix and force vector of the substructure covers the nodes above the mudline, including the tower nodes (see Diagram 3.17).

### 4. *Definition of connection node*

There are 4 connection nodes, one for each pile at the mudline. Below these connection nodes, the non linear behaviour starts due to the soil properties.

$K_s$ , and  $F_s$ , are calculated, that is, the stiffness and forces applied in the substructure as seen by the connection nodes, so in this case they are 24x24 matrices (6 dof for each of the 4 connection nodes).

Diagram 3.17 shows the partition of the whole structure according to the connection nodes.



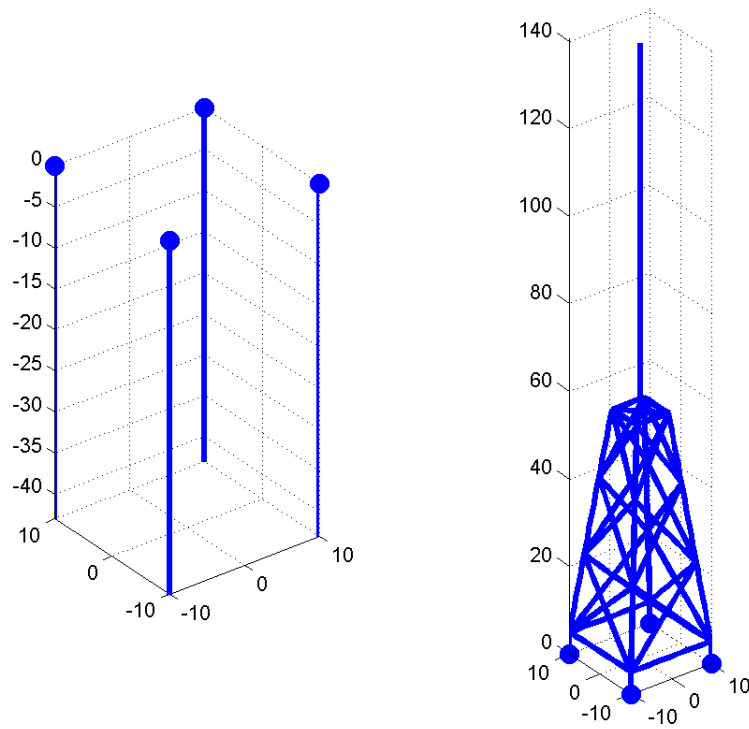


Diagram 3.17 Jacket support structure partition in two, with 4 connection nodes between them

### 5. Calculation of the foundations. Piles under the soil

The same methodology that was explained in the monopile section applies for the soil-pile interaction. The calculations rely on distributed and independent Winkler springs. Hence, p-y curves are used for x and y axes spring stiffness estimation and t-z and q-z curves for the z axis stiffness.

Due to the non linear behaviour of the soil, iteration is carried out until the system converges and deflections of the pile nodes under the soil are obtained.

### 6. Calculation of stresses

Once the non linear part of the structure has been calculated, deflections on the rest of the structure can be obtained in global coordinates, as the connection node displacements are already known.

Then, deflections are transformed into local coordinates and the element forces and stresses can be calculated as shown in Diagram 3.18.

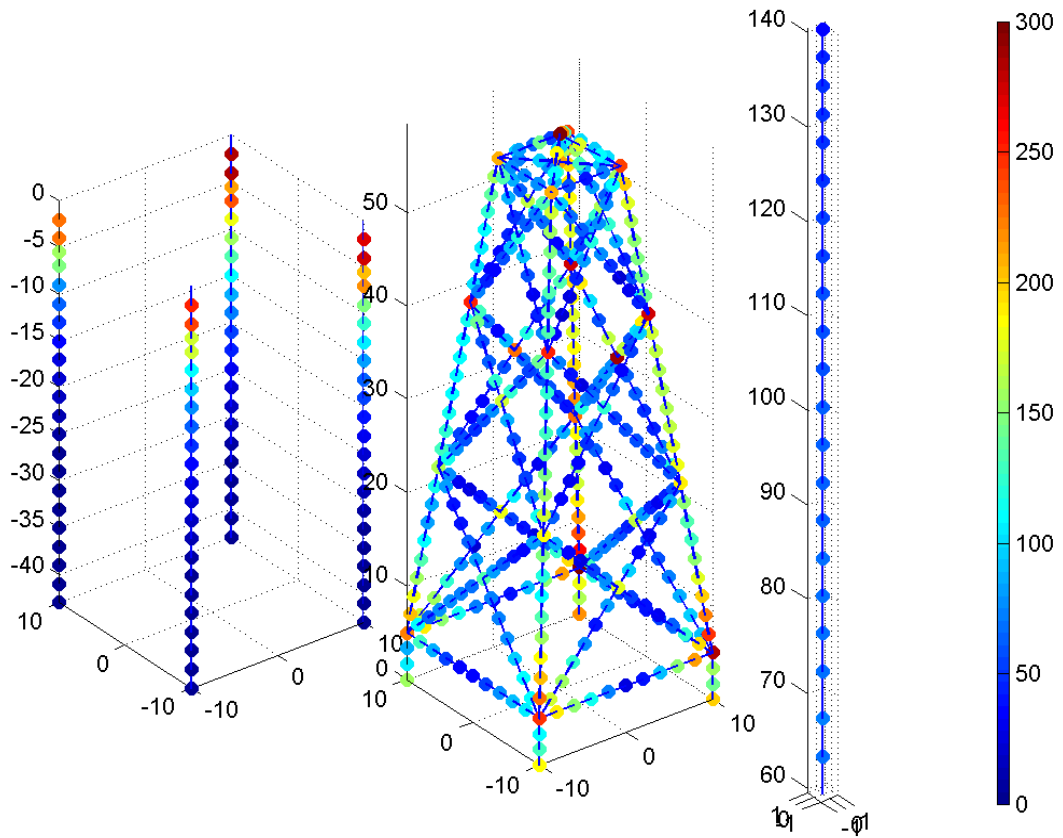


Diagram 3.18 Example of the maximum stress per node (MPa) for the whole structure

### 7. 1<sup>st</sup> natural frequency calculation

Soil stiffness is added to the whole structure matrix for the calculation of the first natural frequency.

Regarding the mass matrix, apart from the weight of the elements, THM is added in the top of the tower node and hydrodynamic added mass in the nodes under water. In this case no water mass inside the jacket lattice is considered, because this can help to find cracks in the structure in the case of leak appearance. Nevertheless, the influence of the water mass and the hydrodynamic added mass in the first natural frequency is insignificant, as stated in [101] and [102].

Finally the eigenvectors and eigenvalues can be calculated and the mode shape depicted as shown in Diagram 3.19.

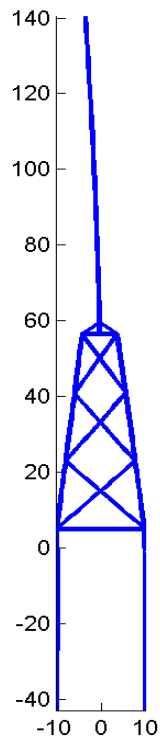


Diagram 3.19 Jacket mode 1 example. Scale 10:1

#### 8. Check results

The following are the design limiting criterion that the structure has to fulfil:

- Maximum axial stress  $< \sigma_{\max}$
- Maximum shear stress  $< \tau_{\max}$
- Pile head tilt angle (mudline)  $< 0.7$
- Fixed pile tip ( $\delta_{\text{tip}} = 0.001 \cdot D$ )
- $D/th < 100$
- No buckling of braces and legs

The same criterion used in the monopile also applies for the jacket substructure, but in this case, buckling of lattice braces and legs is also checked according to [75] for being a critical issue.

Steel Grade 355 is considered, with a material safety factor of 1.1 as per [59]. Maximum axial and shear strength are calculated and limited as per [59], [75].

### *9. Optimization*

The optimization process for the jacket substructure and pile foundations is automatized in several steps. The diameters and thicknesses of the elements, along with the piles penetration is set to minimum initial values and then increase step by step until all the limitations listed before are fulfilled.

### *10. Calculate weight*

The weight of the whole jacket support structure includes the 4 piles, the jacket lattice, the transition piece and the secondary steel, which are calculated with a steel density of  $7850 \text{ Kg/m}^3$ . Secondary steel weight values are according to Table 3.6.

## **3.5.3 Jacket Design**

The design of the jacket is carried out for the ULS. The 1<sup>st</sup> natural frequency is also a limiting factor that can influence the structure final weight if it is out of the allowable boundaries. These boundaries were considered to be the same as with the monopile (see Figure 3.9; **Error! No se encuentra el origen de la referencia.**) so that a proper comparison between the two substructures can be achieved.

Therefore, taking into account the same reasons detailed in the monopile design section, the allowable frequency is set between 0.28 Hz and 0.35 Hz.

The fatigue limit state was not considered due to lack of time. However, it has to be taken into account that a 100% weight optimization cannot be achieved with the partition carried out in the jacket and shown in Diagram 3.14. This is because the

thickness is maintained constant in the whole brace length in each storey and consequently the structure's final weight is a little bit higher than in a perfect optimization. This extra weight can account for the added necessary mass to fulfil the FLS in the lattice joints (roughly estimated to be around 10% more). So, overall the total mass is considered to be realistic.

8 mm corrosion allowance is included in the splash zone. The atmospheric zone is considered to be properly coated and cathodic protection is assumed in the submerged zone.

### 3.5.4 Validation

There is almost no experience for a validation of the results with real projects, even less detailed data regarding environmental conditions of these few locations are available. However, obtained jacket and pile weights showed to be sensible when compared with already accomplished projects (see Table 3.12)

Wind Farm	OWTG	Jacket weight (Tn)	Pile weight (Tn)	Water depth (m)	Pile Diameter (m)	Pile Length (m)
Ormonde	Repower 5 MW	450-500	200-440	17-21	1.82	20-45
Beatrice	Repower 5 MW	750	500	45	1.8	45
Alpha Ventus	Repower 5 MW	500	450	30	1.8	31-44

Table 3.12. Jacket and pile weights for already accomplished projects

Besides, results of a sensitivity analysis for the jacket substructure carried out by an offshore engineering consultancy were used to validate the Matlab programme. In this analysis, several design parameters were modified and the support structure calculated by Finite Element computation.

Despite this study included both ULS and FLS calculations, the comparison of 10 design cases with the Matlab programme showed the following average differences above the consultancy designs, which prove the validity of the tool:

-First natural frequency: +3%

- Jacket lattice weight: +6%

- Piles total weight: +5%

- Pile diameter: +3%

- Pile Penetration: +18%

- Upper leg diameter: +10%

- Lower leg diameter: +14%

As it has already been explained, a 100% weight optimization cannot be achieved with the partition carried out and shown in Diagram 3.14, due to the fact that the thickness of the whole brace length is maintained constant in each storey. However, this extra weight seems to fit correctly with the extra weight necessary to fulfil the FLS as the obtained similar results demonstrate.

### **3.5.5 Jacket Manufacturing**

Compared to the monopile, the jacket lattice and transition piece manufacturing process is more complex, involving many skilled tubular joint's welding and tight tolerance assemblies.

The jacket support structure is also composed of pile foundations. Their manufacturing process is the same as explained for the monopile, but in this case the pile diameters will typically range between 1 and 2.5 m, so the necessary machinery and manipulation requirements will be eased.

A jacket construction can be divided in 3 phases: fabrication, assembly and erection. Their main characteristics are described hereafter [103]:

## *1. Fabrication*

The fabrication phase of the jacket includes cutting, rolling, pressing, fitting, welding, stress relieving, etc., of tubular members, nodes, cones, supports, etc. There are also many quality inspections carried out, including non destructive test (NDTs), welds visual, magnetic particle inspection (MPI) and ultrasonic tests (UT). These processes normally are carried out in a fabrication shop and produce relatively small units.

Nodes fabrication is a critical process due to the frequently encountered geometrical complexity and the particular problems that they present in welding and dimension controlling. The sequential steps in the fabrication of a typical node are as follows:

- Fabrication of the can (with or without stiffeners).
- Cut and profile the stubs. Trace node locations onto the can surface and grind or blast areas. Then the area to be welded is UT inspected.
- Assemble one or two adjacent stubs, tack-weld in position and verify dimensional control.
- Weld according to predetermined sequence to limit deformation. Grinding is performed where necessary and all required inspections of the weld chords carried out.
- Repeat the previous steps for successive stubs.
- If required, carry out a thermal treatment of the welds to ensure that they contain minimal levels of residual stress. Thermal stress relieving or post-weld heat treatment (PWHT) of the heavier more restrained welds may be prescribed.

Although more expensive, alternatively, nodes can be cast steel in order to eliminate critical weld details. Cast nodes have higher fatigue and ultimate capacity

performance and facilitate automation. Comparison between the welded and casted nodes characteristics can be found in [46]



Figure 3.35: Welded joints [104] (to the left) and cast node [46] (to the right) comparison

Jacket sub-assemblies are also included in this phase. They can be considered as an intermediate stage between the standard workshop and the assembly/erection. The aim is to perform as many welds as possible in the shop to maximize the welds quality, since in the workshop many of them can be double-sided and/or automatic.

Sub-assemblies are executed so that at least one of the two edges that will be matching in the subsequent assembly/erection phase has a cut-off allowance. This provides a higher flexibility by cutting to fit once the part is being placed in field.

During these processes the dimensional control is emphasized and tends to be exaggerated, not because of structural consequences (from the structural point of view the tolerances are rather generous), but because of fitting considerations during subsequent phases of construction.

## 2. *Assembly*

Groups of shop fabricated sub-assemblies and loose items are assembled into a unit that constitutes the major lifts for the erection sequence. These processes are normally performed outside the fabrication shop but at ground level.



One of the most fundamental rules in fitting is the avoidance of "force-fitting" of members prior to welding or to create stresses into unwelded members through the welding sequence since such conditions cannot have been foreseen by the designer.



Figure 3.36: Assembled part of jacket substructure [46]

The sequence of events can be summarised as follows:

- Preparation of assembly support and staging.
- Rough setting of assembly main structure, position tacking and dimensional control.
- Infilling of secondary structure, position tacking and dimensional control.
- Weldout of structure and continuous inspection.
- Installation of appurtenances (anodes, walkways, J-tubes, etc.)
- Overall NDT, inspection and dimensional control.
- Blasting and painting or touch up.

### 3. Erection

Assembled, sub-assembled and fabricated structures, together with loose items are incorporated into the final structure. Jacket frames are typically laid out flat and then rolled using multiple cranes.

An outline sequence for the erection phase would be:

- Technical appraisal of lift methods.
- • Preparation of cranes for lift. Preparation for rigging. Transport assembly to lift location. Roll-up into position with scaffolding and staging in position, if possible.
- • Preparation of fixing system and weldout at least sufficient to allow crane release.
- • Crane release. Removal of rigging and temporary attachments.



Figure 3.37: Erection of a jacket substructure [46]

Jacket structural completion is followed by a short phase during which all the jacket systems, are completed and rendered functional.

Regarding the secondary steel, in general, heavier structures are expected for the jacket when compared with the monopile. More complex boat landing and ladders are necessary and a bigger platform. Besides, the use of the J tube is compulsory, whereas the monopile can be installed without J tube if necessary.

As it can be seen, the jacket substructure fabrication process has a lot of manual work due to the high number of welding and operations that are involved. The manufacturing cost is given in a cost per weight basis.

The costs for the jacket substructure are determined as 4 €/kg, based on [81] and the cost for the pile foundations as 2 €/kg according to [81] and [105]

### 3.5.6 Jacket Installation

Jacket support structures installation is more complicated, with higher cycle times and more operations involved in it. However, seabed preparation and/or scour protection is not typically carried out, which simplifies and diminishes costs. Therefore, a local and global scour is included in the calculations, as shown in Figure 3.38.

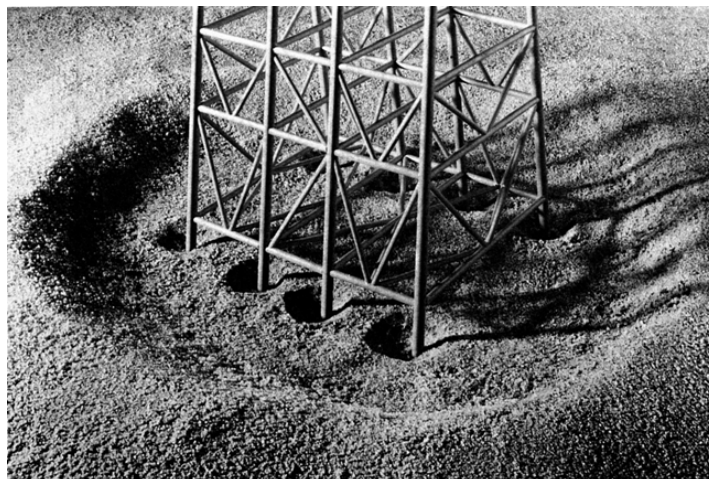


Figure 3.38: Representation of global and local scour in a jacket structure [106]

Installation process can be divided in several stages:

*1. Installation of piles:*

Two different techniques can be used, pre-piling or post-piling

Post piling was used on the Beatrice project, the first OWF using jacket support structures. However, since then, pre-piling has been the preferred choice, for all Alpha Ventus, Ormonde and Thornton Bank phase 2 projects.

Post piling implies a higher cost than pre-piling, due to the fact that you have the same cost for the jacket installation as for the piling operation. These operations are done from the same heavy lift vessel. In this case, the jackets are first placed on the seabed and secured by the mud mats and then piles are placed in each corner sleeves aided by video supervision from an ROV. Besides, post piling requires sleeves (see Figure 3.42) which make the structure heavier (in the Beatrice project the sleeves accounted for around 160 Tn).

For pre-piling however, piles are driven into the sea bed prior to jacket installation. This provides a plane surface for the jackets to stand on and also make the jacket lighter (no need of heavy pile sleeves). Besides, a less expensive pre-piling spread can be used, which just requires a jack up platform to install the foundation piles and do the subsequent jacket installation from a different heavy lift spread, which does not have any downtime due to the piling operations.

For these reasons, the pre-piling technique is being considered in this case study.

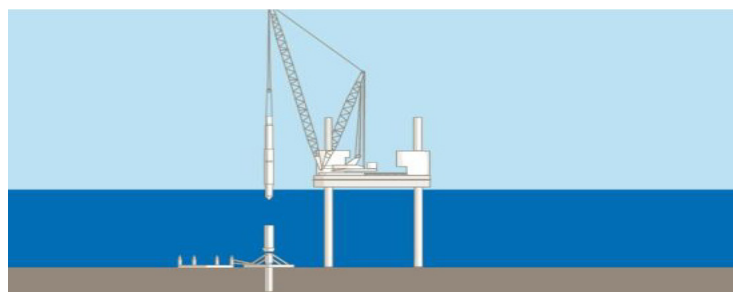


Figure 3.39: Prepiling with seabed template [107]

The same techniques and methods as explained in the monopile foundation apply for the piles installation.

## 2. *Jacket positioning:*

The jacket substructure is lifted and lowered in place. Once positioned, they are supported by temporary grippers and jacks in the piles that enable remote controlled levelling of the structure.

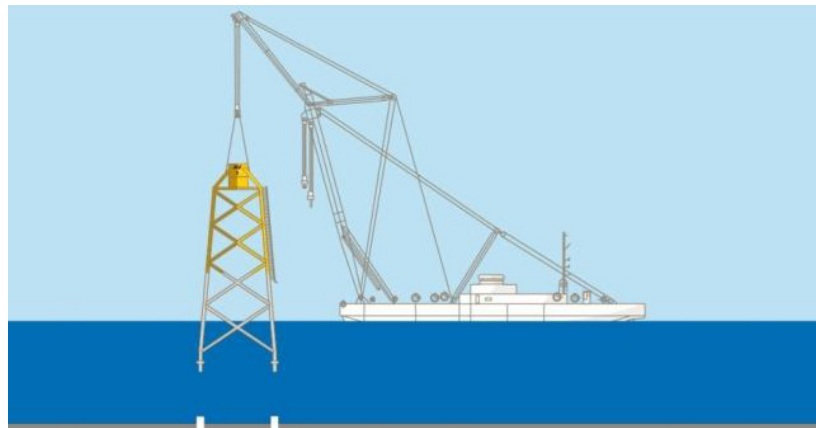


Figure 3.40: Positioning of the jacket substructure (including TP) [107]

If the Transition Piece is made of steel, the positioned jacket substructure already includes the TP, as it is assembled as a whole in the manufacturing field. However, a concrete TP would need two operations for the completion of this stage: one for the jacket steel frame positioning and another one for the concrete TP on it.

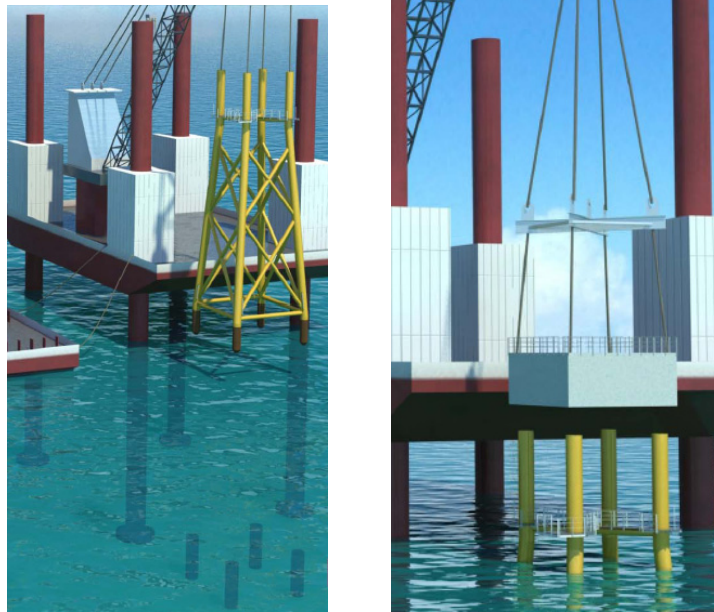


Figure 3.41: Jacket frame (on the left) and TP (on the right) positioning [65]

### 3. *Union of connections:*

Two different techniques can be used for the union of the piles and the jacket frame: grouting or swaging. New connection concepts like Pile Quick Coupling from Leenaars BV [108], have also recently entered the market.

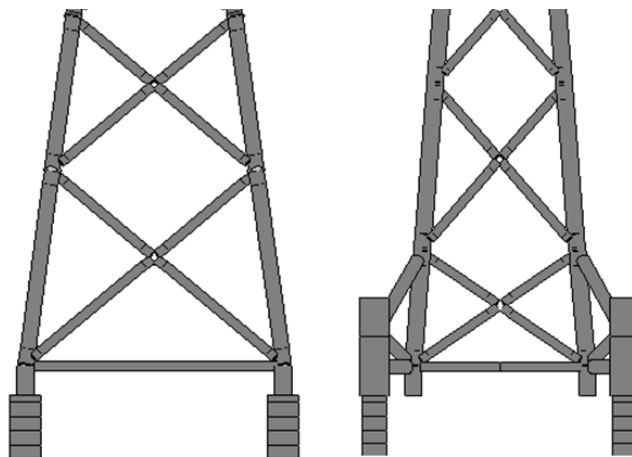


Figure 3.42: Typical jacket and pile connections by in line piles (to the left) and by sleeves (to the right)

Swaging is a forging process, in which the metal is plastically deformed to its final shape using high pressures. Swaging was used in the Beatrice project. In this case, the jacket frame was composed of four additional sleeves in the bottom end corners where the piles were introduced. Then the pile diameter was increased and a permanent connection between the pile and the sleeve was established (see Figure 3.42.).

On the contrary, as explained in the monopile section, the grouted connection is the union between two concentric tubulars formed by the injection of a cementitious material into the annulus space between the tubulars.

Pre-piling and in line grouted piles for the connection of the jacket and the foundation has been the chosen method except on the Beatrice project.

In the case of the concrete TP, after its positioning, the TP would be also grouted or bolted to the jacket legs.

Once all the above operations have been accomplished and the grout dried, the jacket is ready to support the OWTG on top of it.

In spite of their higher complexity, which makes them more time consuming for installation, recent experiences in Ormonde OWF during the jacket installation process, have proved to be as competitive as the monopile [109]. This demonstrated the potential of this technology, which is expected to suffer a huge development over the next years as more experience is gained.

Taking all this into account, the installation costs for an average OWF composed of 100 WTG must include the following:

Barge and tug hiring cost for the transportation of the piles and jacket substructure from the base port to site. Their cost and operation  $H_s$  were summarised in Table 3.8 [84].

HLV hiring costs to accomplish all the installation operations. The cost of such vessels was depicted in Diagram 3.11 as a function of the lifting capacity with an operational  $H_s = 1.2$  m [99].

The cost of a small piling hammer, which is estimated at 11009 €/day [84].

Mob and demob fixed cost of 320000 € is also considered, which means a cost of 3200 € per foundation for the mob and demob expenses.

Average times for each operation are estimated from Ormonde project (see Table 3.9). Then, the weather windows for these operations have to be taken into account as a function of the operational  $H_s$ . A minimum weather window of 6 hours is considered and its results were shown in Diagram 3.12.

<b>Operation</b>	<b>Time (days)</b>
Piles loading & transportation (go & back)	0.5
Jacket loading & transportation (go & back)	0.5
4 piles installation	1.5
Jacket installation	1

Table 3.13. Estimated times for jacket installation operations

Once the total necessary time and the daily rate of each vessel are known, total installation costs can be calculated.